CDX Markets, Time-Varying Fear, and Corporate Leverage*

Artur Anschukov
Imperial Business School
Imperial College

Harjoat S. Bhamra
Imperial Business School
Imperial College

Lars-Alexander Kuehn
Tepper School of Business
Carnegie Mellon University

March 25, 2026

Abstract

CDX spreads and corporate leverage comove strongly and more intensely during crises. Existing CDX pricing models cannot reproduce this because they assume exogenous default and leverage. We develop a consumption-based model where firms optimally choose default and leverage while an Epstein–Zin representative agent learns about crisis risk. The agent's perceived crisis probability, her fear, is self-reinforcing, raising default boundaries and leverage through a fear-driven financing channel that accounts for time variation in CDX spreads. We estimate the model to match the 5-year CDX rate, equity returns, and leverage. The model replicates the CDX term structure and physical default probabilities.

JEL Classification: G12, G13, G32, G33, E44

Keywords: CDX, credit derivatives, credit risk, corporate leverage, default, learning, disaster risk, term structure, structural estimation

*We would like to thank Hui Chen, Alexandre Corhay, Mete Kilic, Sang Seo, Ilya Strebulaev, Pietro Veronesi, Neng Wang, seminar participants at Carnegie Mellon University, and conference participants at the 2024 Oxford Said-VU SBE Macro-Finance Conference, the 9th London-Paris Bachelier Workshop for valuable feedback. Lars-A. Kuehn acknowledges financial support as the Marvin Goodfriend Fellow from the Tepper School of Business. Contacts: a.anschukov17@imperial.ac.uk, h.bhamra@imperial.ac.uk, and kuehn@cmu.edu.

Contents

1 Introduction

CDX spreads and corporate leverage comove strongly over time, see Figure 1. The correlation between the levels of 5-year CDX rates and average cross-sectional leverage is 41%, rising to 60% for monthly changes. This comovement intensifies precisely when credit risk rises: during the 2008–2009 financial crisis, 5-year CDX rates surged from 60 to over 200 basis points while leverage climbed from 32% to 44%; during the COVID-19 shock, CDX rates doubled from 49 to over 100 basis points as leverage rose from 34% to 41%.

Despite its empirical salience, this joint behavior has not been documented in the CDX literature and cannot be quantitatively accounted for by existing CDX pricing models, because they treat default intensities and capital structure as exogenous. Without optimal corporate decisions, these models cannot address the economics linking leverage dynamics to CDX-leverage comovement.[1] At the same time, Seo and Wachter (2018) show that rare economic disasters are a first-order determinant of CDX spreads, establishing macroeconomic tail risk as a central driver of credit index pricing. Structural models require stationary leverage ratios to match observed credit spreads (Collin-Dufresne and Goldstein, 2001), yet a long-standing puzzle is that standard structural determinants explain little of the variation in credit spread changes (Collin-Dufresne, Goldstein, and Martin, 2001), while tail risk premia appear to be a primary determinant of corporate spreads (Culp, Nozawa, and Veronesi, 2018). Corporate default cycles have important asset-pricing implications (Giesecke, Longstaff, Schaefer, and Strebulaev, 2011), yet existing CDX pricing models abstract from these by imposing exogenous leverage. The empirical evidence, therefore, points to a tighter interaction between crisis risk and corporate balance sheets than existing models allow. Understanding how exposure to crises shapes both CDX rates and firms' leverage choices is the central motivation of this paper.

We develop a CDX pricing framework in which firms optimally default and choose leverage while an Epstein–Zin representative agent learns about crisis risk, the unobservable arrival rate of sudden downward jumps in consumption. These jumps, which we call crises, individually average 2.5%; they unfold into disasters only when they cluster into cumulative declines exceeding 10%. Learning about the crisis arrival rate is self-reinforcing: each observed crisis raises the perceived likelihood of the next. We call the agent's subjective assessment of crisis

[1] For example, Collin-Dufresne, Goldstein, and Yang (2012), Seo and Wachter (2018), Collin-Dufresne, Junge, and Trolle (2024), and Doshi, Ericsson, Fournier, and Seo (2024) model default as the outcome of an exogenous policy rule and abstract from firm-level financing choices.

Figure 1: Time Series of CDX and Leverage

This figure displays the 5-year maturity CDX rate (blue lines) and average cross-sectional leverage (red line) for the months from September 2003 to June 2022. The solid blue line is the data, and the dashed one represents the model. The grey bars are NBER recessions. The CDX data represents Markit's North American Investment Grade CDX Index, for which Series 1 started trading in September 2003.

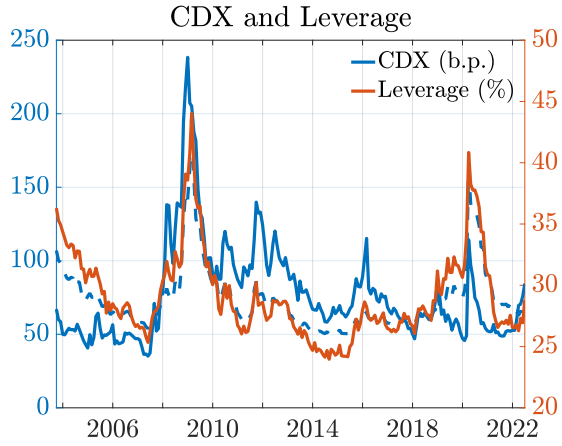

risk her *fear* — it is the state variable that links investor beliefs to corporate decisions and CDX rates. Our framework differs from the existing CDX literature along two key dimensions. First, firms optimally default and choose capital structure in response to macroeconomic conditions, building on Chen (2010); Bhamra, Kuehn, and Strebulaev (2010b); Hackbarth, Miao, and Morellec (2006). Second, investors do not observe the true crisis arrival rate; instead, they infer it from consumption following Benzoni, Collin-Dufresne, and Goldstein (2011), Wachter and Zhu (2025), and Ghaderi, Kilic, and Seo (2022).

By combining optimal corporate financing with learning about crises, the model delivers a disciplined explanation for the joint dynamics of leverage, default, CDX rates, and earnings. As fear rises, optimal default boundaries shift upward and equity values decline, increasing leverage, thereby amplifying and prolonging movements in CDX spreads even in the absence of large realized defaults. This interaction generates a tight link between CDX rates and leverage that is absent from models with exogenous financing policies. We call it the *fear-driven financing channel*: fear is transmitted to credit markets not primarily through risk prices but through its effect on endogenous leverage. Because fear is self-reinforcing, the fear-driven financing channel is dormant in calm times and self-activating during stress — explaining why CDX–leverage comovement intensifies during crises, as documented in Figure

1. Ours is the first framework in which learning about crisis risk generates self-reinforcing fear that propagates to credit markets through endogenous leverage.[2]

Firms issue debt and equity. Default decisions optimize the value of levered equity (Leland, 1994; Goldstein, Ju, and Leland, 2001), while leverage is set by coupon levels chosen to maximize firm value, trading off tax benefits against bankruptcy costs. As shown by Strebulaev (2007), infrequent capital structure adjustment suffices to generate rich leverage dynamics. Our framework exploits this insight: firms set leverage at entry, and aggregate leverage fluctuates as fear alters default boundaries and the cross-sectional distribution of firms. Fear, therefore, shapes both the optimal default boundary and the optimal coupon, so that firm-level default rates and leverage fluctuate with fear in addition to earnings.

We use the same consumption calibration as Anschukov, Bhamra, and Kuehn (2024), which matches the size and duration of the U.S. Great Depression, the likelihood of consumption disasters from Barro and Ursua (2012), and the first four moments of U.S. consumption growth for the calm post-war sample.

As in Seo and Wachter (2018), we price CDX contracts within a consumption-based asset pricing framework. In Seo and Wachter (2018), default is modeled as the event where a firm's value falls below an exogenous threshold – the CDX price is, therefore, a function solely of the aggregate jump intensity. Since we model optimal default, the distance-to-default is firm-specific, and the entire earnings distribution of the 125 index constituents is relevant for pricing. To make the model tractable, we reduce the state space to average cross-sectional leverage and fear, extending the homogeneous-pool approximation used by Doshi, Ericsson, Fournier, and Seo (2024) to account for cross-sectional heterogeneity in leverage.

Following Hennessy and Whited (2007) and Bazdresch, Kahn, and Whited (2018), we structurally estimate four firm-level parameters: the size of idiosyncratic and aggregate Brownian risk, the idiosyncratic jump size, and bankruptcy cost parameters. We use data on all firms in the North American Investment Grade CDX Index from 2003 to 2022. The estimation targets seven moments: the means and standard deviations of excess returns, leverage, and 5-year CDX rates, and the standard deviation of market excess returns. The model generates a large equity premium of 9.5%, volatile equity returns of 33.8%, realistic leverage of 27.4%, market returns with 14.4% dispersion, and a 5-year CDX rate of 72 basis points.

Despite targeting only the 5-year CDX rate, the model closely matches the full 1-to-10-year

[2] Benzoni, Collin-Dufresne, and Goldstein (2011) and Wachter and Zhu (2025) both have self-reinforcing learning processes, but neither studies credit markets.

term structure of CDX rates and physical default probabilities. At the short end, the average 1-year CDX rate is 21 basis points in the model compared to 22 basis points in the data; at the long end, the average 10-year CDX rate is 138 basis points in the model compared to 113 basis points in the data. Physical default probabilities, which are not estimation targets, are also matched closely.[3]

To evaluate the model's time-series performance, we feed the estimated model with two observable inputs: average cross-sectional leverage and a proxy for the latent belief process constructed from large negative equity market returns. The model replicates the cyclical variation of the 5-year CDX rate across the entire 2003–2022 sample, including the prolonged elevation during the Great Recession and the sharp spike during COVID-19. The CDX slope, the difference between 10-year and 5-year rates, is also well matched, with the only notable discrepancy occurring during the months following the onset of COVID-19, when unprecedented policy interventions compressed long-maturity spreads in ways the model does not capture. The model additionally reproduces the time-varying volatility of CDX rates, closely tracking realized volatility estimates throughout the sample. Importantly, the belief proxy is constructed to mirror the model's Bayesian updating rule and is not estimated to fit CDX spreads: the time-series dynamics of CDX rates emerge as an equilibrium outcome rather than a targeted object.

In summary, our paper makes five main contributions. First, we document a strong and systematic comovement between CDX rates and corporate leverage that intensifies during crises, an empirical pattern absent from the CDX literature, and show that models with exogenous default cannot account for it. Second, we develop a structural CDX pricing model in which firm-level default and leverage are endogenous and respond to self-reinforcing fear — an emergent property of Bayesian learning, not an imposed process — generating a nonlinear fear-driven financing channel that is dormant in calm times and self-activating during stress. Third, we structurally estimate the model on CDX data from 2003–2022, jointly matching moments of the 5-year CDX rate, equity returns, and leverage. Fourth, despite targeting only the 5-year CDX rate, the model replicates the full term structure of CDX rates and physical default probabilities out of sample – a result not achieved by existing consumption-based models. Fifth, a decomposition of CDX rates reveals that the fear-driven financing channel is the dominant source of time variation in CDX rates, with leverage effects exceeding direct

[3]Matching the term structure of CDX rates is a key improvement relative to Kuehn, Schreindorfer, and Schulz (2023). In their framework, disaster risk is fully observable via a Markov chain, so there is no learning and no distinction between actual and perceived crisis risk.

belief effects by approximately six to one, while the direct effect of fear on risk prices primarily governs spread levels at short maturities.

The remainder of the paper is organized as follows. Section 2 presents the asset-pricing block of the model: a representative agent consumption-based model with learning and a discussion of how consumption dynamics are calibrated. Section 3 presents the corporate finance block of the model: a firm-level model of optimal default and capital structure decisions is embedded within the asset pricing block. We derive levered equity prices, corporate bond prices, and describe how CDX rates are computed. Section 4 describes the data and presents the empirical results. Finally, Section 5 concludes.

2 Consumption, Fear, and the Stochastic Discount Factor

We embed a model of optimal corporate financing for a cross-section of firms inside a representative agent consumption-based asset pricing model, building on the framework developed in Anschukov, Bhamra, and Kuehn (2024). The key novelty of the framework relative to the existing literature (see Bhamra, Kuehn, and Strebulaev (2010b) and Chen (2010)) is a common negative shock modeled by a downward jump, affecting both aggregate consumption and firm-level earnings, where the jump intensity is stochastic and unobservable. The representative agent forms and updates subjective beliefs about the jump intensity by observing consumption. Subjective beliefs – which we refer to as fear – impact optimal capital structure and default decisions at the firm level, as we show in the following section.

2.1 Consumption Dynamics

While the aggregate consumption process superficially resembles Wachter and Zhu (2025), we use a distinct approach, based on a markedly different calibration. Aggregate consumption follows:

$$\frac{dC_t}{C_{t-}} = \mu_c dt + \sigma_c dB_{c,t} + \left(e^{-Z_{c,t}} - 1\right) dN_t, \tag{1}$$

where B_c is a standard Brownian motion and N is a Poisson process with *unobservable* stochastic intensity λ_t.[4] When N jumps, log consumption drops by $Z_{c,t}$, where the jump sizes $\{Z_{c,t}\}$ are i.i.d. exponentially distributed with mean $1/\epsilon_c$.[5] The Brownian motion B_c, the jump sizes $\{Z_{c,t}\}$, and the Markov chain λ_t are mutually independent. The unobservable λ_t

[4] Since λ_t is itself stochastic, N is formally a Cox process (doubly stochastic Poisson process).

[5] The mean jump in consumption growth is $E_{t-}[e^{-Z_{c,t}} - 1] = -\frac{1}{1+\epsilon_c} \equiv -J_c$.

follows a two-state Markov chain: state L with $\lambda_t = \lambda_L$ and state H with $\lambda_t = \lambda_H$. Physical transition rates are ϕ_{LH} (from L to H) and ϕ_{HL} (from H to L).

The consumption process (1) has seven exogenous parameters, which we calibrate as in Anschukov, Bhamra, and Kuehn (2024) – see Panel A of Table 1. Following Barro (2006) and Barro and Ursua (2012), we define a consumption disaster as a path segment during which consecutive annual growth rates of consumption are negative and cumulatively result in a drop of more than 10%. Empirically, disasters are slow-moving and unfolding gradually (Constantinides, 2008; Julliard and Ghosh, 2012; Nakamura, Steinsson, Barro, and Ursua, 2013; Branger, Kraft, and Meinerding, 2015; Ghaderi, Kilic, and Seo, 2022). Individual jump sizes are calibrated to be small – an average consumption drop of 2.5% per jump – in contrast to the single large instantaneous disaster (Rietz, 1988; Wachter, 2013). A single jump, therefore, does not constitute a disaster. Instead, disasters emerge as sequences of downward jumps in close succession, consistent with the empirical evidence that disasters unfold gradually over several years (Barro, 2006; Barro and Ursua, 2012). Panels B and C of Table 1 show that the calibration matches the statistical properties of post-war consumption and consumption disasters very well.[6]

2.2 Subjective Beliefs, Fear and Belief Uncertainty

We next describe how learning dynamics create belief uncertainty and why the belief that the economy is in the high-risk state can be interpreted as fear. The representative agent observes aggregate consumption and knows all fixed parameters, but cannot observe the jump intensity λ_t. She updates her posterior belief p_t that the current state is H:

$$p_t = Pr(\lambda_t = \lambda_H | \mathcal{F}_t),$$

where $\mathcal{F}_t$ is her information set. Her subjective jump intensity is $\tilde{\lambda}_t = \tilde{\lambda}(p_t) = p_t \lambda_H + (1 - p_t)\lambda_L$.

Intuitively, the subjective belief level p_t can be thought of as a fear of small downward jumps arriving: when p_t rises, the agent acts as if she were facing a more threatening environment, with a higher probability of a downward jump in consumption, with consequences for leverage, default, and credit risk. For simplicity and to clarify that p_t does not measure

[6] We aim to match an average disaster size of 16.59% and an average disaster duration of 44 months, the respective values for the U.S. Great Depression. We take the likelihood of entering a disaster, 3.6%, from Barro and Ursua (2012), close to the value in Wachter (2013).

subjective beliefs about disaster intensity (a single downward jump is relatively small and not a disaster), we shall refer to p_t as fear.[7]

Under Bayesian updating, her belief dynamics follow:

$$dp_t = (\lambda_H - \lambda_L)(p_t - \overline{p})(p_t - p^*)\, dt + \sigma_p(p_{t-})dN_t, \tag{2}$$

where

$$\overline{p} = \frac{1+\overline{\kappa}}{2}\left[1 + \sqrt{1 - \frac{4f_H\overline{\kappa}}{(1+\overline{\kappa})^2}}\right], p^* = \frac{1+\overline{\kappa}}{2}\left[1 - \sqrt{1 - \frac{4f_H\overline{\kappa}}{(1+\overline{\kappa})^2}}\right], \overline{\kappa} = \frac{\kappa}{\lambda_H - \lambda_L}. \tag{3}$$

We note that $\kappa = \phi_{LH} + \phi_{HL}$ is the convergence rate to the long-run mean, $f_H = \phi_{LH}/\kappa$ is the long-run probability of being in state H, and

$$\sigma_p(p) = \frac{\lambda_H - \lambda_L}{\tilde{\lambda}(p)} p(1-p) \geq 0$$

measures *belief uncertainty*, which is concave in the subjective belief p, as shown in Figure 2.[8]

Figure 3 illustrates how the concavity of belief uncertainty impacts the learning mechanism. The dynamics of the subjective belief level p create time variation in fear, and are shown on the left. When there are no jumps in consumption, the agent's fear fades: her belief that the economy is in the high state decays towards the lower bound p^*. When a downward jump in consumption arrives, the agent immediately increases her belief that the economy is in the high-risk state: her fear jumps from p_{t-} to $p_{t-} + \sigma_p(p_{t-})$. Belief uncertainty is therefore a measure of belief fragility: when belief uncertainty is high, any revision in beliefs will be large – fear would rise by a large amount if consumption were to jump downward.

The dynamics of belief uncertainty are subtle, because belief uncertainty increases in p until p reaches $\hat{p} = \frac{\sqrt{\lambda_L}}{\sqrt{\lambda_L}+\sqrt{\lambda_H}}$ and then decreases – see Figure 3. Consequently, if the level of p just prior to a jump is below $\hat{p}$ and remains so after the jump, belief uncertainty will jump up – see the top panel. However, if the level of p just prior to a jump is above $\hat{p}$, belief uncertainty will jump down – see the bottom panel.

[7] In Appendix B, Proposition B2 shows that when fear rises, the agent's conditional consumption growth distribution develops a fatter left tail, more negative skewness, and higher variance. Proposition B3 and Lemma 1 extend this result to arbitrary horizons. Fear thus creates a deterioration of the agent's forward-looking consumption outlook.

[8] The long-run probability of the low-risk state is $f_L = 1 - f_H = \phi_{HL}/\kappa$. We denote by $\tilde{\mathbb{P}}$ the probability measure representing the agent's subjective beliefs and by $\tilde{E}_t[\cdot]$ the time-t conditional expectation given the observable filtration $\mathcal{F}_t$. Formally, $\tilde{E}_t[I_A] = E_t\left[\frac{\tilde{M}_T}{\tilde{M}_t} I_A\right]$, where $\tilde{M}$ is the exponential martingale $\frac{d\tilde{M}_t}{\tilde{M}_{t-}} = \left(\frac{\tilde{\lambda}_{t-}}{\lambda_{t-}} - 1\right)(dN_t - \lambda_{t-}dt)$, $\tilde{M}_0 = 1$, defined on the full filtration $\mathcal{G}_t$ generated by observing both consumption and the latent state λ_t. For $\mathcal{F}_t$-measurable observables, this reduces to the physical conditional expectation: $\tilde{E}_t[I_A] = \mathbb{P}(A \mid \mathcal{F}_t)$.

The belief dynamics (2) make fear self-exciting. Since $\tilde{\lambda}(p) = p\lambda_H + (1-p)\lambda_L$ is increasing in p, each crisis ($dN_t = 1$) raises p_t by $\sigma_p(p_{t-}) > 0$, which in turn raises $\tilde{\lambda}(p_t)$, increasing the agent's expectation of the next crisis. Between crises, p_t decays toward p^*, so the excitation is transient. This self-excitation is not assumed, as in a Hawkes process (Hawkes, 1971), but arises endogenously from Bayesian filtering of an unobservable Markov chain. Moreover, because $\sigma_p(p)$ is state-dependent, the self-excitation of fear is nonlinear: it is strongest at intermediate beliefs, precisely when the agent is most uncertain about the state of the economy.

2.3 Preferences and the Stochastic Discount Factor

The representative agent has the continuous-time analog of Epstein–Zin–Weil preferences with an elasticity of intertemporal substitution ψ equal to 1. The representative agent's value function is given by

$$J_t = \tilde{E}_t \left[\int_t^\infty f\left(C_s, J_s\right) ds \right], \tag{4}$$

where f is given by the normalized Kreps-Porteus aggregator:

$$f(c, v) = \beta(1-\gamma)v \, \ln\left(c/h^{-1}(v)\right), \, h(x) = \frac{x^{1-\gamma}}{1-\gamma}, \tag{5}$$

β is the rate of time preference and $\gamma > 1$ is the coefficient of relative risk aversion.[9]

The representative agent's value function is of the form

$$J(C_t, p_t) = h\Big(e^{V(p_t)} C_t\Big), \tag{6}$$

where the function $V(p_t)$ is monotonically decreasing in p_t and captures how fear impacts the agent's utility.

Proposition 1 *The dynamics of the equilibrium stochastic discount factor π_t are given by*

$$\frac{d\pi_t}{\pi_{t-}} = -r(p_{t-})dt - \Theta_B dB_{c,t} + \left[\Theta_J(Z_{c,t}) + \Theta_L(p_{t-}, Z_{c,t})\right] dN_t - \left(\lambda^{\mathbb{Q}}(p_{t-}) - \tilde{\lambda}(p_{t-})\right) dt, \tag{7}$$

where the locally risk-free rate is given by

$$r(p_t) = \beta + \mu_c - \gamma\sigma_c^2 - \lambda^{\mathbb{Q}}(p_t)\frac{J_c}{1 - J_c\gamma}, \tag{8}$$

[9] The continuous-time version of the recursive preferences introduced by Epstein and Zin (1989) and Weil (1990) is known as stochastic differential utility (SDU) and derived in Duffie and Epstein (1992). Schroder and Skiadas (1999) provide proof of existence and uniqueness. Kraft and Seifried (2010) show the version of SDU we use is well-defined under a mixed Brownian-Poisson filtration.

the price of Brownian risks in log consumption is given by $\Theta_B = \gamma\sigma_c$*; the price of pure jump risk is given by* $\Theta_J(Z_{c,t}) = e^{\gamma Z_{c,t}} - 1 \approx \gamma Z_{c,t}$*; and the risk price of belief uncertainty is given by*

$$\Theta_L(p_t, Z_{c,t}) \approx -(\gamma - 1)\sigma_p(p_t)V'(p_t)\big[1 + \Theta_J(Z_{c,t})\big]. \tag{9}$$

The risk-neutral intensity rate for jump arrivals $\lambda^{\mathbb{Q}}(p_t)$ *is related to the corresponding subjective intensity* $\tilde{\lambda}(p_t)$ *via* $\lambda^{\mathbb{Q}}(p_t) = \omega(p_t)\tilde{\lambda}(p_t)$*. The risk-distortion factor is* $\omega(p_t) = \omega_J + \omega_L(p_t)$*, where* ω_J *is the risk-distortion for pure jump risk and* $\omega_L(p_t)$ *is an additional risk-distortion for belief uncertainty, given by*

$$\omega_J = \frac{1 - J_c}{1 - J_c(1+\gamma)} \qquad \omega_L(p_t) \approx -(\gamma - 1)\sigma_p(p_t)V'(p_t)\omega_J. \tag{10}$$

Three types of aggregate risk are priced: Brownian risk (negligible empirically), pure jump risk, and belief uncertainty. The price of Brownian risk is $\Theta_B = \gamma\sigma_c$, which is small because σ_c is low. When belief uncertainty is zero, jump risk is still priced with the constant risk-distortion factor ω_J, creating a wedge between the risk-neutral and subjective jump intensities – see Rietz (1988) and Barro (2006). The price of belief uncertainty, given by (9), is non-zero because the agent prefers earlier resolution of intertemporal risk (Ai, 2010; Collin-Dufresne, Johannes, and Lochstoer, 2016). It is time-varying and hump-shaped in p (Wachter and Zhu, 2025), declining as the agent becomes increasingly sure which state the economy is in – see Figure 2. Belief uncertainty creates an additional risk distortion $\omega_L(p_t)$, widening the wedge between the risk-neutral and subjective jump intensities.

3 Firm Dynamics and CDX Prices

We embed a structural model of optimal default and capital structure inside the consumption-based framework of Section 2. Once default and leverage are chosen optimally, corporate financing decisions depend on the *level* of beliefs about crisis risk, i.e., fear, rather than on belief uncertainty. This channel is absent in models without optimal default/leverage. We use the model to price firm-level defaultable bonds and CDX contracts – indices of credit default swaps on investment-grade issuers.

Our setup follows the earnings-based structural tradition (Goldstein, Ju, and Leland, 2001; Hackbarth, Miao, and Morellec, 2006; Bhamra, Kuehn, and Strebulaev, 2010a,b; Chen, 2010), augmented with learning about crisis risk that feeds directly into capital structure and default.

3.1 Firms' Earnings Dynamics

There are K firms. Real earnings for firm $k \in \{1, \ldots, K\}$ evolve as

$$\frac{dX_{k,t}}{X_{k,t-}} = \mu_x dt + \sigma_x^{\text{id}} dB_{x,k,t} + \sigma_x^{\text{sys}} dB_{x,t} + (e^{-Z_{k,t}} - 1)dN_t - dN_{k,t},$$

where μ_x is expected earnings growth when there are no jumps; $dB_{x,t}$ and $dB_{x,k,t}$ are systematic and idiosyncratic Brownian shocks; $E_t[dB_{c,t}dB_{x,t}] = \rho_{cx}dt$ and $E_t[dB_{c,t}dB_{x,k,t}] = E_t[dB_{x,k,t}dB_{x,k',t}] = 0$ for $k' \neq k$. Hence σ_x^{sys} and σ_x^{id} are the systematic and idiosyncratic volatilities, and ρ_{cx} is the correlation between the Brownian shock to consumption and the systematic Brownian shock to earnings.

Aggregate jump risk arrives through the Poisson process N_t, which also affects consumption. Earnings jump sizes are heterogeneous: $Z_{k,t}$ is exponentially distributed, independent across firms and from $Z_{c,t}$, with mean $1/\epsilon_x = \varphi/\epsilon_c > 0$. Thus the mean conditional earnings jump is[10]

$$E_{t-}[e^{-Z_{k,t}} - 1] = \tilde{E}_{t-}[e^{-Z_{k,t}} - 1] = -\frac{1}{1+\epsilon_x} \equiv -J_x < 0.$$

To ensure a stationary firm earnings distribution for structural estimation in Section 4, we assume each firm can experience an idiosyncratic exit jump $dN_{k,t} = 1$ with intensity λ_x, driving earnings to zero. Default or exogenous exit triggers replacement by a new entrant with earnings X_{0-} and optimally chosen capital structure. The set of firms in the economy at time-t is denoted by $\mathcal{K}_t$. The number of firms $K = |\mathcal{K}_t|$ hence remains fixed while the set of firms in the economy changes. Gomes and Schmid (2021) use the same approach to ensure leverage does not vanish in the long run.

3.2 Fear and Optimal Default

The optimal default boundary increases with the belief that the economy is in the high-risk state, i.e., fear, and is chosen to maximize the value of the levered equity claim. This is similar to how the optimal exercise policy for an American-style option is obtained by pricing the option.[11]

We assume the initial firm owners have decided on capital structure by optimally fixing the coupon level c. Given coupon c_k, firm k's equity owners optimally choose a default time

[10] For any suitable q, $\tilde{E}_{t-}[q(Z_{c,t}, Z_{k,t})] = E_{t-}[q(Z_{c,t}, Z_{k,t})]$.

[11] We use the Hamilton-Jacobi-Bellman Variational Inequality approach of Pham (1998) and Øksendal (2003) instead of the smooth pasting approach in Leland (1994).

$\tau_{D,k}$ to maximize levered equity value:

$$S_{k,t} = (1-\eta) \sup_{\tau_{D,k} \geq t} \tilde{E}_t \left[\int_t^{\tau_{D,k}} \frac{\pi_u}{\pi_t} \big(X_{k,u} - c_k\big)\, du \right],$$

so $S_{k,t} = S(X_{k,t}, p_t, c_k)$ depends on earnings $X_{k,t}$, the belief p_t about the high-risk state, i.e., fear, and c_k.

Default occurs the first time earnings cross a belief-dependent boundary:

$$\tau_{D,k} = \inf\{t > 0 : X_{k,t} \leq X_D(p_t, c_k)\}.$$

Solving the optimal stopping problem via a Hamilton-Jacobi-Bellman variational inequality (HJB-VI) yields the price–boundary pair (S, X_D), see Proposition B7 in Appendix B. Unlike the risk price for belief uncertainty, which is hump-shaped in belief levels (see Figure 2), the optimal default boundary is *monotone increasing* in the belief level. Figure 4 provides a visualization of the result.[12]

Intuitively, a higher p raises the subjective frequency of large negative earnings moves, shifting the continuation value down and prompting earlier default. Learning thus raises $X_D(p, c)$ in high-risk episodes. Default arises either by diffusion, i.e., touching X_D, or by a jump that simultaneously lowers earnings, increases p, and causes the default boundary to jump upward. This learning-default link amplifies distance-to-default movements and credit risk. Moreover, because the agent's perceived crisis intensity is self-exciting, if crises cluster, then each crisis raises fear, which raises the default boundary, which raises leverage, leaving the firm more fragile when the next crisis arrives. This feedback makes the fear-driven financing channel nonlinear — weak when fear is low, and increasingly powerful as crises cluster into a disaster.

3.3 Corporate Bond Prices and Optimal Capital Structure

We now price firm-level corporate debt. The time-t price of perpetual corporate debt issued by firm k with coupon rate c_k and recovery rate α is given by

$$D_{k,t} = c_k \tilde{E}_t \left[\int_t^{\tau_{D,k}} \frac{\pi_u}{\pi_t} du \right] + \alpha(1-\eta) \tilde{E}_t \left[\frac{\pi_{\tau_{D,k}}}{\pi_t} p_X(p_{\tau_{D,k}}) X_{k,\tau_{D,k}} \right].$$

[12] The monotone increasing property of the optimal default boundary in fear is established via a chain of maximum-principle arguments applied to the HJB-VI. We show that equity is convex in log-earnings $Y = \ln X$ ($S_{YY} \geq 0$), decreasing in fear ($S_p \leq 0$), and that the cross-partial satisfies $S_{Yp} \leq 0$. Applying the implicit function theorem to the smooth pasting condition $S_Y(Y_D(p), p) = 0$ then yields $Y_D'(p) = -S_{Yp}/S_{YY} \geq 0$. Two intermediate conditions are verified at the estimated parameter values. The proof is given in Anschukov, Bhamra, and Kuehn (2024).

Debtholders receive a coupon flow c_k until endogenous default at the random time $\tau_{D,k}$.[13] If endogenous default occurs prior to exogenous exit, then debt holders receive the fraction α of after-tax unlevered firm value. At default, firms become all-equity financed, so firm value is merely the value of unlevered equity, given by $(1-\eta)p_X(p_{\tau_{D,k}})X_{k,\tau_{D,k}}$. The time-$t$ value of perpetual debt depends on current earnings, current beliefs, and the coupon rate, i.e., $D_{k,t} = D(X_{k,t}, p_t, c_k)$.[14]

At firm entry, $t = t_k$, initial owners choose the coupon to maximize firm value net of issuance costs ι:

$$c_k^*(p_{t_k}) = \arg\max_c F_{k,t_k}(c, X_D(p_{t_k}, c)) \quad \text{with} \quad F_{k,t_k} = S_{k,t_k} + (1-\iota)D_{k,t_k}.$$

Because c_k^* depends on the entry belief p_{t_k}, the default boundary depends on both current and entry beliefs: $X_D(p_t, c_k^*(p_{t_k}))$. Across the panel $\mathcal{K}_t$, $\{X_D(p_t, c_k^*(p_{t_k}))\}_{k\in\mathcal{K}_t}$ governs cross-sectional default timing. As firms either default or exit and are replaced, the t_k's are updated. For $X_0 = 1$, optimal coupons $c(p_0)$ (setting $t_k = 0$ for simplicity) decline with p_0 as tax benefits are dominated by bankruptcy costs in high-risk states – see the right panel of Figure 4.

Figure 5 shows how a firm's optimal default boundary and distance-to-default change in the time series, together with belief uncertainty. In the left panel, we simulate a downward jump in consumption, which also decreases belief uncertainty. At the same time, the default boundary rises, pushing down the value of levered equity even though belief uncertainty falls. The right panel shows distance-to-default rather than the optimal default boundary: the effects are even stronger here because increases in the default boundary are compounded by declines in earnings.

3.4 CDX Pricing

In this section, we explain how to price a CDX contract and show how it depends on the prices of the underlying corporate bonds and firm-level default decisions. We price Markit's North American Investment Grade CDX Index (the CDX.NA.IG Index, commonly known as the "IG Index"), which is composed of 125 of the most liquid North American firms with investment grade credit ratings that trade in the CDS market. The index composition is

[13] Exogenous exit at the random time $\tau_{X,k}$, which is exponentially distributed with parameter λ_x, automatically induces default because earnings must cross the default boundary when earnings jump to zero.

[14] The yield on such debt, denoted by $y(X_{k,t}, p_t, c_k)$, is defined by

$$y(X_{k,t}, p_t, c_k) = \frac{c_k}{D(X_{k,t}, p_t, c_k)}.$$

chosen twice annually at times known as roll dates, which we denote by t_{roll}.[15] At each roll date, the CDX index is issued with six maturities: 1 year, 2 years, 3 years, 5 years, 7 years, and 10 years.

Let the time-t price of the corporate debt issued by firm k be $D_{k,t}$. The random default time of firm k's debt is denoted by $\tau_{D,k}$, and so we can define the stochastic recovery rate

$$R_{k,\tau_{D,k}} = \frac{D_{k,\tau_{D,k}}}{D_{k,t_{0,k}}},$$

which is the ratio of corporate debt value for firm k at default relative to the value at the time of issuance, $t_{0,k} = t_k$. We use $n_{t,s}(t_{\text{roll}})$ to represent the fraction of firms in the index defined at the roll date t_{roll} that have defaulted between the times t and $s > t$:

$$n_{t,s}(t_{\text{roll}}) = \frac{1}{N_F} \sum_{k \in \mathcal{N}_F(t_{\text{roll}})} 1_{\{t < \tau_{D,k} \leq s\}},$$

where $N_F = 125$ is the number of firms in the index and $\mathcal{N}_F(t_{\text{roll}})$ is the set of firms in the index. The key variables that impact the value of the CDX index are $\{R_{k,\tau_{D,k}}\}_{k \in \mathcal{N}_F(t_{\text{roll}})}$ and the stochastic process $n_{t,s}(t_{\text{roll}})$.

The N_F firms in the index are selected according to a pre-defined and publicly known set of rules (e.g., credit quality). A CDX contract issued at the roll date t_{roll} has a finite time to maturity, denoted by $T - t$, where t is the current time ($t \in [t_{\text{roll}}, T)$) and $T \in \{t_{\text{roll}} + 1, t_{\text{roll}} + 2, t_{\text{roll}} + 3, t_{\text{roll}} + 5, t_{\text{roll}} + 7, t_{\text{roll}} + 10\}$.

A CDX contract is a swap between a protection buyer and a protection seller. The protection buyer receives default-contingent payments from the protection seller, triggered by defaults among the index constituents and sized by the loss given default. The protection seller receives premium payments from the protection buyer at a fixed rate applied to the surviving notional.

We first describe the cash flows received by the protection buyer. If firm k in the index defaults at time $\tau_{D,k}$, the protection buyer receives a cash flow of $\frac{1}{N_F} \cdot (1 - R_{k,\tau_{D,k}})$, where $R_{k,\tau_{D,k}}$ is the recovery rate for firm k's debt. When the recovery rate is zero, the cash flow is $\frac{1}{N_F}$. Therefore, the sum of the payoffs received by the protection buyer up until time $s > t$ is

$$L_{t,s}(t_{\text{roll}}) = \frac{1}{N_F} \sum_{k \in \mathcal{N}_F(t_{\text{roll}})} 1_{\{t < \tau_{D,k} \leq s\}} \left(1 - R_{k,\tau_{D,k}}\right),$$

[15] The two roll dates for a given year are September 20 (or the Business Day immediately thereafter in the event that September 20 is not a Business Day) and March 20 (or the Business Day immediately thereafter in the event that March 20 is not a Business Day).

which increases with the losses an investor would have incurred, and is known as the cumulative loss. Using increments in $L_{t,s}$, the present value of the cumulative loss under subjective beliefs is given by

$$\text{Prot}(T-t, t_{\text{roll}}) = \tilde{E}_t \left[\int_t^T \frac{\pi_s}{\pi_t} dL_{t,s} \right],$$

where, for ease of notation, we have suppressed the dependence on the roll date. Equivalently,

$$\text{Prot}(T-t, t_{\text{roll}}) = \frac{1}{N_F} \sum_{k \in \mathcal{N}_F(t_{\text{roll}})} \tilde{E}_t \left[\frac{\pi_{\tau_{D,k}}}{\pi_t} (1 - R_{k,\tau_{D,k}}) 1_{\{t < \tau_{D,k} \leq T\}} \right].$$

We evaluate the CDX contract at inception, setting $t = t_{\text{roll}}$. We now describe the cash flows received by the protection seller. The protection seller receives insurance payments which amount to $(S_{\text{CDX}} \cdot \frac{1}{4}) \cdot (1 - n_{t,s})$ every quarter.[16] In addition, as payments are made in arrears, the protection seller receives an accrued premium as compensation for the time the defaulted entity was covered since the last scheduled payment. Suppose, for example, firm k defaults between dates t and $t + \frac{1}{4}$, then firm k was covered for an additional timespan of $(\tau_{D,k} - t)$ since the last quarterly payment: the accrued premium for firm k amounts to $(S_{\text{CDX}} \cdot \frac{1}{4}) \cdot 4(\tau_{D,k} - t) \cdot \frac{1}{N_F}$, reflecting firm k's equal weight in the index. Aggregating both the expected discounted scheduled and default-triggered payments gives the following expression for the present value of cash flows received by the protection seller

$$\begin{aligned} \text{Prem}(T-t, S_{\text{CDX}}, t_{\text{roll}}) = & S_{\text{CDX}} \cdot \frac{1}{4} \cdot \tilde{E}_t \left[\sum_{m=1}^{4(T-t)} \left(\frac{\pi_{t+\frac{m}{4}}}{\pi_t} \left(1 - n_{t,t+\frac{m}{4}} \right) \right. \right. \\ & \left. \left. + \int_{t+\frac{m-1}{4}}^{t+\frac{m}{4}} \frac{\pi_s}{\pi_t} 4 \left(s - t - \frac{m-1}{4} \right) dn_{t,s} \right) \right]. \end{aligned}$$

Finally, S_{CDX} is set such that present values of protection and premium payments are equal when the contract commences at time t_{roll}, and so

$$S_{\text{CDX}} = \frac{\text{Prot}\left(T - t_{\text{roll}}, t_{\text{roll}}\right)}{\text{Prem}\left(T - t_{\text{roll}}, 1, t_{\text{roll}}\right)}.$$

3.5 CDX Simulation

As in Seo and Wachter (2018), we price a CDX contract within a consumption-based asset pricing framework. Since in Seo and Wachter (2018) default is modeled as the event where a firm's value falls below an exogenous threshold, their CDX price is a function solely of the aggregate jump intensity and thus independent of firm-level characteristics.

[16] It is market convention to quote quarterly paid spreads in annual terms, hence $S_{\text{CDX}} \cdot \frac{1}{4}$.

In contrast, we model optimal default, where the distance-to-default is firm-specific. As a result, unlike Seo and Wachter (2018), the entire firm distribution of the 125 index constituents is relevant for the pricing of CDX contracts, specifically, each firm's earnings level and coupon rate. Since it is computationally infeasible to track the full firm distribution, we reduce the state space to two variables: average leverage $\bar{L}_t$ and the current belief p_t. Leverage contains information about both earnings and coupons, making it a natural summary statistic of the cross-section of default risk.

There is no closed-form solution for the CDX spread, so we price the contract under the risk-neutral measure using Monte Carlo simulations. For each point on a grid of average leverage and belief, we draw 125 firm-level leverage ratios from a truncated log-normal distribution with a standard deviation of 15.89%, the unconditional cross-sectional dispersion, and 125 initial beliefs from the stationary distribution of p_t. Within our model, a firm's leverage ratio is

$$L(X_{k,t}, p_t, p_{k,0}) = \frac{D(X_{k,t}, p_t, p_{k,0})}{D(X_{k,t}, p_t, p_{k,0}) + S(X_{k,t}, p_t, p_{k,0})},$$

where $p_{k,0}$ is the entry belief for firm k, as defined in Section 3.3. For each firm, we solve for earnings by numerically inverting the leverage function, then simulate earnings for 10 years and track defaults and losses across the full finite pool. We repeat this 10,000 times, computing the CDX rate for maturity m (in years) as $S_{\text{CDX},m}(\bar{L}_t, p_t)$.

Our CDX pricing methodology extends the homogeneous-pool approximation of Doshi, Ericsson, Fournier, and Seo (2024) in order to preserve cross-sectional heterogeneity. Specifically, we assume that there is both leverage and entry belief heterogeneity because firms enter the economy at different times. Each firm, therefore, carries a different optimal coupon and faces a different default boundary. Because the CDX rate is convex in leverage, evaluating it at the cross-sectional mean misses the contribution of firms in the right tail – precisely those closest to default. A homogeneous-pool approximation assumes this effect away, see Appendix C.5 for details.

4 Structural Estimation and the Fear-Driven Financing Channel

We perform four empirical exercises that directly map into our model's economic mechanisms: (i) a joint moment-matching of equity returns, leverage, and credit spreads (see Section 4.3) tests the fear-driven financing channel; (ii) a CDX term-structure analysis (see Section 4.4)

validates the firm-specific optimal default boundary feature; (iii) the time-series evidence (Section 4.5) tests how fear-driven leverage dynamics shape the cyclical behavior of credit risk; and (iv) a decomposition holding leverage and fear fixed in turn (Section 4.6) isolates the two components of the fear-driven financing channel.

4.1 Firm Level Data

We require data on equity returns, leverage, and CDX prices for the structural estimation. Monthly return and leverage data are from CRSP-Compustat. We define the quarterly book value of debt as the sum of short- and long-term liabilities (DLCQ plus DLTTQ). Monthly leverage is defined as the most recent quarterly book value of debt divided by the sum of the book value of debt and the market value of equity.

We obtain daily data on credit default swaps for the period from September 2003 to June 2022 from ICE Data Services (formerly known as Credit Market Analysis Ltd. (CMA)). We focus on Markit's North American Investment Grade CDX Index, described in Section 3.4. It comprises 125 of the most liquid North American firms with investment-grade credit ratings that trade in the CDS market. The index composition is chosen twice annually at times known as roll dates. We match the sample of firms contained in the on-the-run contract with CRSP-Compustat name by name.

For the structural estimation, we target the pooled average and standard deviation of monthly excess returns and leverage for these matched firms. In addition, we target the mean and standard deviation of the 5-year CDX rate as well as the standard deviation of the equal-weighted portfolio return of matched firms. Empirical CDX moments are computed from monthly averages of daily spreads, matching the model's time-aggregation convention.

4.2 Predefined Parameters

Estimating all model parameters is computationally infeasible because the model must be solved numerically. Therefore, we focus the estimation on parameters for which the existing literature provides weak priors: parameters associated with firms' cash flow risk and bankruptcy costs. The other parameters are predefined based on values in the prior literature and summarized in Table 2.

As in Wachter (2013), we assume that the agent has unit elasticity of substitution. Wachter (2013) models large infrequent jumps using the distribution of consumption declines found by Barro and Ursua (2008). Large infrequent jumps produce extreme realizations of the

stochastic discount factor, allowing Wachter (2013) to generate a realistic equity premium with a risk aversion of only three. In contrast, we model smaller, more frequent jumps, which generate a realistic distribution of consumption growth, as shown in Anschukov, Bhamra, and Kuehn (2024). Smaller jumps produce less extreme SDF realizations, so we assume that the representative agent has a risk aversion of ten, as in Bansal and Yaron (2004). We choose the time discount rate β such that the perpetual risk-free yield is 1%. The correlation between consumption and earnings growth is set at 20%, as estimated by Bhamra, Kuehn, and Strebulaev (2010b).

We set the earnings drift μ_x so that the observed net earnings growth rate equals the net consumption growth rate, i.e.

$$\mu_x = \mu_c - (f_H\lambda_H + f_L\lambda_L)J_c + (f_H\lambda_H + f_L\lambda_L)J_x.$$

In the model, firms issue debt at the initial date of formation. Firms also face exogenous exit and are replaced by firms which choose their leverage afresh. Hence, in panel simulations of the model, average leverage is stationary over time. We set the exogenous exit rate such that the true net earnings growth rate equals zero, which implies that

$$\lambda_x = \mu_c - (f_H\lambda_H + f_L\lambda_L)J_c.$$

We set debt issuance costs to $\iota = 1\%$, based on empirical evidence in Altinkilic and Hansen (2000) for large firms. Graham (2013) shows in his equation (5) that the value of a firm with perpetual debt can be written as

$$F_{\text{with debt}} = F_{\text{no debt}} + \left[1 - \frac{(1-\tau_c)(1-\tau_e)}{(1-\tau_p)}\right] D,$$

where τ_c denotes the corporate tax rate, τ_e the equity payout tax rate, and τ_p the personal tax rate. The term in square brackets captures the tax advantage of debt. Based on estimates from Kuehn, Schreindorfer, and Schulz (2023), who find that $\tau_c = 0.329$, $\tau_e = 0.112$, and $\tau_p = 0.296$, we set $\eta = 1 - \frac{(1-\tau_c)(1-\tau_e)}{(1-\tau_p)} = 0.154$.

4.3 Structural Estimation

Four firm-level parameters remain to be estimated: the amount of idiosyncratic Gaussian risk σ_x^{id}, systematic Gaussian risk σ_x^{sys}, bankruptcy costs $1-\alpha$, and the jump-scaling parameter φ. Following Hennessy and Whited (2007) and Bazdresch, Kahn, and Whited (2018), we do so by the simulated method of moments (SMM) using seven moments: the averages of firm-level

excess returns, leverage, and the 5-year CDX rate, and the standard deviations of firm-level excess returns, market excess returns, leverage, and the 5-year CDX rate. The continuous-time model is simulated at daily frequency and time-aggregated to monthly frequency.

Given the predefined parameters summarized in Table 2, and vector $\theta = (\sigma_x^{\text{id}}, \sigma_x^{\text{sys}}, 1-\alpha, \varphi)^\top \in \mathbb{R}^4$, we solve the model numerically and simulate panels of firms. The SMM objective function is a weighted metric between seven model moments from simulated panels $\Psi^M(\theta) \in \mathbb{R}^7$ and the corresponding seven moments from actual data $\Psi^D \in \mathbb{R}^7$, defined by the quadratic form $[\Psi^D - \Psi^M(\theta)]^\top \mathbf{W} [\Psi^D - \Psi^M(\theta)]$, where $\mathbf{W} \in \mathbb{R}^{7\times 7}$ is the seven by seven weighting matrix. Following Bloom, Floetotto, Jaimovich, Saporta-Eksten, and Terry (2018), we set the diagonal elements of $\mathbf{W}$ to be $(1/\Psi^D)^2$ (where division and exponentiation are performed element-by-element) and the off-diagonal elements to zero. Intuitively, with this weighting matrix, the SMM estimator minimizes the sum of squared percentage deviations of model moments from the corresponding data moments. The parameter estimate $\hat{\theta}$ is found by searching globally over the parameter space, which we implement via a particle swarm algorithm.[17]

A noteworthy feature of our 2003 to 2022 sample period is that it contains the Great Recession and the COVID-19 recession. While annual consumption dropped by only 1.6% during the Great Recession, it dropped by 5.1% in 2020. This value is small relative to the consumption drop in a typical disaster, so estimating the model based on the ergodic distribution is inappropriate. Instead, we base the estimation on simulated data that mimics the macroeconomic risk in our sample. Specifically, we simulate 1,000 daily panels of 125 firms over 29 years, with the first 10 years serving as a burn-in period. We then time aggregate daily consumption to annual frequency and ensure that each panel's worst annual consumption drop does not exceed 5.1%, as in the data. Hence, the consumption growth distribution is consistent with the moments of the post-war sample, as reported in Table 1.

[17] The variance-covariance matrix of the SMM parameter estimate is given by

$$\text{Cov}(\hat{\theta}) = (1 + 1/h)(\mathbf{AD})^{-1}\mathbf{AVA}^\top((\mathbf{AD})^{-1})^\top,$$

where $\mathbf{A} = \mathbf{D}^\top\mathbf{W}$, $\mathbf{W}$ is the weighting matrix used in the estimation, $\mathbf{D}$ the Jacobian matrix, $\mathbf{V}$ the variance-covariance matrix of the sample data, which we estimate via block bootstrap with replacement on the actual data, and $(1+1/h)$ accounts for the sample variation of simulations ($h = 1,000$ panels). The $(ij)^{th}$ element of the Jacobian matrix $\mathbf{D}$ contains the derivative of model moment i with respect to parameter j, $D_{ij} = \frac{\partial \Psi_i^M}{\partial \theta_j}$, which we compute via central finite differences,

$$D_{ij} = \frac{\Psi_i^M(\theta \odot (1 + e_j\epsilon)) - \Psi_i^M(\theta \odot (1 - e_j\epsilon))}{2\theta_j\epsilon},$$

where $\odot$ denotes element-by-element multiplication, e_j is a column vector with 1 in position j and 0 elsewhere, and $\epsilon = 0.03$.

Before explaining the estimation results, we discuss the identification strategy. In Table 3, we report the sensitivity of model-implied moments (in rows) with respect to model parameters (in columns). The sensitivity of moment i with respect to parameter j equals $\frac{\partial \Psi_i^M}{\partial \theta_j} \frac{\theta_j}{\Psi_i^M}$ and is evaluated at the vector of point estimates from Table 4.

Idiosyncratic risk greatly impacts the first two moments of the 5-year CDX rate level and the standard deviation of firm-level returns. The impact of aggregate Brownian risk on the moments is small but helps identify the quantity of aggregate market risk. Jump risk in earnings is well identified because it impacts the first two moments of the CDX rate. As jump risk increases, more firms default, leading to a higher cost of credit risk insurance. Bankruptcy costs significantly negatively impact leverage, as firms optimally delever when they face higher costs of financial distress.

Table 4 summarizes the estimation. Overall, the model fits the data very well. The model generates an annualized average risk premium of 9.5%, compared with 10.8% in the data. While monthly firm-level returns are very volatile at 9.8% relative to 9.2% in the data, market excess returns are slightly less dispersed at 4.2% relative to 5.1% in the data. The model generates these moments with $\sigma_x^{\text{id}} = 18.1\%$ (idiosyncratic risk) and $\sigma_x^{\text{sys}} = 5.2\%$ (aggregate risk).

The model generates realistic leverage moments: a mean of 27.4% relative to 28.9% in the data, and a standard deviation of 15.3% relative to 15.9% in the data. Given tax shields, the key parameter for identifying leverage is bankruptcy costs. Our estimation implies bankruptcy losses of 34.3%, close to the empirical estimates in Glover (2016) and in Davydenko, Strebulaev, and Zhao (2012) for investment-grade firms. As shown in Chen (2010), time-varying bankruptcy costs alleviate the so-called low-leverage puzzle: the typical investment-grade firm appears to be under-levered, given the large tax shields and small default probability. With time-varying bankruptcy costs, firms are reluctant to take on leverage, not because of high average deadweight losses from default, but because the losses are particularly high in states where defaults are more likely and losses more painful. Although the jump intensity is driven by a Markov switching process in our framework, we cannot tie bankruptcy costs to the Markov state because it is not observable to agents. Instead, the fear-driven financing channel provides an alternative resolution: firms internalize that rising fear will raise default boundaries and amplify credit risk, deterring them from taking on more debt at entry even with constant bankruptcy costs.

Lastly, the model generates a realistic 5-year CDX rate for investment-grade firms of 72

basis points, relative to 77 basis points in the data. Five-year CDX rates are also volatile at 38 basis points relative to 34 basis points in the data. The jump-scaling parameter φ is crucial for matching credit market moments. Our estimation implies that earnings jumps are 3.3 times higher than consumption jumps. This estimate is in line with data for the Great Depression, where earnings losses were 3.8 times higher than consumption losses.[18]

Statistically, the model is rejected at the 5% level with a p-value of the J-statistic of 2.9%, even though the economic fit is excellent. This rejection reflects residual tension among the targeted moments, compounded by the weak identification of systematic Brownian risk, rather than a systematic failure of the pricing mechanism. Interestingly, the point estimate for systematic Brownian shocks is not statistically significant. Our model features two sources of aggregate risk: systematic Brownian shocks, which are correlated with consumption, and Poisson jumps. While earnings losses are larger than consumption losses during crises, firm-level earnings and consumption jump simultaneously, thereby generating aggregate risk. Empirically, we find that common jump risk is more important for pricing credit instruments than common Brownian shocks.

The composition of risk between idiosyncratic and aggregate significantly impacts credit risk, as shown by Chen, Collin-Dufresne, and Goldstein (2009). Intuitively, if most risks were aggregate, many firms would default simultaneously, driving up credit risk. Yet, in the data, the firm-level Sharpe ratio is much smaller than the aggregate Sharpe ratio because individual firms are more volatile than the market. Importantly, our framework can match this fact because our estimation targets the composition of idiosyncratic versus aggregate risk.

4.4 Term Structure of CDX

In this section, we explore the pricing of the entire term structure of CDX contracts ranging from 1 to 10 years. One can view this exercise as an out-of-sample validation of the fear-driven financing channel, because we fit the model only to the first and second moments of the 5-year CDX contract, which tends to be the most liquid.

Figure 6 depicts the term structure of CDX rates in the left panel and the term structure of physical and risk-neutral default probabilities in the right panel. CDX spreads are annualized and reported in basis points per unit of notional for contracts with fixed maturities of 1 to 10 years. Empirical averages are computed from daily data on Markit's North American

[18] According to Shiller's stock market data, aggregate real earnings dropped by 62.4% whereas consumption fell by 16.6%.

Investment Grade CDX Index obtained from ICE Data Services for the period from September 2003 to June 2022. Default probabilities are reported in percent for horizons ranging from 1 to 10 years. Empirical default probabilities are the average cumulative issuer-weighted global default rates reported by Moody's over the period 1920 – 2017 for entities categorized as investment-grade (letter rating of Baa3 or better), the standard long-run benchmark for investment-grade default risk in the structural credit literature (e.g., Chen, 2010; Bhamra, Kuehn, and Strebulaev, 2010b). We report corresponding numerical values in Table 5.

We only target the first and second moments of the 5-year CDX contract. Yet our model matches the entire term structure of CDX rates well. In particular, the model generates realistic short-term CDX rates, an average 1-year (3-year) CDX rate of 21 (46) basis points relative to 22 (51) basis points in the data, as well as realistic long-term rates, an average 8-year (10-year) CDX rate of 113 (138) basis points relative to 105 (113) basis points in the data. In contrast, other consumption-based models, such as Bhamra, Kuehn, and Strebulaev (2010b), Chen (2010), and Kuehn, Schreindorfer, and Schulz (2023), can only explain a single point of the term structure.

A resolution of the credit spread puzzle requires a model to match three facts: low leverage, large credit spreads, and low physical default probabilities. Intuitively, market participants demand significant compensation for holding credit instruments, although corporate defaults are rare. As shown above, our framework generates realistic leverage and large credit spreads. Figure 6 and Table 5 report the term structure of physical default probabilities, which were not targets of the structural estimation. Nevertheless, our model matches the data very well. At the short end of the term structure, the model implies 1-year (3-year) average physical default probabilities of 0.18% (0.71%) relative to 0.14% (0.72%) in the data, and at the long end, 8-year (10-year) average physical default probabilities of 2.67% (3.71%) relative to 2.70% (3.56%) in the data.

Although physical default probabilities are low, risk-neutral default probabilities are substantially higher, thereby increasing credit spreads. At the short end, risk-neutral default probabilities are 0.31%, 1.7 times greater than the corresponding physical ones, and at the long end, risk-neutral default probabilities are 17.1%, 4.6 times greater than the corresponding physical ones. Intuitively, over a 1-year horizon, it is unlikely that the economy enters the high-jump risk state, but this risk increases over longer horizons, giving the fear-driven financing channel a greater chance to operate. As a result, credit risk compensation increases with maturity.

4.5 Time Series Implications

In this section, we evaluate the time-series fit of our model. We conduct our analysis for the sample period from September 2003 to June 2022. Specifically, we examine how well the model accounts for the 5-year CDX rate, the CDX slope (10-year minus 5-year), and CDX rate volatility.

This exercise tests the model's CDX pricing surface, the mapping $S_{\text{CDX},m}(\bar{L}_t, p_t)$ from state variables (average cross-sectional leverage and beliefs) to spreads, against realized CDX dynamics. The fear-driven financing channel operates across this surface, as increases in fear drive up leverage. To generate model-implied time series, we therefore feed the model with the empirical time series for average cross-sectional leverage and the subjective beliefs of being in the high-risk state (fear).

The time series for average cross-sectional leverage is directly observable for the firms included in the on-the-run CDX index after September 2003. In contrast, the subjective belief p_t is latent. In the model, the representative agent updates her belief using aggregate consumption as a signal: her fear jumps upward whenever she observes a downward jump in consumption (a realization of N_t), and the jump size equals her belief uncertainty. Unfortunately, the BEA only began releasing high-frequency consumption data in March 2020, and the onset of the COVID-19 pandemic introduced a pronounced structural break. Because these data are unavailable for most of our sample, we cannot use consumption to construct a belief series consistent with the model's information structure.

We therefore construct an empirical proxy for the subjective belief or fear time series that remains grounded in the model's structure. In the model, a negative consumption jump must generate at least a 3% decline in equity valuations. Motivated by this implication, we treat days on which the average ex-dividend CRSP return falls below -5% — a conservative threshold that reduces false positives from continuous volatility — as observable counterparts of the jump process N_t. This choice is consistent with existing work that exploits large negative market moves as signals of tail risk in reduced-form disaster-risk models (e.g., van Binsbergen, Hua, and Wachter (2023)).

Using these indicator events, we generate a belief process that mirrors the model's updating mechanism. The resulting time series is shown in the third panel of Figure 7. Large downward equity moves of this magnitude occur primarily during recessions, consistent with

the interpretation that these episodes deliver sharp information about economic crisis risk.[19] Their tendency to arrive in rapid succession – several within weeks during the Great Recession and COVID-19 – is the empirical signature of the high-intensity regime, which subsequently triggers and is amplified by self-reinforcing fear.

In Figure 7, we display the model inputs on the left-hand side: the average cross-sectional leverage time series and the subjective belief or fear time series. On the right-hand side are the model-based and empirical[20] 5-year CDX rate and CDX slope (10-year minus 5-year CDX rates). The grey bars represent NBER recessions. Overall, the model replicates very well the cyclical variation of the 5-year CDX rate across the entire sample. The cyclical variation of the CDX slope is also replicated well, with the only notable discrepancy occurring during the COVID-19 period. The fear-driven financing channel, fed with observable leverage and a belief proxy, thus accounts for the cyclical dynamics of credit markets across two decades.

The model's difficulty in matching the CDX slope during the COVID-19 episode likely reflects the extraordinary speed and scale of the policy response, which our consumption-based framework does not incorporate. The Federal Reserve announced unlimited asset purchases on March 23, 2020, and established the Secondary Market Corporate Credit Facility shortly thereafter, directly purchasing investment-grade corporate bonds and bond ETFs for the first time in its history. These interventions disproportionately compressed long-maturity credit spreads: the announcement alone narrowed the 10-year CDX rate by more than the 5-year rate, flattening the term structure in a manner that has no counterpart in our model. Because the representative agent in our framework prices credit risk solely through beliefs about crisis intensity and endogenous leverage – without a role for central bank backstops or liquidity provision – the model cannot generate the asymmetric compression of long-end spreads that characterized the post-March 2020 recovery.

Figure 8 confirms that the model closely replicates the time-varying volatility of CDX rates. We compare model-based and empirical 5-year CDX volatility using two approaches: monthly realized volatility computed from daily data (left panel) and a daily exponentially weighted moving-average estimate with a 5% decay rate, initialized over the first 60 trading days (right panel). Both measures tell the same story. The model captures the sharp volatility spikes during the Great Recession and the COVID-19 crisis, as well as the prolonged periods of low volatility that characterize tranquil markets. Importantly, the model generates this

[19] See van Binsbergen, Hua, and Wachter (2023) for a similar construction using international data.

[20] The CDX data represents Markit's North American Investment Grade CDX Index, for which Series 1 started trading in September 2003.

time variation through the fear-driven financing channel – volatility rises when belief updates and leverage adjustments reinforce each other, and subsides as beliefs decay toward their lower bound and leverage stabilizes. The close match across two distinct volatility estimators suggests that the fear-driven financing channel is not only qualitatively correct but also quantitatively disciplined.

4.6 Decomposing the Fear-Driven Financing Channel

Having established that the model matches both unconditional moments and the time-series dynamics of CDX data, we now decompose the drivers of credit index prices to understand the fear-driven financing cycle in detail. Table 6 reports 1-year, 5-year, and 10-year CDX rates as a function of the belief and average leverage, allowing us to separate the contribution of fear from that of leverage and thus decompose how the fear-driven financing cycle operates across maturities.

Standard CDX pricing models typically treat leverage as exogenous – there is no fear-driven financing channel. In contrast, Table 6 shows that when default and leverage are endogenous, firms optimally adjust their capital structure in response to belief shocks, creating the fear-driven financing channel. The table maps the pricing surface $S_{\text{CDX},m}(\bar{L}_t, p_t)$; the model's dynamics are trajectories across this surface as fear and leverage co-evolve. This channel amplifies and prolongs the impact of fear on CDX rates. We use Table 6 to highlight four facts that discipline the mechanism in the model: (i) endogenous leverage dominates time-varying beliefs with fixed leverage as the driver of time variation in CDX rates, (ii) short-maturity CDX rates load more heavily on beliefs than long-maturity rates, (iii) belief uncertainty generates a hump-shaped, non-monotone response of CDX rates to fear, and (iv) leverage steepens the term structure while beliefs shift its level.

Leverage versus Beliefs The central quantitative message of Table 6 is that CDX rates are more sensitive to leverage than to beliefs. Moving leverage from 25% to 45% increases the 5-year CDX rate from 54 bps to 188 bps, holding beliefs fixed, while moving beliefs from $p = 0.1$ to $p = 1$ at that higher leverage increases the CDX rate further from 188 bps to 211 bps. In other words, beliefs matter, but the bulk of the time variation in CDX is transmitted through endogenous leverage adjustments.

Table 6 isolates the two channels within the estimated model. Varying beliefs with leverage held constant measures the direct effect of fear on risk-neutral default intensities; varying

leverage with beliefs held constant measures the sensitivity of spreads to leverage. The latter dominates by approximately six to one, which is precisely why the fear-driven financing channel – the indirect transmission of fear through changes in endogenous leverage – governs time variation in CDX rates.

Short-Maturity CDX Changes in fear directly shift the representative agent's stochastic discount factor and therefore the risk prices embedded in risk-neutral default intensities, even when leverage is held fixed. Table 6 shows that the proportional impact of fear is strongest at the short end. With leverage of 30%, moving from $p = 0.1$ to $p = 1$ raises the 1-year CDX rate from 19 to 23 bps, a 21% increase, while the 10-year CDX rate rises from 151 to 161 bps, a 7% increase. Thus, in proportional terms, belief shocks affect near-term CDX rates more than far-term rates due to mean reversion, because long-maturity contracts discount the belief state more heavily than short-maturity contracts.

Learning about crises is therefore important for matching the level of CDX rates, especially at short maturities, where the fear-driven financing channel has less chance to act. Fear-driven leverage dynamics drive time-series movements.

Belief Uncertainty Beliefs also affect prices through belief uncertainty. Table 6 shows that CDX rates are hump-shaped in beliefs, because learning is most uncertain away from the extremes, and this uncertainty changes risk prices even if the belief level itself rises. This mechanism is consistent with the learning-based amplification emphasized in Wachter and Zhu (2025), and with the surprise nature of crises documented in Krishnamurthy and Muir (2020).

Term Structure Table 6 also sharpens the term structure predictions. Increasing leverage steepens the CDX term structure. At $p = 0.1$, when leverage increases from 25% to 45%, the 10-year minus 5-year slope rises from 56 to 121 basis points.

In contrast, increasing p has only a modest effect on the slope and primarily shifts the level. At low leverage of 25%, the slope is essentially unchanged; it is 56 basis points at both $p = 0.1$ and $p = 1$. At high leverage of 45%, the slope changes only slightly, from 121 basis points at $p = 0.1$ to 126 basis points at $p = 1$. The interpretation is that because mean reversion dampens the long-end response to belief shocks, the absolute steepening of the term structure from beliefs alone is limited relative to the steepening generated by higher leverage.

The Fear-Driven Financing Channel Table 6 highlights the quantitative components of the fear-driven financing channel. Higher fear shifts the optimal default boundary upward, depressing equity values relative to debt and thereby raising both leverage and CDX rates. Because fear is self-reinforcing, each successive crisis amplifies this sequence: fear compounds, leverage rises further, and CDX rates widen. Unlike standard structural credit models with exogenous default boundaries, our default boundary is itself a function of beliefs and corporate choices. Fear, therefore, becomes an economic primitive for firm behavior, not just for risk pricing. This mechanism is distinct from intermediary-based amplification in models such as He and Krishnamurthy (2013) because firms amplify crises through endogenous adjustments to their own corporate policies.

In sum, Table 6 provides a disciplined decomposition of what moves CDX rates. Learning about crises helps in matching levels, especially at the short end, where belief shocks matter and generate hump-shaped responses through belief uncertainty. However, the dominant source of time variation, and the primary driver of term structure steepening, is endogenous leverage from the fear-driven financing channel. This dominance reflects the self-reinforcing nature of fear: during stress, each crisis compounds fear, fear compounds leverage, and leverage compounds CDX rates. At short maturities, there is less time for crises to cluster and for this cascade to operate, so the direct effect of fear on risk prices is relatively more important.

5 Conclusion

We document a new empirical fact: CDX spreads and corporate leverage comove strongly, and this comovement intensifies during crises. Existing CDX pricing models do not account for this pattern because they treat default intensities and capital structure as exogenous.

We develop and estimate a CDX pricing model in which firms optimally choose default boundaries and capital structure while an Epstein–Zin representative investor forms subjective beliefs about the stochastic arrival rate of sharp downward movements in consumption. We refer to these beliefs as the investor's *fear*. When fear rises, optimal default boundaries shift upward and equity values decline, increasing leverage and elevating CDX spreads. Leverage remains elevated long after fear subsides because crises lower earnings while coupons remain fixed, and capital structure adjusts only through firm turnover. This fear-driven financing channel is the model's central economic mechanism and distinguishes it from frameworks in which leverage is exogenous and CDX spread variation is driven entirely through the stochastic

discount factor and exogenous financing rules. A distinctive feature of the model is that Bayesian learning makes the agent's perceived crisis intensity self-exciting: each crisis raises the expectation of the next. Self-reinforcing fear makes the fear-driven financing channel dormant during calm periods and self-activating during stress, generating the crisis-dependent intensification of CDX–leverage comovement documented in Figure 1.

Structurally estimating four firm-level parameters on data from CDX constituents over 2003 to 2022, the model jointly matches the unconditional moments of the 5-year CDX rate, equity returns, and leverage. Despite targeting only the 5-year CDX rate, the model replicates the full 1-to-10-year term structure of CDX rates and physical default probabilities out of sample, a result not achieved by prior consumption-based credit risk models. When fed with observable leverage and a belief proxy constructed from large negative equity market returns, the model also reproduces the time-series dynamics of the 5-year CDX rate, the CDX slope, and CDX volatility across two decades, including the prolonged elevation during the Great Recession and the sharp spike during COVID-19. The only notable discrepancy arises in the CDX slope following March 2020, when unprecedented Federal Reserve interventions compressed long-maturity spreads through channels outside the model.

A decomposition of CDX rates by leverage and beliefs sharpens the economic interpretation. Endogenous leverage is the dominant source of time variation in CDX rates, while subjective beliefs primarily govern the level of CDX rates. The belief effect is most pronounced at short maturities, where the premium for near-term disaster risk is largest. Beliefs also generate a hump-shaped CDX response because belief uncertainty peaks at intermediate belief levels, consistent with the surprise nature of crises. Leverage steepens the term structure, while beliefs shift its level.

There are several directions for future research. Extending the framework to incorporate active monetary and fiscal policy responses, particularly the types of credit market interventions observed during COVID-19, may help explain the behavior of the term structure during episodes of aggressive policy action. Allowing for time-varying bankruptcy costs tied to observable aspects of macroeconomic conditions (Chen, 2010; Bhamra, Kuehn, and Strebulaev, 2010a,b), or considering CDX tranches, which load more heavily on the tail of the loss distribution, would further test the model's ability to capture the cross-section of credit risk. More broadly, the interaction between learning dynamics and corporate financing decisions documented here may provide a useful framework for understanding how subjective beliefs propagate through firm balance sheets to affect credit supply and the real economy.

References

Ai, Hengjie, 2010, Information quality and long-run risk: Asset pricing implications, *Journal of Finance* 65, 1333–1367.

Altinkilic, Oya, and Robert S. Hansen, 2000, Are there economies of scale in underwriting fees? evidence of rising external financing costs, *Review of Financial Studies* 1, 191–218.

Anschukov, Artur, Harjoat S Bhamra, and Lars-Alexander Kuehn, 2024, Leverage dynamics and learning about economic crises, Unpublished working paper.

Bansal, Ravi, and Amir Yaron, 2004, Risks for the long run: A potential resolution of asset pricing puzzles, *Journal of Finance* 59, 1481–1509.

Barro, Robert J., 2006, Rare disasters and asset markets in the twentieth century, *Quarterly Journal of Economics* 121, 823–866.

Barro, Robert J, and Jose F Ursua, 2008, Consumption disasters in the twentieth century, *American Economic Review* 98, 58–63.

Barro, Robert J., and Jose F. Ursua, 2012, Rare macroeconomic disasters, *Annual Review of Economics* 4, 83–109.

Bazdresch, Santiago, R. Jay Kahn, and Toni M. Whited, 2018, Estimating and testing dynamic corporate finance models, *Review of Financial Studies* 31, 322–361.

Benzoni, Luca, Pierre Collin-Dufresne, and Robert S. Goldstein, 2011, Explaining asset pricing puzzles associated with the 1987 market crash, *Journal of Financial Economics* 101, 552–573.

Bhamra, Harjoat S, Lars-Alexander Kuehn, and Ilya A Strebulaev, 2010a, The aggregate dynamics of capital structure and macroeconomic risk, *Review of Financial Studies* 23, 4187–4241.

Bhamra, Harjoat S., Lars-Alexander Kuehn, and Ilya A. Strebulaev, 2010b, The levered equity risk premium and credit spreads: A unified framework, *Review of Financial Studies* 23, 645–703.

Bloom, Nicholas, Max Floetotto, Nir Jaimovich, Itay Saporta-Eksten, and Stephen J. Terry, 2018, Really uncertain business cycles, *Econometrica* 86, 1031–1065.

Branger, Nicole, Holger Kraft, and Christoph Meinerding, 2015, The dynamics of crises and the equity premium, *Review of Financial Studies* 29, 232–270.

Brémaud, Pierre, 1981, *Point Processes and Queues: Martingale Dynamics* (Springer-Verlag: New York).

Chen, Hui, 2010, Macroeconomic conditions and the puzzles of credit spreads and capital structure, *Journal of Finance* 65, 2171–2212.

Chen, Long, Pierre Collin-Dufresne, and Robert S. Goldstein, 2009, On the relation between the credit spread puzzle and the equity premium puzzle, *Review of Financial Studies* 22, 3367–3409.

Collin-Dufresne, Pierre, Robert Goldstein, and J. Spencer Martin, 2001, The determinants of credit spread changes, *Journal of Finance* 56, 2177–2207.

Collin-Dufresne, Pierre, and Robert S. Goldstein, 2001, Do credit spreads reflect stationary leverage ratios?, *Journal of Finance* 56, 1929–1957.

——— , and Fan Yang, 2012, On the relative pricing of long-maturity index options and collateralized debt obligations, *Journal of Finance* 67, 1983–2014.

Collin-Dufresne, Pierre, Michael Johannes, and Lars A Lochstoer, 2016, Parameter learning in general equilibrium: The asset pricing implications, *American Economic Review* 106, 664–698.

Collin-Dufresne, Pierre, Benjamin Junge, and Anders B. Trolle, 2024, How integrated are credit and equity markets? evidence from index options, *Journal of Finance* 79, 949–992.

Constantinides, George M., 2008, Macroeconomic crises since 1870: Comments and discussion., *Brookings Papers on Economic Activity* pp. 341–349.

Culp, Christopher L., Yoshio Nozawa, and Pietro Veronesi, 2018, Option-based credit spreads, *American Economic Review* 108, 454–488.

David, Alexander, 1997, Fluctuating confidence in stock markets: Implications for returns and volatility, *Journal of Financial and Quantitative Analysis* 32, 427–462.

Davydenko, Sergei, Ilya A. Strebulaev, and Xiaofei Zhao, 2012, A market-based study of the costs of default, *Review of Financial Studies* 25, 2959–2999.

Doshi, Hitesh, Jan Ericsson, Mathieu Fournier, and Sang Byung Seo, 2024, The risk and return of equity and credit index options, *Journal of Financial Economics* 161, 103932.

Duffie, Darrell, and Larry Epstein, 1992, Stochastic differential utility, *Econometrica* 60, 353–394.

Duffie, Darrell, and Costis Skiadas, 1994, Continuous-time security pricing: A utility gradient approach, *Journal of Mathematical Economics* 23, 107–131.

Epstein, Larry, and Stanley Zin, 1989, Substitution, risk aversion, and the temporal behavior of consumption and asset returns: A theoretical framework, *Econometrica* 57, 937–969.

Ghaderi, Mohammad, Mete Kilic, and Sang Byung Seo, 2022, Learning, slowly unfolding disasters, and asset prices, *Journal of Financial Economics* 143, 527–549.

Giesecke, Kay, Francis A. Longstaff, Stephen Schaefer, and Ilya Strebulaev, 2011, Corporate bond default risk: A 150-year perspective, *Journal of Financial Economics* 102, 233–250.

Glover, Brent, 2016, The expected cost of default, *Journal of Financial Economics* 119, 284–299.

Goldstein, Robert S., Nengjiu Ju, and Hayne E. Leland, 2001, An ebit-based model of dynamic capital structure, *Journal of Business* 74, 483–512.

Gomes, Joao F., and Lukas Schmid, 2021, Equilibrium credit spreads and the macroeconomy, *Journal of Finance* 76, 977–1018.

Graham, John R, 2013, Do taxes affect corporate decisions? a review, *Handbook of the Economics of Finance* 2, 123–210.

Grushka, Eli, 1972, Characterization of exponentially modified Gaussian peaks in chromatography, *Analytical Chemistry* 44, 1733–1738.

Hackbarth, Dirk, Jianjun Miao, and Erwan Morellec, 2006, Capital structure, credit risk, and macroeconomic conditions, *Journal of Financial Economics* 82, 519–550.

Hawkes, Alan G., 1971, Spectra of some self-exciting and mutually exciting point processes, *Biometrika* 58, 83–90.

He, Zhiguo, and Arvind Krishnamurthy, 2013, Intermediary asset pricing, *American Economic Review* 103, 732–770.

Hennessy, Christopher A., and Toni M. Whited, 2007, How costly is external financing? evidence from a structural estimation, *Journal of Finance* 62, 1705–1745.

Julliard, Christian, and Anisha Ghosh, 2012, Can rare events explain the equity premium puzzle?, *Review of Financial Studies* 25, 3037–3076.

Kalambet, Yuri, Yuri Kozmin, Ksenia Mikhailova, Igor Nagaev, and Pavel Tikhonov, 2011, Reconstruction of chromatographic peaks using the exponentially modified Gaussian function, *Journal of Chemometrics* 25, 352–356.

Kraft, Holger, and Frank Thomas Seifried, 2010, Foundations of continuous-time recursive utility: Differentiability and normalization of certainty equivalents, *Mathematics and Financial Economics* 3, 115–138.

Krishnamurthy, Arvind, and Tyler Muir, 2020, How credit cycles across a financial crisis, Unpublished working paper.

Kuehn, Lars-Alexander, David Schreindorfer, and Florian Schulz, 2023, Persistent crises and levered asset prices, *Review of Financial Studies* 36, 2571–2616.

Leland, Hayne E., 1994, Corporate debt value, bond covenants, and optimal capital structure, *Journal of Finance* 49, 1213–52.

Liptser, Robert S, and Albert N Shiryaev, 2013, *Statistics of random processes II: Applications* . vol. 6 (Springer-Verlag).

Nakamura, Emi, Jon Steinsson, Robert Barro, and Jose Ursua, 2013, Crises and recoveries in an empirical model of consumption disasters, *American Economic Journal: Macroeconomics* 5, 35–74.

Ogata, Yosihiko, 1981, On lewis' simulation method for point processes, *IEEE transactions on information theory* 27, 23–31.

Øksendal, Bernt, 2003, *Stochastic Differential Equations* (Springer-Verlag).

Pham, Huyên, 1998, Optimal stopping of controlled jump diffusion processes: a viscosity solution approach, *J. Math. Syst. Estimat. Control* 8, 1.

Rietz, Thomas A., 1988, The equity risk premium: a solution, *Journal of Monetary Economics* 22, 117–131.

Schroder, Mark, and Costis Skiadas, 1999, Optimal consumption and portfolio selection with stochastic differential utility, *Journal of Economic Theory* 89, 68–126.

Seo, Sang Byung, and Jessica A. Wachter, 2018, Do rare events explain cdx tranche spreads?, *Journal of Finance* 73, 2343–2383.

Strebulaev, Ilya A., 2007, Do tests of capital structure theory mean what they say?, *Journal of Finance* 62, 1747–1787.

van Binsbergen, Jules, Sophia Hua, and Jessica A. Wachter, 2023, Is the united states a lucky survivor: A hierarchical bayesian approach, Journal of Finance, forthcoming.

Veronesi, Pietro, 1999, Stock market overreaction to bad news in good times: A rational expectations equilibrium model, *Review of Financial Studies* 12, 975–1007.

——— , 2000, How does information quality affect stock returns?, *Journal of Finance* 55, 807–837.

Wachter, Jessica A., 2013, Can time-varying risk of rare disasters explain aggregate stock market volatility?, *Journal of Finance* 68, 987–1035.

——— , and Yicheng Zhu, 2025, Learning with rare disasters, *Quantitative Economics*.

Weil, Philippe, 1990, Nonexpected utility in macroeconomics, *Quarterly Journal of Economics* 105, 29–42.

Wonham, W Murray, 1964, Some applications of stochastic differential equations to optimal nonlinear filtering, *Journal of the Society for Industrial and Applied Mathematics, Series A: Control* 2, 347–369.

Figure 2: Belief Uncertainty

This figure illustrates the agent's belief uncertainty $\sigma_p(p)$, representing the deterministic discontinuous change in the belief p realized upon observing an increment in the Poisson process N_t.

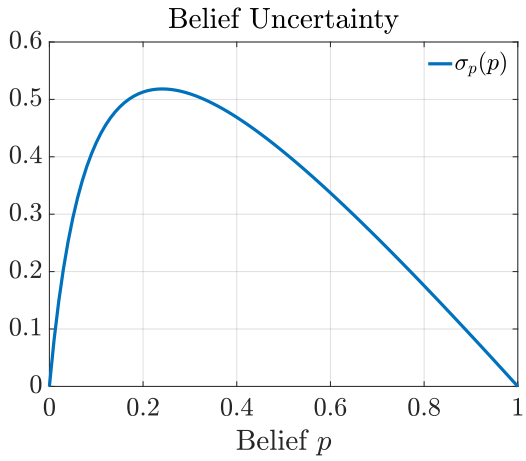

Figure 3: Subjective Beliefs, Fear and Learning Dynamics

This figure illustrates how the agent learns over time. It shows how a downward jump in consumption at time 0 can either lead to an increase or a decrease in belief uncertainty. In the first row, the belief level is low at the time of the observed consumption jump (first panel), and belief uncertainty increases as a result (second panel). In the second row, the belief level is high at the time of the observed consumption jump (third panel), and belief uncertainty decreases as a result (fourth panel).

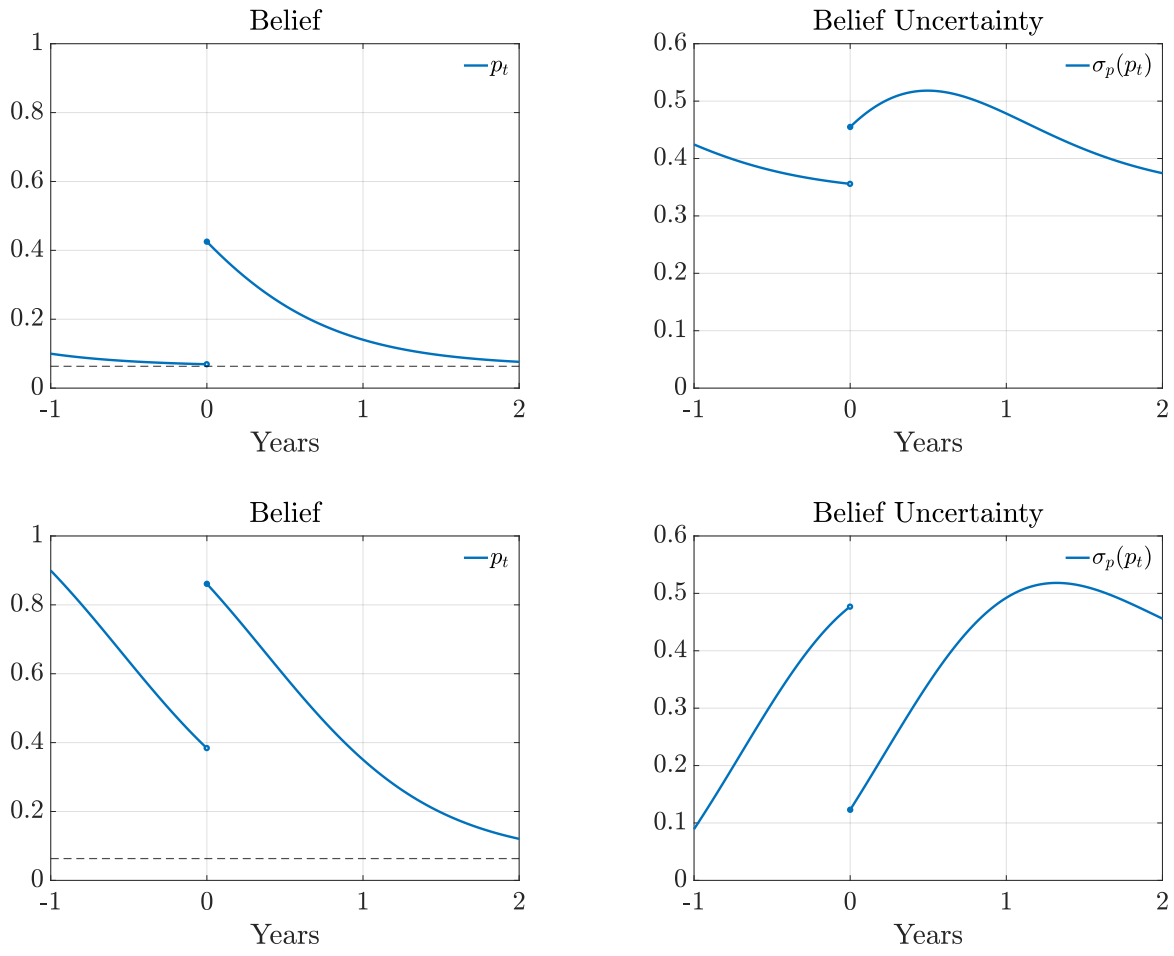

Figure 4: Optimal Corporate Policies

This figure shows the optimal default boundary $X_D(p)$ and the optimal coupon rate $c^*(p_0)$. The optimal default boundary shown corresponds to a firm that issued debt when its earnings were $X_0 = 1$ and the belief about the Markov state was $p_0 = p^*$. The optimal default boundary varies with the current belief p. The optimal coupon rate $c(p_0)$ is chosen when debt is issued and remains constant. The graph represents the firm-value-maximizing coupon rates for a firm that issues debt when its earnings were $X_0 = 1$ for different levels of initial beliefs p_0.

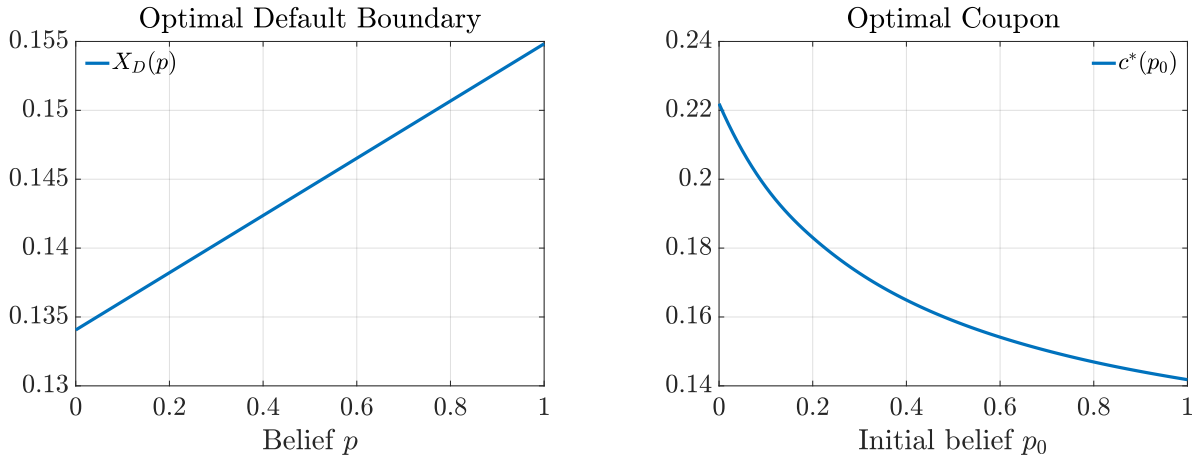

Figure 5: Dynamics of Corporate Default Policy

This figure illustrates the dynamics of the optimal corporate default policy. At time 0, a downward jump in consumption is observed and belief uncertainty drops, as in Figure 3. The first panel depicts the dynamics of the optimal default boundary $X_D(p_t)$, and the second panel depicts the distance to default $\ln(X_t/X_D(p_t))$, where initial earnings are normalized to one and then grow deterministically at rate μ_x unless there is a jump in earnings.

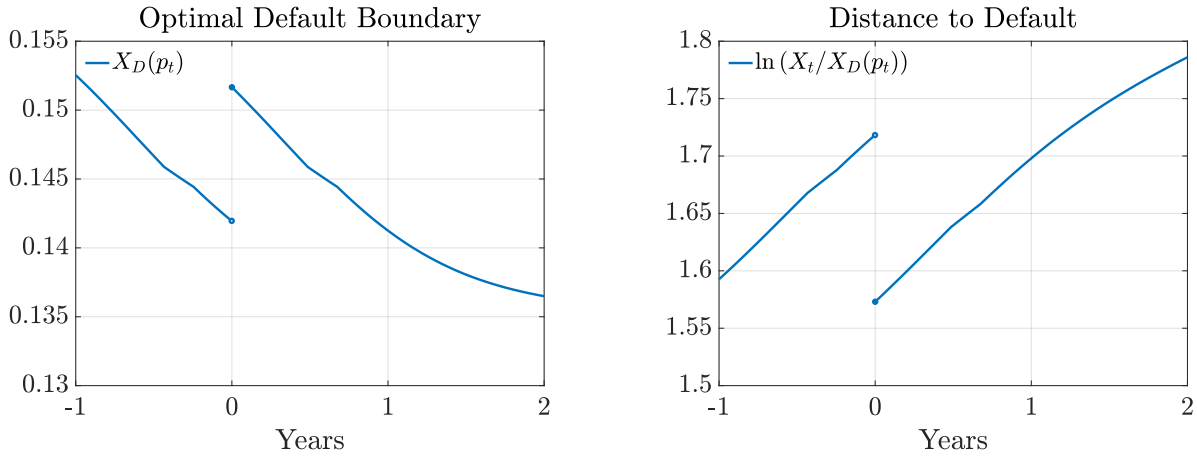

Figure 6: CDX Pricing

This figure depicts the term structure of CDX rates in the left panel and the term structure of physical and risk-neutral default probabilities in the right panel. CDX spreads are annualized and reported in basis points per unit of notional for contracts with a fixed maturity from 1 to 10 years. Empirical averages are computed from daily data on Markit's North American Investment Grade CDX Index for the period from September 2003 to June 2022. Default probabilities are reported in percent for horizons ranging from 1 to 10 years. Empirical default probabilities are the average cumulative issuer-weighted global default rates reported by Moody's spanning the period from 1920 to 2017 for entities categorized as investment grade (letter rating of Baa3 or better).

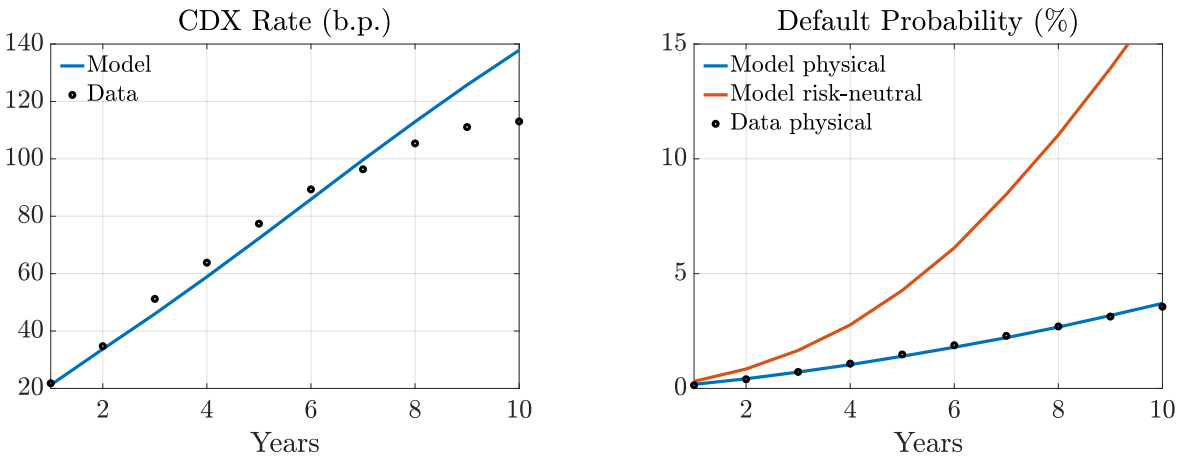

Figure 7: Time Series of CDX and Leverage

This figure displays average cross-sectional leverage (top left), the 5-year CDX rate (top right), the belief p (bottom left), and the 10-year minus 5-year CDX slope (bottom right) for September 2003 to June 2022. The CDX data represents Markit's North American Investment Grade CDX Index, for which Series 1 started trading in September 2003. The model-implied CDX series is based on observed leverage and a constructed belief proxy. To construct a proxy for the unobserved belief, we assume that days on which the average ex-dividend CRSP return is less than -5% are days on which increments in N_t are realized, which allows us to update the daily belief dynamics. The grey bars represent NBER recessions.

Figure 8: CDX Volatility

This figure shows the volatility of Markit's North American Investment Grade CDX Index, expressed in basis points. The left panel plots the monthly realized volatility based on daily data. The right panel shows the daily exponentially weighted moving-average model with a 5% decay rate and a 60-day window length.

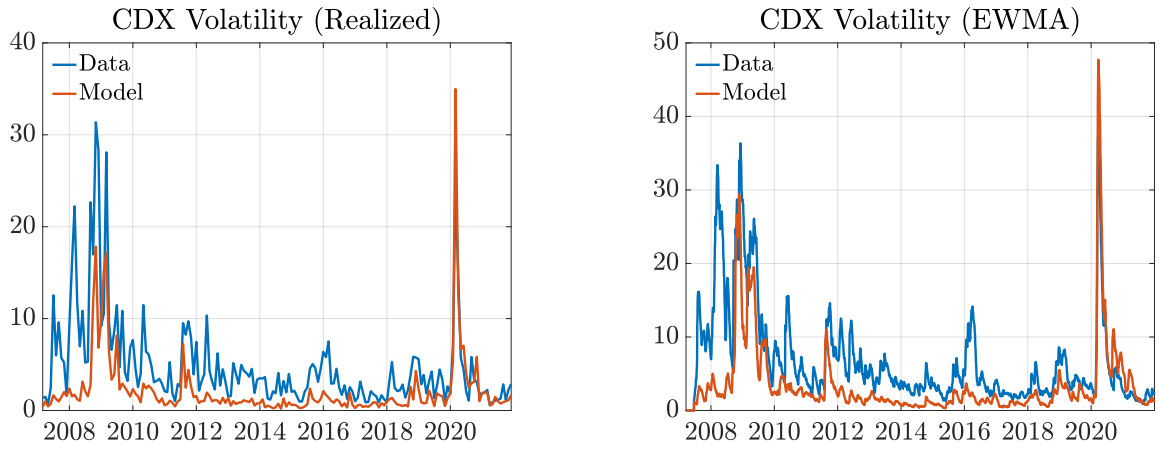

Table 1: Consumption Dynamics

This table summarizes the calibration of the consumption process. Panel A reports the seven parameters of the consumption process. These parameters are chosen so that annual consumption growth matches three moments from the long sample (Panel B), going back to 1929 and thus containing the Great Depression, and four moments from the calm post-war sample starting in 1947 (Panel C). Following Barro (2006), we define consumption disasters as consecutive negative annual consumption growth rates where the cumulative drop exceeds 10%. For the long sample, we simulate 10,000 daily consumption paths for 141 years—matching the average country-level sample length in Barro and Ursua (2012)—which we time aggregate to an annual frequency, and aim to match an average disaster size of 16.59% and an average disaster duration of 44 months, which are the respective values for the U.S. Great Depression. Since the long U.S. sample contains only one disaster, we take the likelihood of entering a disaster from Barro and Ursua (2012). In the post-war sample, the worst consumption drop occurred during the COVID-19 pandemic in 2020, when annual consumption growth fell by 5.11%. To mimic the post-war sample, we simulate 10,000 daily consumption paths for 74 years and only retain the consumption path when the worst cumulative annual consumption drop does not exceed 5.11%. For the post-war sample, we target the mean, standard deviation, skewness, and kurtosis of annual consumption growth.

Panel A: Parameters		
Consumption growth rate	μ_c	0.0240
Consumption growth volatility	σ_c	0.0113
Jump intensity state L	λ_L	0.1708
Jump intensity state H	λ_H	1.6960
Markov chain transition intensity from state L to H	ϕ_{LH}	0.1224
Markov chain transition intensity from state H to L	ϕ_{HL}	0.3816
Jump size	$1/\epsilon_c$	0.0247

Panel B: Long Sample		
	Data	Model
Mean disaster size	0.1659	0.1661
Mean disaster duration	3.6667	3.6567
Likelihood of disasters	0.0360	0.0360

Panel C: Post-War Sample		
	Data	Model
Mean consumption growth	0.0183	0.0183
Std. dev. of consumption growth	0.0154	0.0151
Skewness of consumption growth	-1.1000	-1.1017
Kurtosis of consumption growth	5.7480	4.9636

Table 2: Predefined Parameters

This table summarizes the predefined parameters, which are not estimated.

Parameter		Value
Time discount rate	β	0.0435
Risk aversion	γ	10
Elasticity of intertemporal substitution	ψ	1
Consumption-earnings correlation	ρ_{cx}	0.2
Earnings growth rate	μ_x	0.0511
Exogenous exit rate	λ_x	0.011
Corporate tax rate	η	0.154
Debt issuance costs	ι	0.01

Table 3: Sensitivity Matrix

This table shows the sensitivity of model-implied moments (in rows) with respect to model parameters (in columns). The sensitivity of moment i with respect to parameter j equals $\frac{\partial \Psi_i^M}{\partial \theta_j} \frac{\theta_j}{\Psi_i^M}$ and is evaluated at the vector of point estimates from Table 4.

	σ_x^{id}	σ_x^{sys}	$1-\alpha$	φ
Average excess return	0.31	-0.05	-0.39	1.13
Average leverage	0.75	-0.19	-1.04	0.11
Average 5-year CDX rate	1.87	-0.12	-1.26	2.04
Std. dev. of excess returns	1.30	-0.01	-0.61	0.36
Std. dev. of market excess returns	0.40	0.21	-0.38	0.79
Std. dev. of leverage	0.70	-0.02	-0.39	0.10
Std. dev. of 5-year CDX rate	1.27	-0.11	-1.55	2.64

Table 4: Structural Estimation

This table summarizes the structural estimation of model parameters. We estimate four model parameters, the amount of idiosyncratic Gaussian risk σ_x^{id}, systematic Gaussian risk σ_x^{sys}, bankruptcy costs $1-\alpha$, and the jump scaling parameter φ, with the simulated method of moments using seven moments, which are the average of firm-level excess returns, leverage, and 5-year CDX rate, and the standard deviation of firm-level and market excess returns, leverage, and 5-year CDX rate.

Panel A: Estimated Parameters		
Parameter		Value
Idiosyncratic risk	σ_x^{id}	0.1809
		(0.0073)
Systematic risk	σ_x^{sys}	0.0522
		(0.0437)
Bankruptcy costs	$1-\alpha$	0.3435
		(0.0841)
Jump scaling parameter	φ	3.2787
		(0.3282)

Panel B: Moments		
Moments	Data	Model
Average excess return	0.0090	0.0079
Average leverage	0.2894	0.2737
Average 5-year CDX rate	0.0077	0.0072
Std. dev. of excess returns	0.0917	0.0977
Std. dev. of market excess returns	0.0505	0.0418
Std. dev. of leverage	0.1589	0.1533
Std. dev. of 5-year CDX rate	0.0034	0.0038

Table 5: CDX Moments

This table summarizes the term structure of CDX rates, physical and risk-neutral default probabilities ranging from 1 to 10 years. CDX spreads are annualized and reported per unit of notional for contracts with a fixed time to maturity. Empirical averages are computed from daily data on Markit's North American Investment Grade CDX Index obtained from ICE Data Services for the period from September 2003 to June 2022. Empirical default probabilities are the average cumulative issuer-weighted global default rates reported by Moody's spanning the period from 1920 to 2017 for entities categorized as investment grade (letter rating of Baa3 or better).

	CDX Rate		$\mathbb{P}$ Def. Prob.		$\mathbb{Q}$ Def. Prob.
Horizon	Data	Model	Data	Model	Model
1-year	0.0022	0.0021	0.0014	0.0018	0.0031
2-year	0.0035	0.0034	0.0040	0.0042	0.0085
3-year	0.0051	0.0046	0.0072	0.0071	0.0166
4-year	0.0064	0.0059	0.0108	0.0103	0.0277
5-year	0.0077	0.0072	0.0148	0.0140	0.0427
6-year	0.0089	0.0086	0.0188	0.0179	0.0612
7-year	0.0096	0.0100	0.0229	0.0221	0.0845
8-year	0.0105	0.0113	0.0270	0.0267	0.1104
9-year	0.0111	0.0126	0.0313	0.0318	0.1394
10-year	0.0113	0.0138	0.0356	0.0371	0.1707

Table 6: CDX Pricing

This table reports the 1-year, 5-year, and 10-year CDX rates in basis points as a function of the belief p_t (across columns) and average leverage (across rows).

Belief	0	0.1	0.2	0.3	0.4	0.5	0.6	0.7	0.8	0.9	1
						1-year CDX					
20%	12	15	18	20	21	20	20	20	19	19	18
25%	13	16	20	22	22	22	21	21	20	20	20
30%	15	19	24	26	27	26	25	25	24	24	23
35%	20	25	31	33	34	33	32	32	31	30	30
40%	28	35	42	46	47	46	45	43	43	42	41
45%	41	50	61	66	69	68	66	63	62	61	60
50%	59	73	89	96	99	98	95	91	89	87	86
						5-year CDX					
20%	38	41	44	46	47	47	47	46	46	46	46
25%	50	54	58	61	62	62	61	61	60	60	60
30%	68	74	80	83	85	85	84	83	82	82	82
35%	94	101	110	114	117	117	116	115	114	113	113
40%	129	139	150	157	161	160	159	158	157	156	155
45%	174	188	204	212	218	217	217	216	214	212	211
50%	237	256	277	289	296	296	295	295	291	290	289
						10-year CDX					
20%	73	76	80	82	83	83	82	81	81	81	80
25%	106	110	116	119	120	120	119	118	118	117	116
30%	146	151	159	163	166	165	164	163	163	162	161
35%	191	198	208	214	217	217	217	215	215	214	212
40%	240	250	263	271	275	275	275	274	273	272	271
45%	294	309	324	334	339	340	340	339	339	338	337
50%	364	383	402	414	421	422	422	422	422	421	420

Internet Appendix

In the Internet Appendix, we summarize the notation used in the paper in Appendix A, derive the representative agent's stochastic discount factor and equity valuation in Appendix B, and describe how we solve the model numerically in Appendix C.

A Notation

In this appendix, we summarize the notation used in the paper.

A.1 Consumption, Fear, and the Stochastic Discount Factor

$\mathbb{P}$	objective physical probability measure
$E_t[\cdot]$	time-t conditional expectation operator under $\mathbb{P}$
C	stochastic process for aggregate consumption
μ_c	drift of aggregate consumption growth
B_c	standard Brownian motion under $\mathbb{P}$, dB_c is a Brownian shock to aggregate consumption growth
σ_c	volatility of aggregate consumption growth driven by Brownian shocks
N	Poisson process under $\mathbb{P}$, dN is a Poisson shock to aggregate consumption growth and firm-level earnings growth
λ_t	stochastic intensity of N under $\mathbb{P}$
λ_H	value of the intensity λ in the high risk-state (state H)
λ_L	value of the intensity λ in the low risk-state (state L)
ϕ_{HL}	intensity of transitions from state H to state L under $\mathbb{P}$
ϕ_{LH}	intensity of transitions from state L to state H under $\mathbb{P}$
Z_c	exponentially distributed downward jump in log aggregate consumption
ϵ_c	rate (or inverse scale parameter) for distribution of Z_c under $\mathbb{P}$, $1/\epsilon_c$ is the mean of Z_c under $\mathbb{P}$
$J_c = \frac{1}{1+\epsilon_c}$	mean size of jump in consumption growth under $\mathbb{P}$
$\tilde{\mathbb{P}}$	probability measure representing the representative agent's subjective beliefs
$\widetilde{M}$	exponential martingale under $\mathbb{P}$ used to change measure from $\mathbb{P}$ to $\tilde{\mathbb{P}}$
$\tilde{E}_t[\cdot]$	time-t conditional expectation operator under $\tilde{\mathbb{P}}$
$\mathcal{F}_t$	the σ-algebra representing the representative agent's information set at time-t
$p_t = Pr(\lambda_t = \lambda_H \vert \mathcal{F}_t)$	fear, the representative agent's belief that $\lambda_t = \lambda_H$ conditional on time-t information
$\tilde{\lambda}_t = \tilde{\lambda}(p_t) = p_t\lambda_H + (1-p_t)\lambda_L$	stochastic intensity of N under $\tilde{\mathbb{P}}$
$\kappa = \phi_{LH} + \phi_{HL}$	rate at which λ converges to its long-run mean under $\mathbb{P}$
$f_H = \phi_{LH}/\kappa$	long-run probability under $\mathbb{P}$ that the stochastic intensity of N is in the high-risk state
$f_L = \phi_{HL}/\kappa$	long-run probability under $\mathbb{P}$ that the stochastic intensity of N is in the low-risk state
$\sigma_p(p) = \frac{\lambda_H - \lambda_L}{\tilde{\lambda}(p)} p(1-p)$	representative agent's belief uncertainty
p^*	attractor of the representative agent's belief in between jumps

J	representative agent's value function
$f(\cdot,\cdot)$	normalized Kreps-Porteus aggregator
β	representative agent's rate of time preference
ψ	representative agent's elasticity of intertemporal substitution
γ	representative agent's relative risk aversion
$V(p_t)$	impact of learning on J measured in units of log consumption
$a(p_{t-}) = V\left(p_{t-} + \sigma_p(p_{t-})\right) - V(p_{t-})$	jump in V caused by a jump in p
π	representative agent's equilibrium stochastic discount factor
$r(p)$	equilibrium risk-free rate
$\Theta_B = \gamma\sigma_c$	price of Brownian risk in log aggregate consumption
$\Theta_J(Z_{c,t}) = e^{\gamma Z_{c,t}} - 1$	price of pure jump risk in log aggregate consumption
$\Theta_L(p_{t-}, Z_{c,t}) = \left[1 + \Theta_J(Z_{c,t})\right]\left[e^{-(\gamma-1)a(p_{t-})} - 1\right]$	price of belief uncertainty
$\omega(p)$	risk distortion factor
ω_J	risk distortion factor for pure jump risk
$\omega_L(p)$	additional risk distortion for belief uncertainty
$\lambda^{\mathbb{Q}}(p)$	stochastic intensity of N under $\mathbb{Q}$
$\lambda_J^{\mathbb{Q}}(p)$	stochastic intensity of N under $\mathbb{Q}$ when $\sigma_p(p) = 0$
M_π	exponential martingale used to change measure from $\tilde{\mathbb{P}}$ to $\mathbb{Q}$

A.2 Firms' Dynamics and CDX Prices

t_{roll}	roll date (date at which the composition of the CDX Index is chosen)
t_{issue}	time at which corporate debt is issued
$\mathcal{N}_F(t_{\text{roll}})$	set of firms in the CDX Index at the roll date t_{roll}
N_F	number of firms in the CDX Index
$D_{k,t}$	time-t market value of firm k's debt
$\tau_{D,k}$	random default time for firm k's debt
$R_{k,\tau_{D,k}}$	stochastic recovery rate
$n_{t,s}(t_{\text{roll}})$	fraction of firms in the CDX Index defined at the roll date t_{roll}, that have defaulted between the times t and $s > t$
$L_{t,s}(t_{\text{roll}})$	sum of the payoffs received by the protection buyer up until time $s > t$
$\text{Prot}\,(T-t)$	present value of the cumulative loss
S_{CDX}	CDX spread
$\text{Prem}\,(T-t, S_{\text{CDX}})$	present value of cash flows received by the protection seller
X_k	stochastic process for real earnings of firm k
μ_x	drift in real earnings growth rate
σ_x^{id}	idiosyncratic Brownian volatility in real earnings growth
$B_{x,k}$	standard Brownian motion under $\mathbb{P}$, $dB_{x,k}$ is an idiosyncratic Brownian shock to earnings growth for firm k
σ_x^{sys}	systematic Brownian volatility in real earnings growth
B_x	standard Brownian motion under $\mathbb{P}$, dB_x is a systematic Brownian shock to earnings growth
$\sigma_x = \sqrt{(\sigma_x^{\text{id}})^2 + (\sigma_x^{\text{sys}})^2}$	total Brownian volatility in real earnings growth
ρ_{cx}	correlation between the Brownian shock to consumption growth and systematic Brownian shock to earnings growth
Z_k	exponentially distributed downward jump in log earnings of firm k
ϵ_x	rate (or inverse scale parameter) for distribution of Z_k under $\mathbb{P}$ $1/\epsilon_x$ is the mean of Z_k under $\mathbb{P}$
$\varphi = (1/\epsilon_x)/(1/\epsilon_c)$	scaling parameter for mean log earnings jumps relative to mean log consumption jumps

$J_x = \frac{1}{1+\epsilon_x}$	mean size of jump in earnings growth under $\mathbb{P}$
N_k	Poisson process under $\mathbb{P}$, dN_k is an idiosyncratic Poisson shock that leads to the exit of firm k by driving its earnings to zero
τ_X	random exogenous exit time
λ_x	exogenous exit intensity
η	tax rate
c	coupon rate for debt
p_X	unlevered price-earnings ratio
dR_X^{unlev}	cum-dividend return on unlevered equity
dR_X	cum-dividend return on levered equity
$\Phi(X,p)$	fractional loss for levered equity relative to unlevered equity
S	stochastic process for price of levered equity
$\Pi_L(X,p)^{\text{lev}}$	conditional levered equity risk premium from belief uncertainty
$b(p_t)$	time-t price of a perpetual bond which pays one unit of consumption per unit time until a jump in $N_{k,t}$ is realized
D	stochastic process for price of perpetual corporate debt
α	recovery fraction – fraction of after-tax unlevered firm value recovered by debtholders at default
$X_D(p)$	optimal default boundary as function of p
ι	debt issuance costs
F_{0-}	firm-value at time 0− net of debt issuance costs

A.3 Empirics

$F_{\text{with debt}}$	firm value with perpetual debt
$F_{\text{no debt}}$	firm value with no debt
τ_c	corporate tax rate
τ_e	equity payout rate
τ_p	personal rate
$\theta = (\sigma_x^{\text{id}}, \sigma_x^{\text{sys}}, 1-\alpha, \varphi)^\top$	vector of estimated parameters
$\hat{\theta}$	estimate of θ
$\Psi^M(\theta)$	vector of seven model moments
Ψ^D	vector of seven targeted empirical moments
$\mathbf{W} \in \mathbb{R}^{7\times 7}$	seven by seven weighting matrix used in SMM

B Proofs

Proposition B1 *We assume the representative agent observes aggregate consumption and knows all fixed parameters, but cannot observe the jump intensity λ_t. She updates her posterior belief p_t that the current state is H, $p_t = Pr(\lambda_t = \lambda_H|\mathcal{F}_t)$, where $\mathcal{F}_t$ is her information set. Her subjective jump intensity is $\tilde{\lambda}_t = \tilde{\lambda}(p_t) = p_t\lambda_H + (1-p_t)\lambda_L$. Under Bayesian updating, her belief dynamics follow (2). In between jump times:*

$$p_t = p^* + \frac{1}{(p_\tau - p^*)^{-1}e^{(\lambda_H-\lambda_L)\Delta(t-\tau)} + \Delta^{-1}[1-e^{(\lambda_H-\lambda_L)\Delta(t-\tau)}]}, \tag{B1}$$

where τ is the most recent jump time, $t > \tau$, and

$$\Delta = (1+\overline{\kappa})\sqrt{1-\frac{4f_H\overline{\kappa}}{(1+\overline{\kappa})^2}}.$$

Furthermore, if no further jumps were to occur, then p_t would converge to p^*.

Proof of Proposition B1. Equation (2) is the counterpart of the Wonham filter[21] for the case where updating is based on observing a jump process instead of a continuous-path process – the filter can be obtained as a special case of Theorem 19.6, page 332 of Liptser and Shiryaev (2013), and is used in Benzoni, Collin-Dufresne, and Goldstein (2011) and Wachter and Zhu (2025). Between jump times, equation (2) reduces to a Riccati ordinary differential equation given by

$$\frac{dp_t}{dt} = (\lambda_H - \lambda_L)\left[\overline{\kappa}(f_H - p_t) - p_t(1-p_t)\right],$$

which can be rewritten as

$$\frac{dp_t}{dt} = (\lambda_H - \lambda_L)(p_t - \overline{p})(p_t - p^*), \tag{B2}$$

where $\overline{p}, p^*$, and $\overline{\kappa}$ are defined in (3).

We now show that p^* is the unique steady state solution of (B2), i.e., if no further jumps were to occur, then p_t would converge to p^*. We do so by showing that $\overline{p} > 1$ and $p^* \in (0,1)$.

From $\overline{p}$ in (3) and the fact that $f_H \in (0,1)$, we see that

$$\overline{p} > \frac{1+\overline{\kappa}}{2}\left[1+\sqrt{1-\frac{4\overline{\kappa}}{(1+\overline{\kappa})^2}}\right] = \frac{1}{2}\left[(1+\overline{\kappa}) + \sqrt{(1-\overline{\kappa})^2}\right].$$

We have either $\overline{\kappa} > 1$, $\overline{\kappa} = 1$, or $\overline{\kappa} < 1$. If $\overline{\kappa} > 1$, then $\sqrt{(1-\overline{\kappa})^2} = \overline{\kappa}-1$, and so $\overline{p} > \overline{\kappa} > 1$. If $\overline{\kappa} = 1$, then $\sqrt{(1-\overline{\kappa})^2} = 0$, and so $\overline{p} > (1+\overline{\kappa})/2 = 1$. If $\overline{\kappa} < 1$, then $\sqrt{(1-\overline{\kappa})^2} = 1-\overline{\kappa}$, and so $\overline{p} > 1$. Therefore $\overline{p} > 1$.

Similarly, via p^* in (3) and the fact that $f_H \in (0,1)$, we see that

$$p^* < \frac{1+\overline{\kappa}}{2}\left[1-\sqrt{1-\frac{4\overline{\kappa}}{(1+\overline{\kappa})^2}}\right],$$

from which it follows that $p^* < 1$. It follows immediately from (3) and $f_H \in (0,1)$ that $p^* > 0$. Therefore, $p^* \in (0,1)$.

If the last jump time is denoted by τ, then we can solve the Riccati differential equation (B2) to obtain (B1). ■

Proposition B2 (Conditional consumption growth density and fear) *Let $g_{\Delta t} = \ln(C_{t+\Delta t}/C_t)$ denote log consumption growth over a horizon $\Delta t > 0$. Under the agent's subjective measure $\tilde{\mathbb{P}}$, the conditional density of $g_{\Delta t}$ given her information set $\mathcal{F}_t$ is*

$$f(g \mid p_t) = \left(1 - \tilde{\lambda}(p_t)\Delta t\right)\cdot f_0(g) + \tilde{\lambda}(p_t)\Delta t \cdot f_1(g) + R(g, p_t, \Delta t), \tag{B3}$$

where:

(i) The no-jump component is Gaussian:

$$f_0(g) = \frac{1}{\sigma_g}\phi\left(\frac{g-\mu_g}{\sigma_g}\right), \tag{B4}$$

with $\mu_g = (\mu_c - \frac{1}{2}\sigma_c^2)\Delta t$ and $\sigma_g = \sigma_c\sqrt{\Delta t}$.

[21] See Wonham (1964) and applications in David (1997), Veronesi (1999), and Veronesi (2000).

(ii) The one-jump component is the convolution of a Gaussian and an exponential:

$$f_1(g) = \int_0^\infty \frac{1}{\sigma_g}\phi\left(\frac{g+z-\mu_g}{\sigma_g}\right)\epsilon_c\, e^{-\epsilon_c z}\, dz = \epsilon_c\, e^{\epsilon_c(g-\mu_g)+\frac{1}{2}\epsilon_c^2\sigma_g^2}\,\Phi\left(\frac{-(g-\mu_g)-\epsilon_c\sigma_g^2}{\sigma_g}\right), \tag{B5}$$

where Φ denotes the standard normal cumulative distribution function.

(iii) The remainder satisfies

$$\int_{-\infty}^{\infty} |R(g, p_t, \Delta t)|\, dg \le \frac{3[\tilde\lambda(p_t)\Delta t]^2}{1-\tilde\lambda(p_t)\Delta t}, \tag{B6}$$

provided $\tilde\lambda(p_t)\Delta t < 1$.

The density (B3) depends on p_t only through $\tilde\lambda(p_t) = p_t\lambda_H + (1-p_t)\lambda_L$. Since $\tilde\lambda$ is strictly increasing in p_t, a rise in fear shifts weight from the Gaussian component f_0 to the left-tailed component f_1, increasing the left-tail probability, negative skewness, and variance of the conditional consumption growth distribution.

Proof. Under $\tilde{\mathbb{P}}$, the jump process N has $\mathcal{F}_t$-intensity $\tilde\lambda(p_t)$ at time t.[22] The number of jumps $n = N_{t+\Delta t} - N_t$ satisfies

$$\tilde P(n = k \mid \mathcal{F}_t) = e^{-\tilde\lambda(p_t)\Delta t}\frac{[\tilde\lambda(p_t)\Delta t]^k}{k!} + O((\Delta t)^2), \quad k = 0, 1, 2, \ldots,$$

where the $O((\Delta t)^2)$ term accounts for the variation of $\tilde\lambda(p_s)$ over $[t, t+\Delta t]$; see Brémaud (1981), Chapter VIII, Theorem T2, for the locally constant intensity approximation.

Step 1: Decomposition by number of jumps. Log consumption growth decomposes as

$$g_{\Delta t} = \mu_g + \sigma_g\,\xi - \sum_{i=1}^{n} Z_{c,i},$$

where $\xi \sim N(0,1)$ and $Z_{c,1}, Z_{c,2}, \ldots$ are i.i.d. Exp(ϵ_c), all mutually independent under $\tilde{\mathbb{P}}$. Conditioning on n:

$$f(g \mid p_t) = \sum_{k=0}^{\infty} \tilde P(n = k \mid \mathcal{F}_t)\cdot f_{g|k}(g), \tag{B7}$$

where $f_{g|k}$ is the density of $\mu_g + \sigma_g\xi - S_k$ and $S_k = \sum_{i=1}^k Z_{c,i} \sim \text{Gamma}(k, \epsilon_c)$ for $k \ge 1$, with $S_0 = 0$.

Step 2: The $k = 0$ and $k = 1$ terms. For $k = 0$: $f_{g|0}(g) = f_0(g)$ as defined in (B4).

For $k = 1$: $S_1 = Z_{c,1} \sim \text{Exp}(\epsilon_c)$, and the density of $\mu_g + \sigma_g\xi - Z_{c,1}$ is the convolution

$$f_{g|1}(g) = \int_0^\infty \frac{1}{\sigma_g}\phi\left(\frac{g+z-\mu_g}{\sigma_g}\right)\epsilon_c\, e^{-\epsilon_c z}\, dz.$$

This integral evaluates in closed form. Completing the square in the exponent of $\phi(\cdot)\cdot e^{-\epsilon_c z}$:

$$\begin{aligned} f_{g|1}(g) &= \epsilon_c\, e^{\epsilon_c(g-\mu_g)+\frac{1}{2}\epsilon_c^2\sigma_g^2}\int_0^\infty \frac{1}{\sigma_g}\phi\left(\frac{z+(g-\mu_g)+\epsilon_c\sigma_g^2}{\sigma_g}\right)dz \\ &= \epsilon_c\, e^{\epsilon_c(g-\mu_g)+\frac{1}{2}\epsilon_c^2\sigma_g^2}\,\Phi\left(\frac{-(g-\mu_g)-\epsilon_c\sigma_g^2}{\sigma_g}\right), \end{aligned}$$

which is (B5). This closed-form expression for the Gaussian-exponential convolution follows from the standard result for the difference of a normal and an exponential random variable; see Grushka (1972) or Kalambet, Kozmin, Mikhailova, Nagaev, and Tikhonov (2011).

Step 3: Remainder bound. Define $\lambda^* = \tilde\lambda(p_t)\Delta t$. The approximation in (B3) involves three sources of error: (a) neglecting the probability of two or more jumps in $[t, t+\Delta t]$, (b) treating the intensity $\tilde\lambda(p_s)$ as constant at $\tilde\lambda(p_t)$ over

[22] Between t and $t+\Delta t$, the intensity $\tilde\lambda(p_s)$ evolves as p_s decays deterministically (absent jumps) or jumps upward (upon a jump arrival). The proposition conditions on $\tilde\lambda(p_t)$ at time t and treats the intensity as locally constant over $[t, t+\Delta t]$. The remainder R bounds the error from this approximation and from neglecting multiple jumps.

$[t, t+\Delta t]$, and (c) replacing the exact Poisson weights $e^{-\lambda^*}$ and $\lambda^* e^{-\lambda^*}$ with the first-order approximations $1-\lambda^*$ and λ^*.

Error from multiple jumps. The remainder from truncating the mixture (B7) at $k=1$ is

$$R_1(g) = \sum_{k=2}^{\infty} \tilde{P}(n=k \mid \mathcal{F}_t) \cdot f_{g|k}(g).$$

Since each $f_{g|k}$ is a probability density ($\int f_{g|k}\, dg = 1$), we have $\int |R_1|\, dg \le \sum_{k=2}^{\infty} \tilde{P}(n=k)$. Under the locally constant intensity approximation, n is Poisson(λ^*), so

$$\sum_{k=2}^{\infty} e^{-\lambda^*} \frac{(\lambda^*)^k}{k!} \le \sum_{k=2}^{\infty} (\lambda^*)^k = \frac{(\lambda^*)^2}{1-\lambda^*},$$

where the inequality uses $e^{-\lambda^*} \le 1$ and $k! \ge 1$ for $k \ge 2$.

Error from intensity variation. Between t and $t+\Delta t$, the intensity $\tilde{\lambda}(p_s)$ evolves as p_s decays deterministically at rate $|\mu_p(p_t)|$. By the mean value theorem, $|\tilde{\lambda}(p_s) - \tilde{\lambda}(p_t)| \le (\lambda_H - \lambda_L)|\mu_p(p_t)|\Delta t$ for $s \in [t, t+\Delta t]$. The resulting error in the Poisson probabilities is $O((\lambda_H - \lambda_L)|\mu_p(p_t)|(\Delta t)^2)$, which is of the same order as $(\lambda^*)^2$ for Δt small.

Error from weight approximation. The exact Poisson weights for the $k=0$ and $k=1$ terms are $e^{-\lambda^*}$ and $\lambda^* e^{-\lambda^*}$. Replacing these with $1-\lambda^*$ and λ^* introduces errors of $|e^{-\lambda^*} - (1-\lambda^*)| = O((\lambda^*)^2)$ and $|\lambda^* e^{-\lambda^*} - \lambda^*| = O((\lambda^*)^2)$, both bounded by $(\lambda^*)^2$.

Combined bound. Combining all three sources, the total remainder $R = R_1 + R_2 + R_3$ satisfies

$$\int_{-\infty}^{\infty} |R(g, p_t, \Delta t)|\, dg \le \frac{3(\lambda^*)^2}{1-\lambda^*} + O\big((\lambda_H - \lambda_L)|\mu_p(p_t)|(\Delta t)^2\big).$$

The leading constant of 3 accounts for all three sources: $(\lambda^*)^2/(1-\lambda^*)$ from multiple jumps, at most $2(\lambda^*)^2$ from the weight approximation, and $(\lambda^*)^2/(1-\lambda^*) \ge (\lambda^*)^2$ absorbs the sum.[23] The intensity variation term R_2 is dominated for Δt small, since both are $O((\Delta t)^2)$. For daily frequency $\Delta t = 1/252$ and $\tilde{\lambda}(p_t) \le \lambda_H = 1.70$, the bound evaluates to $\lambda^* = 1.70/252 \approx 0.0067$, giving $3(\lambda^*)^2/(1-\lambda^*) \le 1.4 \times 10^{-4}$. The two-term approximation is therefore accurate to within 0.014% of total probability mass at daily frequency.

Validity as a density. The two-term approximation $(1-\lambda^*)f_0 + \lambda^* f_1$ is itself a valid probability density: both components are non-negative, and the weights sum to one. The remainder R integrates to zero exactly, since both the true density and the approximation integrate to one. The bound (B6) therefore measures the total variation distance between the true and approximate densities. ■

Lemma 1 (Occupation time density for a two-state Markov chain) *Let $\lambda_t \in \{\lambda_L, \lambda_H\}$ be a continuous-time Markov chain with transition rate ϕ_{HL} from H to L and ϕ_{LH} from L to H. Let $T_H = \int_t^{t+\tau} \mathbf{1}_{\{\lambda_s = \lambda_H\}}\, ds$ denote the total time spent in state H during $[t, t+\tau]$. Write $a = \phi_{HL}$ and $b = \phi_{LH}$. Then:*

(i) Starting from $\lambda_t = \lambda_H$, the density of T_H for $0 < t_H < \tau$ is

$$f_{T_H}(t_H \mid H) = e^{-a t_H - b(\tau - t_H)} \left[a \cdot I_0\big(2\sqrt{a b t_H (\tau - t_H)}\big) + \sqrt{\frac{a b t_H}{\tau - t_H}} \cdot I_1\big(2\sqrt{a b t_H (\tau - t_H)}\big) \right], \tag{B8}$$

with a point mass $P(T_H = \tau \mid H) = e^{-a\tau}$.

(ii) Starting from $\lambda_t = \lambda_L$, the density of T_H for $0 < t_H < \tau$ is

$$f_{T_H}(t_H \mid L) = e^{-a t_H - b(\tau - t_H)} \left[b \cdot I_0\big(2\sqrt{a b t_H (\tau - t_H)}\big) + \sqrt{\frac{a b (\tau - t_H)}{t_H}} \cdot I_1\big(2\sqrt{a b t_H (\tau - t_H)}\big) \right], \tag{B9}$$

with a point mass $P(T_H = 0 \mid L) = e^{-b\tau}$.

[23] More precisely: $R_1 \le (\lambda^*)^2/(1-\lambda^*)$, $R_3 \le 2(\lambda^*)^2$, and $(\lambda^*)^2/(1-\lambda^*) + 2(\lambda^*)^2 = (3-2\lambda^*)(\lambda^*)^2/(1-\lambda^*) \le 3(\lambda^*)^2/(1-\lambda^*)$.

Here I_0 and I_1 are modified Bessel functions of the first kind.

Proof. We derive (B8); expression (B9) follows by symmetry ($a \leftrightarrow b$, $t_H \leftrightarrow \tau - t_H$).

Starting from H, the chain alternates between sojourns in H (each Exp(a)) and sojourns in L (each Exp(b)). We condition on the number of transitions during $[t, t+\tau]$.

Even transitions ($2k$, chain in H at $t+\tau$, $k \geq 1$). The chain completes k sojourns in each state: $h_1, l_1, h_2, l_2, \ldots, h_k, l_k$, then remains in H for a residual $r_H = t_H - S_H > 0$, where $S_H = \sum_{i=1}^{k} h_i$. The total time in L is $S_L = \sum_{i=1}^{k} l_i = \tau - t_H$.

The density of $S_H = s$ is Gamma(k, a): $\frac{a^k s^{k-1}}{(k-1)!} e^{-as}$. The survival probability during the residual is $e^{-ar_H} = e^{-a(t_H - s)}$. Integrating over $s \in (0, t_H)$:

$$\int_0^{t_H} \frac{a^k s^{k-1}}{(k-1)!} e^{-as} \cdot e^{-a(t_H - s)}\, ds = e^{-at_H} \int_0^{t_H} \frac{a^k s^{k-1}}{(k-1)!}\, ds = e^{-at_H} \frac{(at_H)^k}{k!}.$$

The density of $S_L = \tau - t_H$ is Gamma(k, b): $\frac{b^k (\tau - t_H)^{k-1}}{(k-1)!} e^{-b(\tau - t_H)}$. So the contribution from $2k$ transitions is

$$f_{2k}(t_H) = e^{-at_H} \frac{(at_H)^k}{k!} \cdot \frac{b^k (\tau - t_H)^{k-1}}{(k-1)!}\, e^{-b(\tau - t_H)}.$$

Odd transitions ($2k+1$, chain in L at $t+\tau$, $k \geq 0$). The chain completes $k+1$ sojourns in H and k sojourns in L: $h_1, l_1, \ldots, l_k, h_{k+1}$, then remains in L for a residual $r_L = \tau - t_H - S_L > 0$. By an identical calculation (with the roles exchanged), the contribution is

$$f_{2k+1}(t_H) = \frac{a^{k+1} t_H^k}{k!}\, e^{-at_H} \cdot e^{-b(\tau - t_H)} \frac{(b(\tau - t_H))^k}{k!}.$$

Summation and Bessel identification. Combining and setting $u = at_H$, $v = b(\tau - t_H)$:

$$\begin{aligned} f_{T_H}(t_H \mid H) &= \sum_{k=0}^{\infty} f_{2k+1}(t_H) + \sum_{k=1}^{\infty} f_{2k}(t_H) \\ &= e^{-u-v} \left[a \sum_{k=0}^{\infty} \frac{(uv)^k}{(k!)^2} + \frac{1}{\tau - t_H} \sum_{k=1}^{\infty} \frac{(uv)^k}{k!(k-1)!} \right]. \end{aligned} \tag{B10}$$

The modified Bessel functions of the first kind satisfy

$$I_0(z) = \sum_{m=0}^{\infty} \frac{(z/2)^{2m}}{(m!)^2}, \qquad I_1(z) = \sum_{m=0}^{\infty} \frac{(z/2)^{2m+1}}{m!(m+1)!}.$$

Setting $z = 2\sqrt{uv}$, so that $(z/2)^{2m} = (uv)^m$, the first sum in (B10) is $I_0(2\sqrt{uv})$. For the second sum, re-indexing $j = k - 1$:

$$\sum_{k=1}^{\infty} \frac{(uv)^k}{k!(k-1)!} = uv \sum_{j=0}^{\infty} \frac{(uv)^j}{(j+1)!j!} = \sqrt{uv}\, I_1(2\sqrt{uv}).$$

Substituting $\frac{\sqrt{uv}}{\tau - t_H} = \sqrt{\frac{abt_H}{\tau - t_H}}$ yields (B8). ∎

Proposition B3 (Exact conditional consumption growth density at arbitrary horizons) *For any horizon $\tau > 0$, the conditional density of log consumption growth $g_\tau = \ln(C_{t+\tau}/C_t)$ given the agent's information set $\mathcal{F}_t$ is*

$$f(g \mid p_t) = p_t \cdot F_H(g, \tau) + (1 - p_t) \cdot F_L(g, \tau), \tag{B11}$$

where, for $j \in \{H, L\}$,

$$F_j(g, \tau) = \sum_{n=0}^{\infty} P_j(n, \tau) \cdot f_{g|n}(g),$$

with

$$P_j(n, \tau) = \int_0^{\tau} \frac{[\lambda_L(\tau - t_H) + \lambda_H t_H]^n}{n!}\, e^{-\lambda_L(\tau - t_H) - \lambda_H t_H}\, f_{T_H}(t_H \mid j)\, dt_H + \Delta_j(n, \tau),$$

where

$$\Delta_H(n,\tau) = e^{-\phi_{HL}\tau}\,\frac{(\lambda_H\tau)^n}{n!}\,e^{-\lambda_H\tau}, \qquad \Delta_L(n,\tau) = e^{-\phi_{LH}\tau}\,\frac{(\lambda_L\tau)^n}{n!}\,e^{-\lambda_L\tau}$$

account for the point masses at $T_H = \tau$ (starting from H, no regime switch, probability $e^{-\phi_{HL}\tau}$) and $T_H = 0$ (starting from L, no regime switch, probability $e^{-\phi_{LH}\tau}$) established in Lemma 1. The probability of n jumps given initial state j integrates against both the continuous density and the boundary atoms (where f_{T_H} is given by Lemma 1), and

$$f_{g|n}(g) = \begin{cases} \dfrac{1}{\sigma_c\sqrt{\tau}}\,\phi\!\left(\dfrac{g-\mu_\tau}{\sigma_c\sqrt{\tau}}\right) & n = 0, \\ \displaystyle\int_0^\infty \frac{1}{\sigma_c\sqrt{\tau}}\,\phi\!\left(\frac{g+s-\mu_\tau}{\sigma_c\sqrt{\tau}}\right)\frac{\epsilon_c^n\, s^{n-1}\, e^{-\epsilon_c s}}{(n-1)!}\,ds & n \geq 1, \end{cases}$$

the Normal-Gamma(n,ϵ_c) convolution, with $\mu_\tau = (\mu_c - \frac{1}{2}\sigma_c^2)\tau$.

The density depends on fear p_t only through the mixture weights in (B11). The sum over n converges rapidly, and each $P_j(n,\tau)$ requires a one-dimensional numerical integration against the Bessel-function density from Lemma 1. The representation is exact: no approximation error is incurred.

Proof. Since $p_t = P(\lambda_t = \lambda_H \mid \mathcal{F}_t)$ is a sufficient statistic for the agent's information about λ_t, the law of total probability gives

$$f(g \mid \mathcal{F}_t) = p_t \cdot f(g \mid \lambda_t = \lambda_H) + (1-p_t)\cdot f(g \mid \lambda_t = \lambda_L).$$

Conditional on $\lambda_t = \lambda_j$, the Markov chain $\{\lambda_s\}_{s\in[t,t+\tau]}$ evolves independently of the Brownian motion B_c. The integrated jump intensity is $\Lambda_\tau = \int_t^{t+\tau}\lambda_s\,ds = \lambda_L(\tau - T_H) + \lambda_H T_H$, where T_H is the occupation time from Lemma 1. Conditional on the path of λ_s (equivalently, on T_H), the jump process N is an inhomogeneous Poisson process with n jumps occurring with probability $\frac{\Lambda_\tau^n}{n!}e^{-\Lambda_\tau}$. The Brownian component $\sigma_c(B_{c,t+\tau} - B_{c,t}) \sim N(0,\sigma_c^2\tau)$ and the jump sizes $Z_{c,1},\ldots,Z_{c,n} \overset{\text{i.i.d.}}{\sim} \text{Exp}(\epsilon_c)$ are mutually independent. Integrating over T_H using the density from Lemma 1 yields $P_j(n,\tau)$, and convolving the Gaussian and Gamma components yields $f_{g|n}$. ■

Proposition B4 *The representative agent's stochastic discount factor is given by*

$$\pi(C_t,p_t) = \beta e^{-\beta\int_0^t[1-(\gamma-1)V(p_s)]ds}C_t^{-\gamma}e^{-(\gamma-1)V(p_t)}, \tag{B12}$$

where for $p\in[0,1]$, $V(p)$ satisfies the functional differential equation

$$0 = \mu_p(p)V'(p) + \tilde{\lambda}(p)\frac{\frac{1-J_c}{1-\gamma J_c}e^{(1-\gamma)[V(p+\sigma_p(p))-V(p)]} - 1}{1-\gamma} - \beta V(p) + \mu_c - \frac{1}{2}\gamma\sigma_c^2, \tag{B13}$$

where

$$\mu_p(p) = \kappa(f_H - p) - (\lambda_H - \lambda_L)p(1-p), \tag{B14}$$

where at the internal point $p^*\in(0,1)$, given by (3), we have

$$0 = \tilde{\lambda}(p^*)\frac{\frac{1-J_c}{1-\gamma J_c}e^{(1-\gamma)[V(p^*+\sigma_p(p^*))-V(p^*)]} - 1}{1-\gamma} - \beta V(p^*) + \mu_c - \frac{1}{2}\gamma\sigma_c^2. \tag{B15}$$

Using $V(p)$, we can quantify the learning-based amplification of welfare losses from downward consumption jumps via

$$a(p_{t-}) = V\big(p_{t-} + \sigma_p(p_{t-})\big) - V(p_{t-}) < 0. \tag{B16}$$

Proof of Proposition B4. We derive the functional differential equation for $V(p)$, given in (B21). Let J_t be the value function for exogenous aggregate consumption as defined in (4). The Feynman-Kac theorem implies

$$f(C_{t-},J_{t-})dt + \tilde{E}_{t-}\left[dJ(C_t,p_t)\right] = 0.$$

Using Ito's Lemma we rewrite the above equation as

$$0 = f\left(C_{t-},J_{t-}\right) + \mu_c C_{t-}J_{t-,C} + \frac{1}{2}\sigma_c^2 C_{t-}^2 J_{t-,CC} + \mu_p(p_{t-})J_{t-,p} + \tilde{\lambda}(p_{t-})\tilde{E}_{t-}\left[J(C_{t-}e^{-Z_{c,t}},p_{t-}+\sigma_p(p_{t-})) - J(C_{t-},p_{t-})|dN_t = 1\right], \tag{B17}$$

where $\mu_p(\cdot)$ is defined in (B14). Note that when $dN_t = 1$ both arguments change in $J(C,p)$. We guess and verify that the representative agent's value function is given by (6). Therefore,

$$J(C_t,p_t) - J(C_{t-},p_{t-}) = \frac{(C_{t-}e^{-Z_{c,t}})^{1-\gamma}}{1-\gamma} e^{(1-\gamma)V\left(p_{t-}+\sigma_p(p_{t-})\right)} - J(C_{t-},p_{t-}) \tag{B18}$$
$$= J(C_{t-},p_{t-})\left[e^{(1-\gamma)\left[-Z_{c,t}+V\left(p_{t-}+\sigma_p(p_{t-})\right)-V(p_{t-})\right]}-1\right] = J(C_{t-},p_{t-})\left[e^{-(1-\gamma)Z_{c,t}}e^{(1-\gamma)a(p_{t-})}-1\right]$$

where $a(p)$ is defined in (B16).

Substituting (6) and (B18) into (B17) yields

$$0 = \mu_c - \frac{1}{2}\gamma\sigma_c^2 - \beta V(p_{t-}) + \mu_p(p_{t-})V'(p_{t-}) + \tilde{\lambda}(p_{t-})\frac{\tilde{E}_{t-}[e^{-(1-\gamma)Z_{c,t}}]e^{(1-\gamma)\left[V\left(p_{t-}+\sigma_p(p_{t-})\right)-V(p_{t-})\right]}-1}{1-\gamma}, \tag{B19}$$

where $\mu_p(p)$ is defined in (B14). We know that $Z_{c,t}$ is exponentially distributed with mean $1/\epsilon_c > 0$ under $\mathbb{P}$ (and hence $\tilde{\mathbb{P}}$). The probability density function for $Z_{c,t}$ is given by $f(x) = \epsilon_c e^{-\epsilon_c x}$, $x \geq 0$, and so

$$E_{t-}\left[e^{-\delta Z_{c,t}}\right] = \tilde{E}_{t-}\left[e^{-\delta Z_{c,t}}\right] = \int_0^\infty \epsilon_c e^{-\epsilon_c x - \delta x}dx = \int_0^\infty \epsilon_c e^{-(\epsilon_c+\delta)x}dx = \frac{\epsilon_c}{\epsilon_c+\delta} = \frac{1-J_c}{1-(1-\delta)J_c},$$

which implies

$$E_{t-}\left[e^{-(1-\gamma)Z_{c,t}}\right] = \tilde{E}_{t-}\left[e^{-(1-\gamma)Z_{c,t}}\right] = \frac{1-J_c}{1-\gamma J_c},$$

where J_c is the average drop in consumption due to a jump, i.e., $\epsilon_c = \frac{1}{J_c} - 1$. Therefore, (B19) can be written as

$$0 = \mu_c - \frac{1}{2}\gamma\sigma_c^2 - \beta V(p_{t-}) + \mu_p(p_{t-})V'(p_{t-}) + \tilde{\lambda}(p_{t-})\frac{\frac{1-J_c}{1-\gamma J_c}e^{(1-\gamma)\left[V\left(p_{t-}+\sigma_p(p_{t-})\right)-V(p_{t-})\right]}-1}{1-\gamma},$$

and so, setting $p_{t-} = p$ gives the functional differential equation (B21). We set $p = p^*$ in (B21) to obtain the condition (B15).

Duffie and Skiadas (1994) show that the SDF for a general normalized aggregator f is given by

$$\pi_t = e^{\int_0^t f_v(C_s,J_s)ds} f_c\left(C_t,J_t\right),$$

where $f_c(\cdot,\cdot)$ and $f_v(\cdot,\cdot)$ are the partial derivatives of f with respect to its first and second arguments, respectively, and J is the value function given in (4). Thus, taking the derivatives of (5) and substituting (6) we obtain (B20). ■

We recall the following key definitions used throughout. The representative agent's stochastic discount factor is

$$\pi(C_t,p_t) = \beta e^{-\beta\int_0^t[1-(\gamma-1)V(p_s)]ds}C_t^{-\gamma}e^{-(\gamma-1)V(p_t)}, \tag{B20}$$

where $V(p)$ satisfies the functional differential equation

$$0 = \mu_p(p)V'(p) + \tilde{\lambda}(p)\frac{\frac{1-J_c}{1-\gamma J_c}e^{(1-\gamma)\left[V\left(p+\sigma_p(p)\right)-V(p)\right]}-1}{1-\gamma} - \beta V(p) + \mu_c - \frac{1}{2}\gamma\sigma_c^2. \tag{B21}$$

Proof of Proposition 1.

We now derive the dynamics of the SDF. Applying Ito's Lemma to (B20) we obtain

$$d\pi_t = \frac{\partial\pi_t}{\partial t}dt + C_{t-}\frac{\partial\pi_t}{\partial C_t}(\mu_c dt + \sigma_c dB_{c,t}) + \frac{\partial\pi_t}{\partial p_t}\mu_p(p_{t-})dt + \frac{1}{2}C_{t-}^2\frac{\partial^2\pi_t}{\partial C_t^2}\sigma_c^2 dt + \pi_{t-}\left(e^{\gamma Z_{c,t}+(1-\gamma)a(p_{t-})}-1\right)dN_t$$
$$\frac{d\pi_t}{\pi_{t-}} = -\beta[1+(1-\gamma)V(p_{t-})]dt - \gamma(\mu_c dt + \sigma_c dB_{c,t}) + (1-\gamma)V'(p_{t-})\mu_p(p_{t-})dt + \frac{1}{2}\gamma(1+\gamma)\sigma_c^2 dt + \left(e^{\gamma Z_{c,t}+(1-\gamma)a(p_{t-})}-1\right)dN_t$$

and so

$$\frac{d\pi_t}{\pi_{t-}} = -\kappa(p_{t-})dt - \gamma\sigma_c dB_{c,t} + \left(e^{\gamma Z_{c,t}+(1-\gamma)a(p_{t-})}-1\right)dN_t,$$

where $a\left(p_{t-}\right)$ is defined in (B16) and $\kappa(p_{t-})$ is given by the following function

$$\kappa(p) = \beta + \gamma\mu_c - \frac{1}{2}\gamma(1+\gamma)\sigma_c^2 + (\gamma-1)\left(\mu_p(p)V'(p) - \beta V(p)\right).$$

We now use the functional differential equation (B21) to eliminate the dependence of $\kappa(p)$ on $V'(p)$, i.e.

$$\begin{aligned}
\kappa(p) &= \beta + \gamma\mu_c - \frac{1}{2}\gamma(1+\gamma)\sigma_c^2 - (\gamma-1)\left(\mu_c - \frac{1}{2}\gamma\sigma_c^2 + \tilde{\lambda}(p)\frac{\frac{1-J_c}{1-\gamma J_c}e^{(1-\gamma)[V(p+\sigma_p(p))-V(p)]} - 1}{1-\gamma}\right), \\
&= \beta + \gamma\mu_c - \frac{1}{2}\gamma(1+\gamma)\sigma_c^2 - (\gamma-1)\left(\mu_c - \frac{1}{2}\gamma\sigma_c^2 + \tilde{\lambda}(p)\frac{\frac{1-J_c}{1-\gamma J_c}e^{(1-\gamma)a(p)} - 1}{1-\gamma}\right), \\
&= \beta + \mu_c - \gamma\sigma_c^2 + \tilde{\lambda}(p)\left(\frac{1-J_c}{1-\gamma J_c}e^{(1-\gamma)a(p)} - 1\right).
\end{aligned}$$

Now, in the absence of arbitrage, we have

$$\tilde{E}_{t-}[d\pi_t] = -r_{t-}\pi_{t-}dt,$$

where r_{t-} is the time-$t-$ risk-free rate. Therefore,

$$\begin{aligned}
\frac{d\pi_t}{\pi_{t-}} &= -r_{t-}dt - \gamma\sigma_c dB_{c,t} + \left(e^{\gamma Z_{c,t} + (1-\gamma)a(p_{t-})} - 1\right)dN_t - \tilde{\lambda}(p_{t-})\left(E_{t-}[e^{\gamma Z_{c,t}}]e^{(1-\gamma)a(p_{t-})} - 1\right)dt \\
&= -r_{t-}dt - \gamma\sigma_c dB_{c,t} + \left(e^{\gamma Z_{c,t} + (1-\gamma)a(p_{t-})} - 1\right)dN_t - \tilde{\lambda}(p_{t-})\left(\frac{1-J_c}{1-J_c(1+\gamma)}e^{(1-\gamma)a(p_{t-})} - 1\right)dt,
\end{aligned}$$

and $r_{t-} = r(p_{t-})$, where

$$r(p) = \kappa(p) - \left(\frac{1-J_c}{1-J_c(1+\gamma)}e^{(1-\gamma)a(p)} - 1\right)\tilde{\lambda}(p),$$

and we have used the fact that $\tilde{E}_{t-}[e^{\gamma Z_{c,t}}] = \frac{1-J_c}{1-J_c(1+\gamma)}$. Using the definition of the risk distortion factor

$$\omega(p) = \frac{1-J_c}{1-J_c(1+\gamma)}e^{(1-\gamma)a(p)},$$

we see that

$$\frac{d\pi_t}{\pi_{t-}} = -r_{t-}dt - \gamma\sigma_c dB_{c,t} + \left(e^{\gamma Z_{c,t} + (1-\gamma)a(p_{t-})} - 1\right)dN_t - \tilde{\lambda}(p_{t-})\left(\omega(p_{t-}) - 1\right)dt, \tag{B22}$$

where $r_{t-} = r(p_{t-})$, and

$$r(p) = \beta + \mu_c - \gamma\sigma_c^2 - \omega(p)\tilde{\lambda}(p)\frac{J_c}{1-J_c\gamma}. \tag{B23}$$

In order to distinguish the impact of jumps in beliefs from jumps in consumption, we rewrite (B22) as

$$\frac{d\pi_t}{\pi_{t-}} = -r_{t-}dt - \gamma\sigma_c dB_{c,t} + \left[e^{\gamma Z_{c,t}} - 1 + e^{\gamma Z_{c,t}}\left(e^{(1-\gamma)a(p_{t-})} - 1\right)\right]dN_t - \tilde{\lambda}(p_{t-})\left(\omega(p_{t-}) - 1\right)dt. \tag{B24}$$

We now define the stochastic process M_π as the solution to the following stochastic differential equation under $\tilde{\mathbb{P}}$

$$\frac{dM_{\pi,t}}{M_{\pi,t-}} = \left[e^{\gamma Z_{c,t}}e^{(1-\gamma)a(p_{t-})} - 1\right]dN_t - \tilde{\lambda}(p_{t-})\left(\omega(p_{t-}) - 1\right)dt, M_{\pi,0} = 1.$$

We see that M_π is an exponential martingale under $\tilde{\mathbb{P}}$ and defines the change of measure from $\tilde{\mathbb{P}}$ to $\mathbb{Q}$, and so the risk-neutral intensity of N, denoted by $\lambda^{\mathbb{Q}}(p_{t-})$, is given by

$$\lambda^{\mathbb{Q}}(p_{t-}) = E^{\mathbb{Q}}_{t-}\left[\frac{dN_t}{dt}\right] = \tilde{E}_{t-}\left[\frac{M_{\pi,t}}{M_{\pi,t-}}\frac{dN_t}{dt}\right],$$

where, of course, $\tilde{E}_{t-}[M_{\pi,t}] = M_{\pi,t-}$. We now evaluate $\tilde{E}_{t-}\left[\frac{M_{\pi,t}}{M_{\pi,t-}}dN_t\right]$.

$$\begin{aligned}\tilde{E}_{t-}\left[\frac{M_{\pi,t}}{M_{\pi,t-}}dN_t\right] &= \tilde{E}_{t-}\left[\left\{1+\left[e^{\gamma Z_{c,t}}e^{(1-\gamma)a(p_{t-})}-1\right]dN_t - \tilde{\lambda}(p_{t-})\left(\omega(p_{t-})-1\right)dt\right\}dN_t\right] \\ &= \tilde{E}_{t-}\left[\left\{1+\left[e^{\gamma Z_{c,t}}e^{(1-\gamma)a(p_{t-})}-1\right] - \tilde{\lambda}(p_{t-})\left(\omega(p_{t-})-1\right)dt\right\}\right]\tilde{\lambda}(p_{t-})dt \\ &= \tilde{E}_{t-}\left[e^{\gamma Z_{c,t}}\right]e^{(1-\gamma)a(p_{t-})}\tilde{\lambda}(p_{t-})dt + o(dt).\end{aligned}$$

Hence,

$$\lambda^{\mathbb{Q}}(p_{t-}) = \tilde{E}_{t-}\left[e^{\gamma Z_{c,t}}\right]e^{(1-\gamma)a(p_{t-})}\tilde{\lambda}(p_{t-}) = \frac{1-J_c}{1-(1+\gamma)J_c}e^{(1-\gamma)a(p_{t-})}\tilde{\lambda}(p_{t-}) = \omega(p_{t-})\tilde{\lambda}(p_{t-}).$$

We can hence obtain (8) from (B23). To distinguish between the impact of pure jump risk versus belief uncertainty, we rewrite the above expression as

$$\lambda^{\mathbb{Q}}(p_{t-}) = \left[\frac{1-J_c}{1-(1+\gamma)J_c} + \frac{1-J_c}{1-(1+\gamma)J_c}\left(e^{(1-\gamma)a(p_{t-})}-1\right)\right]\tilde{\lambda}(p_{t-}) = (\omega_J + \omega_L(p_{t-}))\tilde{\lambda}(p_{t-}).$$

We can now rewrite (B24) as (7), where

$$\Theta_J(Z_{c,t}) = e^{\gamma Z_{c,t}} - 1,$$

and

$$\Theta_L(p_t, Z_{c,t}) = \left[1+\Theta_J(Z_{c,t})\right]\left[e^{-(\gamma-1)a(p_t)}-1\right].$$

By exploiting the power series expression for the exponential function, we see that

$$\Theta_J(Z_{c,t}) = \sum_{n=1}^{\infty}\frac{(\gamma Z_{c,t})^n}{n!} \approx \gamma Z_{c,t}.$$

Recalling the definition of $a(p_t)$ in (B16), we see that

$$e^{-(\gamma-1)a(p_t)} - 1 = e^{-(\gamma-1)[V\left(p_t+\sigma_p(p_t)\right)-V(p_t)]} - 1.$$

Using a linear approximation for a Taylor series expansion of $e^{-(\gamma-1)[V\left(p_t+\sigma_p(p_t)\right)-V(p_t)]}$ around $\sigma_p(p_t) = 0$, we obtain

$$e^{-(\gamma-1)a(p_t)} - 1 \approx -(\gamma-1)\sigma_p(p_t)V'(p_t), \tag{B25}$$

and hence (9). We can decompose the risk-distortion factor as follows $\omega(p_t) = \omega_J + \omega_L(p_t)$, where ω_J is the risk-distortion for pure jump risk defined in (10) and $\omega_L(p_t)$ is an additional risk-distortion for belief uncertainty, given by

$$\omega_L(p_t) = \omega_J\left[e^{-(\gamma-1)a(p_t)}-1\right],$$

which vanishes when belief uncertainty is zero, i.e., $\sigma_p(p) = 0$. Using (B25), we obtain the approximation for $\omega_L(p_t)$ in (10). ■

Proposition B5 *The unlevered price-earnings ratio of a firm is given by*

$$p_{X,t} = \tilde{E}_t\left[\int_t^{\infty}\frac{\pi_s}{\pi_t}\frac{X_s}{X_t}ds\right],$$

where we omit the subscript k for ease of notation. The unlevered price-earnings ratio will depend on the representative agent's belief that the economy is in the high-risk state, i.e., $p_{X,t} = p_X(p_t)$.

The price-earnings ratio $p_X(p)$ solves the functional differential equation

$$0 = \mu_p(p)p_X'(p) - \left(r(p)+\lambda_x+\gamma\sigma_c\sigma_x^{sys}\rho_{cx}-\mu_x\right)p_X(p) + \omega(p)\tilde{\lambda}(p)\left[p_X\left(p+\sigma_p(p)\right)\left(1-J_x\right)-p_X(p)\right]+1, \tag{B26}$$

with condition

$$0 = -\left(r(p^*)+\lambda_x+\gamma\sigma_c\sigma_x^{sys}\rho_{cx}-\mu_x\right)p_X(p^*) + \omega(p^*)\tilde{\lambda}(p^*)\left[p_X\left(p^*+\sigma_p(p^*)\right)\left(1-J_x\right)-p_X(p^*)\right]+1. \tag{B27}$$

Proof of Proposition B5.

The cum-dividend return on a firm's unlevered equity is denoted by $dR^{\text{unlev}}_{X,t}$, where, using Ito's Lemma, we obtain

$$\begin{aligned}
dR^{\text{unlev}}_{X,t} &= \frac{p'_X(p_{t-})}{p_X(p_{t-})}\mu_p(p_{t-})dt + \mu_x dt + \sigma_x^{\text{id}} dB_{x,k,t} + \sigma_x^{\text{sys}} dB_{x,t} + \frac{1}{p_X(p_{t-})}dt \\
&+ \frac{\left[p_X\left(p_{t-}+\sigma_p(p_{t-})\right)X_{t-}e^{-Z_{k,t}} - p_X(p_{t-})X_{t-}\right]dN_t - p_X(p_{t-})X_{t-}dN_{k,t}}{p_X(p_{t-})X_{t-}} \\
&= \frac{p'_X(p_{t-})}{p_X(p_{t-})}\mu_p(p_{t-})dt + \mu_x dt + \sigma_x^{\text{id}} dB_{x,k,t} + \sigma_x^{\text{sys}} dB_{x,t} + \frac{1}{p_X(p_{t-})}dt + \left[\frac{p_X\left(p_{t-}+\sigma_p(p_{t-})\right)e^{-Z_{k,t}}}{p_X(p_{t-})} - 1\right]dN_t - dN_{k,t} \\
&= \left(\mu_x + \frac{p'_X(p_{t-})}{p_X(p_{t-})}\mu_p(p_{t-}) + \frac{1}{p_X(p_{t-})}\right)dt + \sigma_x^{\text{id}} dB_{x,k,t} + \sigma_x^{\text{sys}} dB_{x,t} - dN_{k,t} + \left[\frac{p_X\left(p_{t-}+\sigma_p(p_{t-})\right)e^{-Z_{k,t}}}{p_X(p_{t-})} - 1\right]dN_t.
\end{aligned}$$

Therefore,

$$\tilde{E}_{t-}\left[\frac{dR^{\text{unlev}}_{X,t}}{dt} - r(p_{t-})\right] = \mu_x + \frac{p'_X(p)}{p_X(p)}\mu_p(p) + \frac{1}{p_X(p)} - \lambda_x + \left[\frac{p_X\left(p+\sigma_p(p)\right)}{p_X(p)}\frac{\epsilon_x}{1+\epsilon_x} - 1\right]\tilde{\lambda}(p) - r(p),$$

and

$$\tilde{E}_{t-}\left[\frac{dR^{\text{unlev}}_{X,t}}{dt} - r(p_{t-})\right] = \gamma\sigma_c\sigma_x^{\text{sys}}\rho_{cx} - (\omega(p)-1)\tilde{\lambda}(p)\left[\frac{p_X\left(p+\sigma_p(p)\right)}{p_X(p)}\frac{\epsilon_x}{1+\epsilon_x} - 1\right]$$

We now use the basic asset pricing equation

$$\tilde{E}_{t-}\left[dR^{\text{unlev}}_{X,t} - r(p_{t-})dt\right] = -\tilde{E}_{t-}\left[dR^{\text{unlev}}_{X,t}\frac{d\pi_t}{\pi_{t-}}\right],$$

obtain the following functional differential equation

$$\mu_x + \frac{p'_X(p)}{p_X(p)}\mu_p(p) + \frac{1}{p_X(p)} - \lambda_x + \left[\frac{p_X\left(p+\sigma_p(p)\right)}{p_X(p)}\frac{\epsilon_x}{1+\epsilon_x} - 1\right]\tilde{\lambda}(p) - r(p) = \gamma\sigma_c\sigma_x^{\text{sys}}\rho_{cx} - (\omega(p)-1)\tilde{\lambda}(p)\left[\frac{p_X\left(p+\sigma_p(p)\right)}{p_X(p)}\frac{\epsilon_x}{1+\epsilon_x} - 1\right],$$

and so

$$0 = \mu_p(p)p'_X(p) - \left(r(p) + \lambda_x + \gamma\sigma_c\sigma_x^{\text{sys}}\rho_{cx} - \mu_x\right)p_X(p) + \omega(p)\tilde{\lambda}(p)\left[p_X\left(p+\sigma_p(p)\right)\frac{\epsilon_x}{1+\epsilon_x} - p_X(p)\right] + 1,$$

from which we obtain (B26). Setting $p = p^*$, we obtain the following condition

$$0 = -\left(r(p^*) + \lambda_x + \gamma\sigma_c\sigma_x^{\text{sys}}\rho_{cx} - \mu_x\right)p_X(p^*) + \omega(p^*)\tilde{\lambda}(p^*)\left[p_X\left(p^*+\sigma_p(p^*)\right)\frac{\epsilon_x}{1+\epsilon_x} - p_X(p^*)\right] + 1,$$

which gives (B27). ■

Proposition B6 *The time-t price of a perpetual bond which pays one unit of consumption per unit time until a jump in $N_{k,t}$ is realized is denoted by $b(p_{t-})$, where $b(p)$ satisfies the following functional ordinary differential equation*

$$0 = \mu_p(p)b'(p) - \left(r(p) + \lambda_x\right)b(p) + \omega(p)\tilde{\lambda}(p)\left[b\left(p+\sigma_p(p)\right) - b(p)\right] + 1, \tag{B28}$$

with condition

$$0 = -\left(r(p^*) + \lambda_x\right)b(p^*) + \omega(p^*)\tilde{\lambda}(p^*)\left[b\left(p^*+\sigma_p(p^*)\right) - b(p^*)\right] + 1. \tag{B29}$$

Setting $\lambda_x = 0$ in the above equations gives the price of the perpetual bond $b_{rf}(p)$.

Proof of Proposition B6. The instantaneous return on the bond, including the coupon flow, is given by

$$\frac{db(p_{t-})+dt}{b(p_{t-})} = \left(\frac{b'(p_{t-})}{b(p_{t-})}\mu_p(p_{t-}) + \frac{1}{b(p_{t-})}\right)dt - dN_{k,t} + \left[\frac{b\left(p_{t-}+\sigma_p(p_{t-})\right)}{b(p_{t-})} - 1\right]dN_t.$$

From the principle of no arbitrage, we obtain

$$\tilde{E}_t\left[\frac{db(p_{t-})+dt}{b(p_{t-})} - r(p_{t-})dt\right] = -\tilde{E}_{t-}\left[\frac{d\pi_t}{\pi_{t-}}\frac{db(p_{t-})}{b(p_{t-})}\right]$$

Therefore, we obtain

$$0 = \mu_p(p)b'(p) - \left(r(p)+\lambda_x\right)b(p) + \omega(p)\tilde{\lambda}(p)\left[b\left(p+\sigma_p(p)\right) - b(p)\right] + 1,$$

from which we obtain (B28). Setting $p = p^*$, we obtain the following condition

$$0 = \omega(p^*)\tilde{\lambda}(p^*)\left[b\left(p^*+\sigma_p(p^*)\right) - b(p^*)\right] - \left(r(p^*)+\lambda_x\right)b(p^*) + 1,$$

which gives (B29). We solve for $b(p)$ via Chebyshev collocation. ■

Proposition B7 *The price of levered equity $S(X_t, p_t)$ satisfies the following Hamilton-Jacobi-Bellman Variational Inequality (HJB-VI):*

$$min\Big\{(\lambda_x + r(p))S(X,p) - (1-\eta)(X-c) - (\mu_x - \gamma\sigma_c\sigma_x^{sys}\rho_{cx})XS_X(X,p) - \mu_p(p)S_p(X,p)$$
$$-\frac{1}{2}X^2\sigma_x^2 S_{XX}(X,p) - \tilde{E}_{t-}[S(Xe^{-Z_{k,t}}, p+\sigma_p(p)) - S(X,p)|dN_t = 1]\tilde{\lambda}(p)\omega(p), S(X,p)\Big\} = 0,$$

with boundary conditions

$$\lim_{X\to 0} S(X,p) = 0$$

and

$$\lim_{X\to\infty} S(X,p) = (1-\eta)\left(p_X(p)X - b(p)c\right).$$

Proof of Proposition B7. The cum-dividend return on a firm's levered equity is given by $dR_t = \frac{dS_t}{S_{t-}} + \frac{(1-\eta)(X_t-c)}{S_{t-}}dt$, and so using Ito's Lemma, we obtain

$$\begin{aligned}
dR_t &= \frac{X_{t-}}{S_{t-}}\frac{\partial S_{t-}}{\partial X_{t-}}\left(\mu_x dt + \sigma_x^{\text{id}}dB_{x,k,t} + \sigma_x^{\text{sys}}dB_{x,t}\right) + \frac{1}{S_{t-}}\frac{\partial S_{t-}}{\partial p_t}\mu_p(p_{t-})dt + \frac{(1-\eta)(X_{t-}-c)}{S_{t-}}dt \\
&+ \frac{1}{S_{t-}}\left[S(X_{t-}e^{-Z_{k,t}}, p_{t-}+\sigma_p(p_{t-})) - S(X_{t-}, p_{t-})\right]dN_t + \frac{1}{S_{t-}}\left[0 - S(X_{t-}, p_{t-})\right]dN_{k,t} + \frac{1}{2}\frac{X_{t-}^2}{S_{t-}}\frac{\partial^2 S_{t-}}{\partial X_{t-}^2}\sigma_x^2 dt \\
&= \left(\frac{X_{t-}}{S_{t-}}\frac{\partial S_{t-}}{\partial X_{t-}}\mu_x + \frac{1}{S_{t-}}\frac{\partial S_{t-}}{\partial p_t}\mu_p(p_{t-}) + \frac{1}{2}\frac{X_{t-}^2}{S_{t-}}\frac{\partial^2 S_{t-}}{\partial X_{t-}^2}\sigma_x^2 + \frac{(1-\eta)(X_{t-}-c)}{S_{t-}}\right)dt + \frac{X_{t-}}{S_{t-}}\frac{\partial S_{t-}}{\partial X_{t-}}\left(\sigma_x^{\text{id}}dB_{x,k,t} + \sigma_x^{\text{sys}}dB_{x,t}\right) \\
&+ \left[\frac{S(X_{t-}e^{-Z_{k,t}}, p_{t-}+\sigma_p(p_{t-}))}{S(X_{t-}, p_{t-})} - 1\right]dN_t - dN_{k,t}
\end{aligned}$$

where

$$\sigma_x^2 = \left(\sigma_x^{\text{id}}\right)^2 + \left(\sigma_x^{\text{sys}}\right)^2.$$

Thus, from the basic asset pricing equation

$$\tilde{E}_{t-}\left[dR_t - r(p_{t-})dt\right] = -\tilde{E}_{t-}\left[dR_t\frac{d\pi_t}{\pi_{t-}}\right],$$

we see that the conditional levered equity risk premium for a firm is

$$\tilde{E}_{t-}\left[\frac{dR_t}{dt}\right] - r(p_{t-}) = \gamma\sigma_c\sigma_x^{\text{sys}}\rho_{cx}\frac{\partial \ln S_{t-}}{\partial \ln X_{t-}} - \left\{\frac{\tilde{E}_{t-}[S(X_{t-}e^{-Z_{k,t}}, p_{t-}+\sigma_p(p_{t-}))]}{S(X_{t-}, p_{t-})} - 1\right\}\tilde{\lambda}(p_{t-})(\omega(p_{t-}) - 1).$$

By applying the basic asset pricing equation, we obtain the following functional partial differential equation

$$\frac{X_{t-}}{S_{t-}}\frac{\partial S_{t-}}{\partial X_{t-}}(\mu_x-\gamma\sigma_c\sigma_x^{\text{sys}}\rho_{cx})+\frac{1}{S_{t-}}\frac{\partial S_{t-}}{\partial p_t}\mu_p(p_{t-})+\frac{1}{2}\frac{X_{t-}^2}{S_{t-}}\frac{\partial^2 S_{t-}}{\partial X_{t-}^2}\sigma_x^2+\frac{(1-\eta)(X_{t-}-c)}{S_{t-}}-(r(p_{t-})+\lambda_x)$$
$$=-\left\{\frac{\tilde{E}_{t-}[S(X_{t-}e^{-Z_{k,t}},p_{t-}+\sigma_p(p_{t-}))|dN_t=1]}{S(X_{t-},p_{t-})}-1\right\}\tilde{\lambda}(p_{t-})\omega(p_{t-}),$$

when the firm is not in default, i.e., $X_{t-} > X_D(p_{t-})$. When $X_{t-} \leq X_D(p_{t-})$, we have $S(X_{t-},p_{t-})=0$. Hence, we obtain (B30).

■

C Numerical Appendix

In this Appendix, we describe how we solve numerically for the representative agent's value function, levered and unlevered asset prices, firm-value maximizing leverage and CDX spreads, and simulate the aggregate economy.

C.1 Functional Differential Equations

C.1.1 Value function and unlevered prices

The representative agent's value function and unlevered asset prices can be obtained by solving functional ordinary differential equations, where the belief p is the single state variable: see Equations (B21), (B26), and (B28) (with $\lambda_x = 0$ for the risk-free perpetual bond).

Rather than solve for the price-earnings ratio $p_X(p)$ directly, we solve for the log price-earnings ratio $p_\xi(p) = \ln p_X(p)$, which satisfies the functional differential equation

$$0 = \mu_p(p)p'_\xi(p) - [r(p) + \lambda_x + \gamma\sigma_c\sigma_x^{\text{sys}}\rho_{cx} - \mu_x] + \omega(p)\tilde{\lambda}(p)\left[(1 - J_x)e^{p_\xi(p+\sigma_p(p))-p_\xi(p)} - 1\right] + e^{-p_\xi(p)}.$$

C.1.2 Solving the functional equations

All functional ordinary differential equations are solved using a collocation approach. Let $0 = g\left(p, F(p)\right)$ be a functional ordinary differential equation. We approximate the true solution $F(p)$ on the interval $p \in [0, 1]$ by

$$\tilde{F}\left(p, \theta\right) = \sum_{i=1}^{n} \theta_i \Psi_i(p),$$

where we set $n = 10$ and use the first 10 Chebyshev polynomials, i.e., polynomials up to the 9th order, as the basis Ψ. To obtain θ we numerically solve the system of residual equations

$$0 \approx g\left(p_i, \tilde{F}(p_i, \theta)\right), \ \forall i = 1, ..., 10.$$

The first nine p_i we choose correspond to the first nine Chebyshev nodes. The last equation is evaluated at $p_{10} = p^*$ to accommodate the boundary condition.

C.1.3 Determining the time discount rate

We set the time discount rate β such that the unconditional average yield of the risk-free perpetual bond equals 1%. To achieve this, we first simulate a stationary distribution of p_t to approximate $E\left[y_{rf}(p_t)\right]$ for a given $y_{rf}(p_t) = \frac{1}{b_{rf}(p_t)}$. Next, starting from an initial guess for β we iteratively solve equations (B28) and (B29) with $\lambda_x = 0$ until

$$0 \approx \frac{1}{n}\sum_{i=1}^{n} y_{rf}(p_i) - 0.01$$

is reached. Once we have determined β, we proceed with solving for the price-earnings and price-coupon ratios.

C.2 Levered Equity, Corporate Debt and Capital Structure

The most commonly used approach to solve optimal stopping problems in Finance and Economics is to derive first an option's value assuming an exogenous exercise boundary and then maximize the option's value by imposing value matching and smooth pasting conditions. This approach becomes difficult to implement in more than one dimension as exercise and continuation regions can have complex shapes that are difficult to characterize a priori. In contrast, solving optimal stopping problems using the variational inequality (VI) approach directly yields an option's value under the value-maximizing policy in a single step. Exercise and continuation regions can be identified based on whether an option value equals the continuation or exercise value at any particular point.

As the levered equity owner's optimal stopping problem is one in two dimensions, we will use the VI approach in combination with finite differences. Considering standard value matching and smooth pasting arguments as well as our knowledge about boundary conditions, we know that the price of levered equity $S(X_t, p_t)$ will be flat to the left of the default threshold $X_D(p_t)$, exhibit the most curvature to the right of it and be approximately linear for large X (because of boundary condition (C3)). To accurately capture these features and obtain a more precise estimate of the default

boundary, we introduce the change of variable $X_t = e^{Y_t}$ as this way, more grid points are allocated where the function changes rapidly and eventually pastes into zero. To reduce the presence of minus signs, we rewrite the jump in earnings $X_{t-}e^{-Z_{k,t}}$ as $X_{t-}e^{Z_{k,t}}$, with probability density function $f(Z_k) = \epsilon_x e^{\epsilon_x Z_k}$ for $Z_k \leq 0$ and $f(Z_k) = 0$ for $Z_k > 0$.

For exogenous coupon rate c and change of variable $X = e^Y$, the price of levered equity $S(Y,p)$ (with slight abuse of notation) solves the following HJB-VI

$$\min\Bigg\{\Big[r(p) + \lambda_x + \tilde{\lambda}(p)\omega(p)\Big]S(Y,p) - (1-\eta)(e^Y - c) - \Big[(\mu_x - \gamma\sigma_c\sigma_x^{\text{sys}}\rho_{cx}) - \frac{1}{2}\sigma_x^2\Big]S_Y(Y,p)$$
$$- \frac{1}{2}\sigma_x^2 S_{YY}(Y,p) - \mu_p(p)S_p(Y,p) - \tilde{\lambda}(p)\omega(p)\int_{-\infty}^{0} S\Big(Y + Z_k,\ p + \sigma_p(p)\Big)f(Z_k)dZ_k,\ S(Y,p)\Bigg\} = 0, \quad \text{(C1)}$$

where $\sigma_x = \sqrt{(\sigma_x^{\text{id}})^2 + (\sigma_x^{\text{sys}})^2}$ with boundary conditions

$$\lim_{Y\to-\infty} S(Y,p) = 0 \quad \text{(C2)}$$

and

$$\lim_{Y\to\infty} S(Y,p) = (1-\eta)\left(p_X(p)e^Y - b(p)c\right). \quad \text{(C3)}$$

C.2.1 Discretization scheme

We discretize the (Y,p) plane by taking $n_Y + 2$ steps in the Y direction and n_p steps in the p direction. Let S be a lexicographically ordered column vector with elements $S = (S_1, S_2, \cdots, S_N)'$ where $S_1 = S(Y_1,p_1)$, $S_2 = S(Y_2,p_1)$, ..., $S_{n_Y} = S(Y_{n_Y},p_1)$, $S_{n_Y+1} = S(Y_1,p_2)$, ..., $S_N = S(Y_{n_Y},p_{n_p})$.[24] In order to estimate the price of levered equity, we derive a set of discretized operators, allowing us to write the associated partial integro-differential equation for each grid point i as

$$(r_i + \lambda_x + \hat{\lambda}_i)S_i = (1-\eta)\left(e^{Y_i} - c\right) + \hat{\mu}_x\partial_y(S_i)$$
$$+\frac{1}{2}\sigma_x^2\partial_{yy}(S_i) + \mu_p(p_i)\partial_p(S_i) + \hat{\lambda}_i \mathrm{J}_i S,$$

where $\hat{\lambda}_i = \tilde{\lambda}_i\omega_i$, $\hat{\mu}_x = \Big[(\mu_x - \gamma\sigma_c\sigma_x^{\text{sys}}\rho_{cx}) - \frac{1}{2}\sigma_x^2\Big]$, $\partial.(\ \cdot\ )$ are differentiation operators, vector J_i is a jump operator containing the discretized jump size distribution and vector S is the lexicographically ordered column vector of levered equity prices. Equivalently, in matrix notation, with likewise lexicographically ordered rows, we can write the problem as

$$(r + \lambda_x + \hat{\lambda}) \circ S = u + (A_G + A_J)S$$
$$\rho \circ S = u + AS, \quad \text{(C4)}$$

where u is the vector of intermediate payoffs to equity, matrix A_G is the discretized version of the infinitesimal generator $\hat{\mu}_x\partial_y + \frac{1}{2}\sigma_x^2\partial_{yy} + \mu_p(p)\partial_p$ and A_J is a matrix with vectors $\hat{\lambda}_i\mathrm{J}_i$ as rows. We describe the translation of (C1) into (C4) in three separate steps. First, we derive the coefficient matrix A_G approximating partial derivatives with finite differences. Secondly, we discuss the necessary adjustments of A_G and u to account for boundary conditions. Lastly, we discuss how we set up A_J to approximate the integral term.

Throughout, we will refer back to variations of the following two figures as visual aids. Here, for simplicity, we assume a uniform grid with $n_Y = 5$, i.e., $n_Y + 2$ points in the direction of Y_t and $n_p = 3$ points in the direction of p_t.

[24] Vector S does not contain points at Y_0 and Y_{n_y+1} as those will be given by boundary conditions.

Figure C1: : Equidistant $7 \times (3+2)$ grid in Y_t and p_t directions.

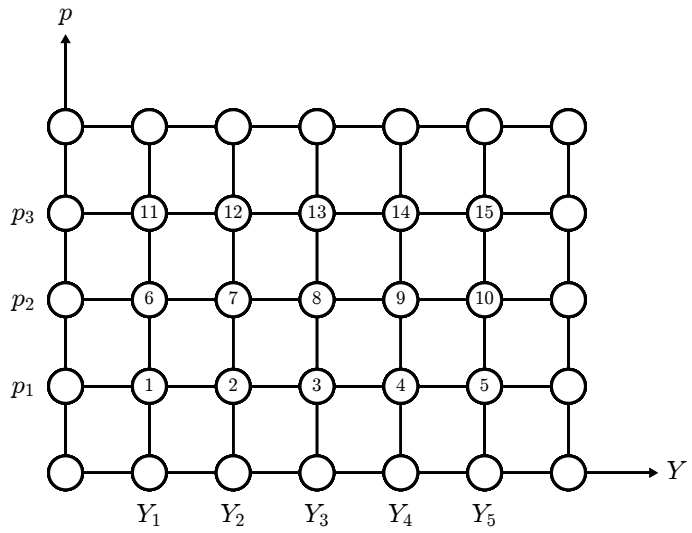

Figure C2: : Schematic representation of coefficient matrix A_G.

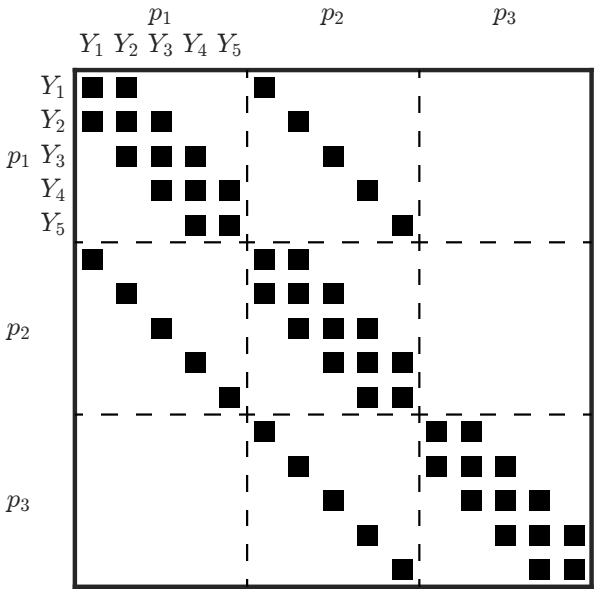

Figure C1 visually represents the resulting 7×3 grid. $Y_0 = Y^{min}$, $Y_6 = Y^{max}$, $p_1 = 0$ and $p_3 = 1$ represent respectively the lower and upper cut-off points in both directions. The numbered inner nodes can be thought of as the 15 unknown entries of the value function vector S identified by their lexicographical index. Given that p_t is a probability, the unindexed nodes at the top and bottom of the grid can be thought of as ghost nodes, i.e., pseudo nodes lying outside the domain of p_t. The remaining six nodes, of which three are located to the far left and the far right of the inner grid each, represent values of the value function for the case that $S(Y^{min}, p_t)$ and $S(Y^{max}, p_t)$ and will be given by boundary conditions. For ease of comprehension, we will switch between the earlier introduced lexicographical, single integer indexing scheme using symbol i and Cartesian indexing of elements. When using Cartesian indexing, we identify elements by the integer pair (j, k) where j is the coordinate in Y_t direction and k is the coordinate in p_t direction.

For example, node S_{15} in Figure C1 can alternatively be referred to as node $S_{(5,3)}$. Under lexicographical indexing, $Y_i \equiv Y_{j(i)}$ and $p_i \equiv p_{k(i)}$ denote the Y- and p-coordinates of the i-th grid point.

Figure C2 represents schematically how coefficient matrix A_G will be populated. Black squares indicate non-zero matrix entries. The main and co-diagonals will be populated due to the first and second derivatives in the direction of Y_t, and the far-off diagonals are due to the first derivative in the direction of p_t. In this visualization, it is implicitly assumed that p^*, i.e., the level of the belief toward which p_t reverts, lies somewhere between p_1, and p_2. As a result, the drift of dp_t changes signs going from p_1 to p_2 and, as we will be using an upwind scheme when approximating the derivative in the direction of p_t, the right far-off diagonal is discontinued in the sub-matrix p_2,p_3.

C.2.2 Populating coefficient matrix A_G

To discretize the infinitesimal generator

$$\hat{\mu}_x \partial_y(S_i) + \frac{1}{2}\sigma_x^2 \partial_{yy}(S_i) + \mu_p(p)\partial_p(S_i) \tag{C5}$$

we approximate derivatives by finite differences. For first-order derivatives, we employ the following upwind scheme

$$\mu(x_n)V'(x_n) \approx \mu(x_n)^- \frac{V_n - V_{n-1}}{\Delta x} + \mu(x_n)^+ \frac{V_{n+1} - V_n}{\Delta x}$$

where $\mu(x)^- = min\Big(\mu(x), 0\Big)$ and $\mu(x)^+ = max\Big(\mu(x), 0\Big)$, i.e., we use backward differences if the drift coefficient is negative and forward differences if the drift coefficient is positive. We approximate the second order derivative by central differences

$$V''(x_n) \approx \frac{V_{n+1} - 2V_n + V_{n-1}}{(\Delta x)^2}.$$

Substituting the approximations into (C5) we obtain

$$\begin{aligned}
&\hat{\mu}_x^- \frac{S_{(j,k)} - S_{(j-1,k)}}{\Delta Y} + \hat{\mu}_x^+ \frac{S_{(j+1,k)} - S_{(j,k)}}{\Delta Y} \\
&\qquad + \frac{1}{2}\sigma_x^2 \frac{S_{(j+1,k)} - 2S_{(j,k)} + S_{(j-1,k)}}{(\Delta Y)^2} \\
&+\mu_p(k)^- \frac{S_{(j,k)} - S_{(j,k-1)}}{\Delta p} + \mu_p(k)^+ \frac{S_{(j,k+1)} - S_{(j,k)}}{\Delta p}.
\end{aligned}$$

By collecting terms and rearranging we obtain

$$\underbrace{\left[-\frac{\mu_p(k)^-}{\Delta p}\right]}_{A_{\alpha,i}} S_{(j,k-1)} \tag{C6a}$$

$$+\underbrace{\left[-\frac{\hat{\mu}_x^-}{\Delta Y} + \frac{\frac{1}{2}\sigma_x^2}{(\Delta Y)^2}\right]}_{A_{\beta}} S_{(j-1,k)} \tag{C6b}$$

$$+\underbrace{\left[\frac{\hat{\mu}_x^-}{\Delta Y} - \frac{\hat{\mu}_x^+}{\Delta Y} - \frac{\sigma_x^2}{(\Delta Y)^2} + \frac{\mu_p(k)^-}{\Delta p} - \frac{\mu_p(k)^+}{\Delta p}\right]}_{A_{\gamma,i}} S_{(j,k)} \tag{C6c}$$

$$+\underbrace{\left[\frac{\hat{\mu}_x^+}{\Delta Y} + \frac{\frac{1}{2}\sigma_x^2}{(\Delta Y)^2}\right]}_{A_{\delta}} S_{(j+1,k)} \tag{C6d}$$

$$+\underbrace{\left[\frac{\mu_p(k)^+}{\Delta p}\right]}_{A_{\epsilon,i}} S_{(j,k+1)}. \tag{C6e}$$

The term to the left of the value highlighted in yellow will appear on the main diagonal of A_G. The terms to the left of the values highlighted in blue will appear on the co-diagonals to the left and right of the main diagonal A_G. The terms to the left of the values highlighted in green will appear on the far-off diagonals in A_G.

Going back to the initial example of a 5×3 grid of unknown values, the 7th row in matrix A_G will look as follows

$$\begin{pmatrix} 0 & A_{\alpha,7} & 0 & 0 & 0 & |A_\beta & A_{\gamma,7} & A_\delta & 0 & 0 & |0 & A_{\epsilon,7} & 0 & 0 & 0 \end{pmatrix}.$$

Note that, under the assumption made earlier that p^* is somewhere between p_1 and p_2, the element $A_{\epsilon,7}$ and all elements $A_{\epsilon,i}$ for $i > 5$ would be zero because of the upwind scheme we employ. Unlike in Figure C2, we include these elements for illustrative purposes as they are populated with zeros rather than being left empty. Figure C3 displays coefficient matrix A_G, highlighting the corresponding generator elements.

Figure C3: : Coefficient matrix A_G with elements highlighted in the 7-th row.

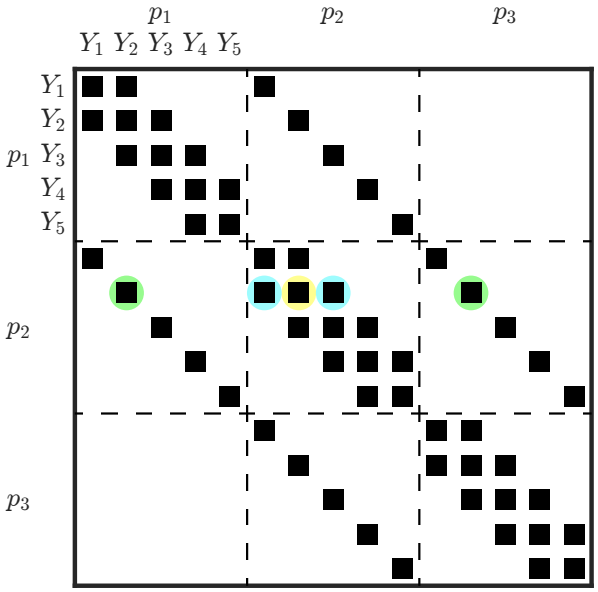

Similarly, Figure C4 highlights the locations of the corresponding value function values on the $7 \times (3+2)$ grid.

Figure C4: : Equidistant $7 \times (3+2)$ grid with highlighted 5-point stencil.

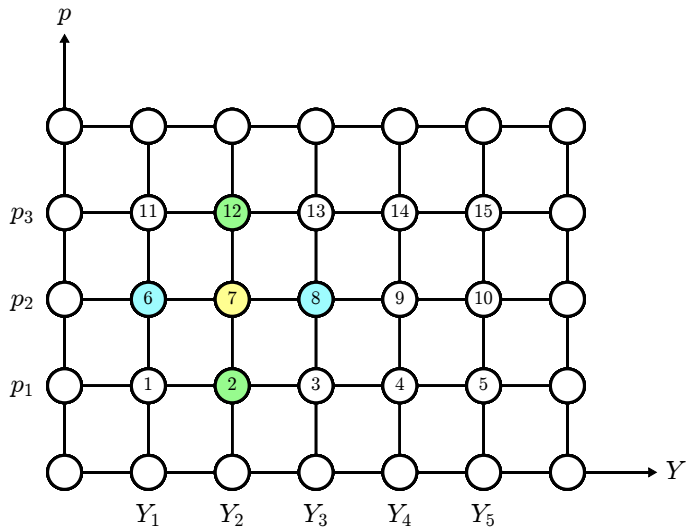

Multiplying the 7-th row of A_G with vector S yields (C6) for $j = 2$ and $k = 2$.

C.2.3 Adjusting A_G and u for boundary conditions

Whenever the 5-point stencil illustrated in Figure C4 encompasses elements outside the 5×3 inner grid, we must impose boundary conditions.

We first consider the case when elements from the left edge of the grid are required. As an example, we illustrate the case for $S_{(1,2)}$ in Figure C5.

Figure C5: : 5-point stencil centered on $S_{(1,2)}$ encompassing $S_{(0,2)}$.

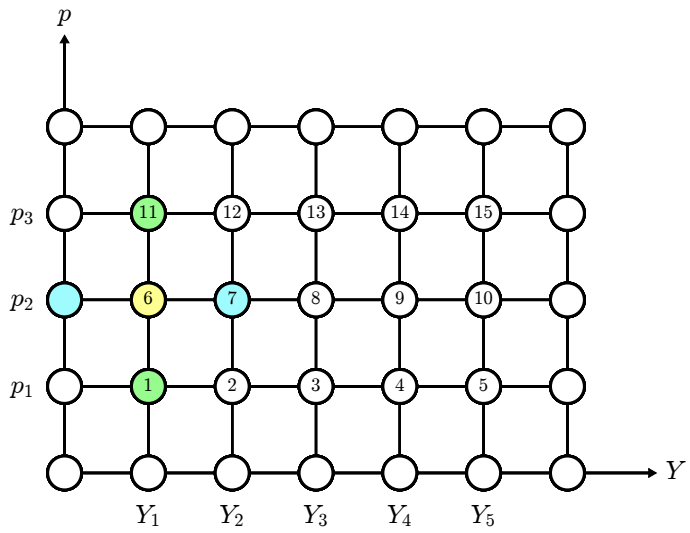

Setting $j = 1$ in (C6) we need to make an assumption for the values of $S_{0,k} = S(Y^{min}, p_k)$. Boundary condition (C2) must hold when $X_t \to 0$. Thus, if Y^{min} is chosen to be sufficiently small, we can set $S_{(0,k)} = 0$ for all levels of p_k. Given this, the term $A_\beta S_{(0,k)}$ vanishes from equation (C6). Going further, we choose to partition matrix A_G, i.e., exclude nodes with ex-ante *known* values from vector S. This way, vector S, which we obtain as a solution to (C4), will only contain the *unknown* values from the $n_Y \times n_p$ inner grid. In order to achieve this, it has to be ensured that, counting from the end (bottom right), every n_Y-th element on the left co-diagonal is set to zero. Vector u, on the other hand, remains unchanged.

Figure C6: : Coefficient matrix A_G with $A_{\beta,6} = 0$ highlighted in red.

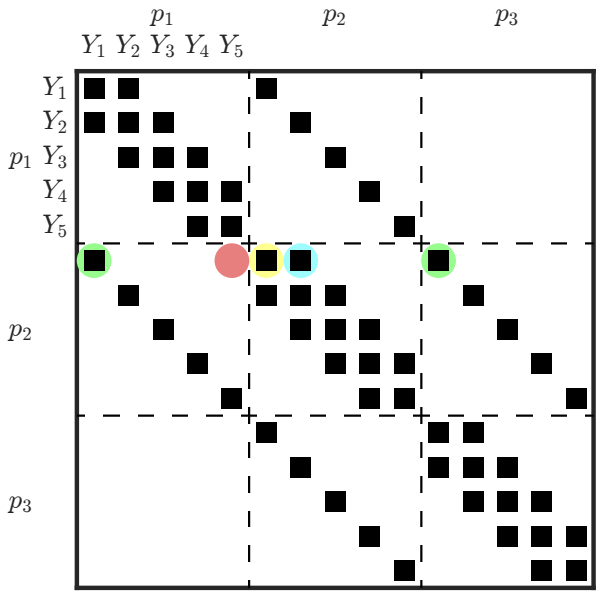

We once again illustrate the case for when the stencil is centered on $S_{(1,2)}$, i.e., S_6, in Figure C6. Had we not adjusted A_G for boundary conditions by setting $A_{\beta,6} = 0$ (element highlighted in red), it would be incorrectly multiplied with S_5. Multiplying the 6-th row of A_G with vector S yields (C6) for $j = 1$ and $k = 2$, assuming the boundary condition that $S_{(0,2)} = 0$ holds.

Next, we consider the case when elements from the right edge of the grid are required. As an example, we illustrate the case for $S_{(5,2)}$ in Figure C7.

Figure C7: : 5-point stencil centered on $S_{(5,2)}$ encompassing $S_{(6,2)}$.

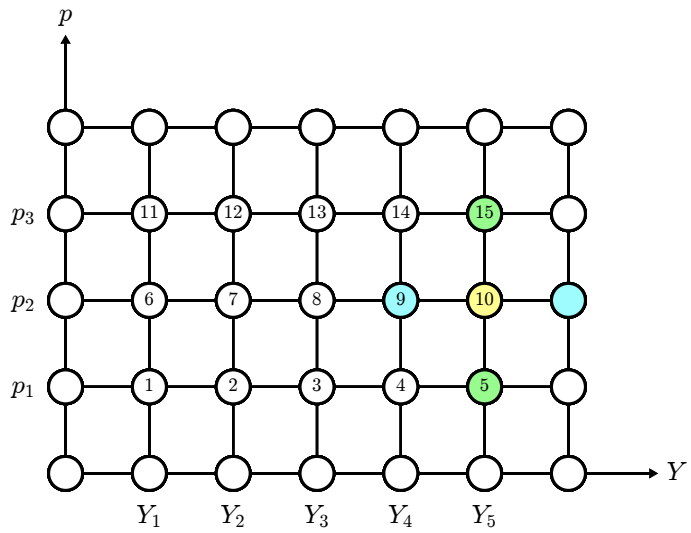

Setting $j = 5$ in (C6) we now need to make an assumption for the values of $S_{(6,k)} = S(Y^{max}, p_k)$. Boundary condition (C3) must hold when $X_t \to \infty$. Thus, if Y^{max} is chosen to be sufficiently large, we can approximate the value of levered

equity by setting

$$S_{(n_Y+1,k)} = (1-\eta)\left(e^{p_{\xi_k}+Y^{max}} - b_k c\right).$$

This time, in order for the discretized HJB-VI to correctly reflect this assumption, we have to ensure that every n_Y-th element on the right co-diagonal is set to zero. In addition, we now also have to adjust u by setting $u_{(n_Y,k)} = (1-\eta)\left(e^{Y_{n_Y}} - c\right) + A_\delta S_{(n_Y+1,k)}$ for all k. We once again illustrate the case for when the stencil is centered on $S_{(5,2)}$, i.e., S_{10}, in Figure C8.

Figure C8: : Coefficient matrix A_G with $A_{\delta,10} = 0$ highlighted in red.

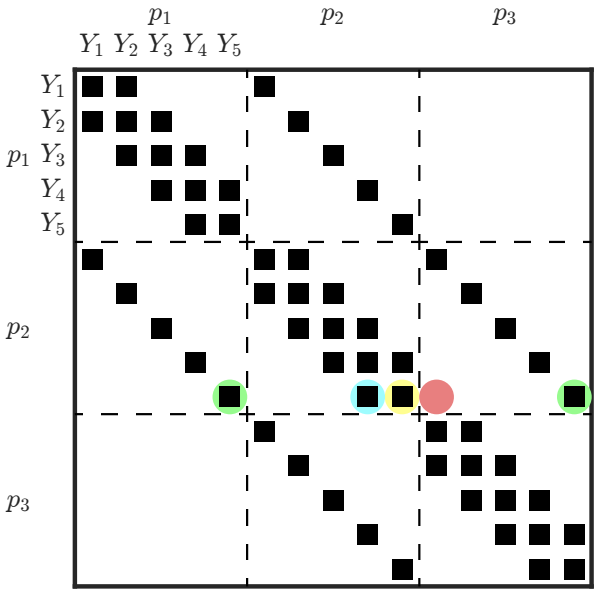

Multiplying the 10-th row of A_G with vector S and adding u_{10} yields (C6) $+(1-\eta)\left(e^{Y_{n_Y}} - c\right)$ for $j = 5$ and $k = 2$, given boundary condition $S_{(6,2)} = (1-\eta)\left(e^{p_{\xi_2}+Y^{max}} - b_2 c\right)$.

Next, we consider the cases when elements from the top or the bottom edge of the grid are required. We limit our discussion to the case of the top edge of the grid, as equivalent arguments can be used in both cases. As an example, we illustrate the case for $S_{(2,3)}$ in Figure C9.

Figure C9: : 5-point stencil centered on $S_{(2,3)}$ encompassing $S_{(2,4)}$.

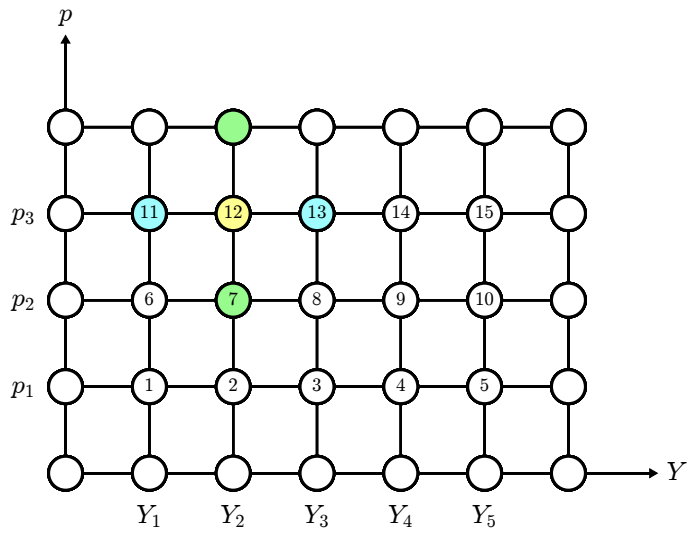

As p_t is a probability, setting the upper cut-off point $p_{n_p} = 1$ from the outset is sensible. Therefore, all nodes in the top row are pseudo nodes as they lie outside the domain. Unlike in the previous cases, in the direction of Y_t, it is not necessary to make additional assumptions about their values. To see this, recall that we employ an upwind scheme when discretizing first derivatives and that between jumps p_t will mean revert towards p^*. As a result, we know that $p_{n_p} \geq p^*$, thus $\mu_p(n_p) \leq 0$ and $\mu_p(n_p)^+ = 0$. This means that when $k = 3$ in (C6) the last term (C6e) will be zero for all possible values of $S_{(j,4)}$. As $A_{\epsilon,(j,3)} = 0$ for all j, no further adjustments of A_G or u are necessary, i.e., no elements have to be manually set to zero. Strictly speaking, a hypothetical $A_{\epsilon,(2,3)} = A_{\epsilon,12}$ would in fact lie outside of A_G as illustrated in Figure C10.

Figure C10: : Coefficient matrix A_G with hypothetical $A_{\epsilon,12} = 0$ highlighted in red.

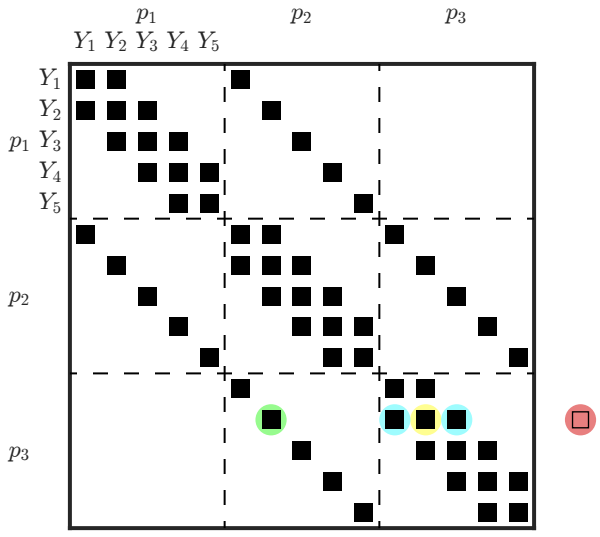

Multiplying the 12-th row of A_G with vector S yields (C6) for $j = 2$ and $k = 3$.

Following the same reasoning, no assumptions have to be made for values of the pseudo nodes of the bottom row, and likewise, no further corrections of A_G or u are necessary.

C.2.4 Populating matrix A_J

As a last step, we discretize the term which appears due to the presence of jumps in firm earnings,

$$\tilde{\lambda}(p)\omega(p)\int_{-\infty}^{0} S\Big(Y+Z_k, p+\sigma_p(p)\Big)f(Z_k)dZ_k, \tag{C7}$$

and construct A_J. As $p+\sigma_p(p)$ is non-random and otherwise does not affect the jump-size distribution in any way, we suppress this argument together with $\tilde{\lambda}(p)\omega(p)$ for notational clarity for the moment. Effectively, we have to discretely approximate the expected post-jump value $S(Y_j+Z_k)$ for a given initial log-earnings level Y_j

$$E\left[S(Y_j+Z_k)\right] = \int_{-\infty}^{0} S(Y_j+Z_k)f(Z_k)dZ_k.$$

We do so by means of numerical integration. Applying the simple trapezoidal quadrature rule and assuming that the value function is currently in state $S_j = S(Y_j)$ before the jump occurs, its expected post-jump value can be written as

$$\begin{aligned}
\int_{-\infty}^{0} S(Y_j+Z)f(Z)dZ &\approx \frac{S(Y_j+Z_j)f(Z_j)}{2}h + \sum_{l=2}^{j-1} S(Y_j+Z_l)f(Z_l)h + \frac{S(Y_j+Z_1)f(Z_1)}{2}h && \text{(C8a)}\\
&= \Big(\tfrac{f(Z_j)}{2}h \quad f(Z_{j-1})h \quad \cdots \quad f(Z_2)h \quad \tfrac{f(Z_1)}{2}h \quad \underbrace{0 \quad \cdots \quad 0}_{1\times(n_Y-j)}\Big)\, S && \text{(C8b)}\\
&= \mathrm{J}_j S, && \text{(C8c)}
\end{aligned}$$

where vector $Z = \left[(Y_{n_Y}\cdots Y_1)' - Y_{n_Y}\right]$ contains all possible on-grid earnings jump sizes, $h = \Delta Y$ is the uniform grid spacing, and $S = (S_1 = S(Y_1), \cdots, S_{n_Y} = S(Y_{n_Y}))'$. Thus J_j, becomes a vector of probabilities. Its first j probabilities correspond to jumps of size $\{Z_j, \cdots, Z_1\}$, of which Z_1 is a jump of size zero and Z_j represents the maximum possible jump given an initial level Y_j to the last value on the far left of the grid for Y, i.e., $Y_j + Z_j = Y_1$.[25] Essentially, each J_j is a probability mass function approximating the density $f(Z)$. Note that the trailing zeros in (C8b) are due to the fact that we only allow for negative jumps, i.e., states higher than the current one are reached with probability zero when a jump occurs. The number of non-zero elements decreases with decreasing j as the pre-jump level S_j approaches the grid's lower cut-off point.

A common concern in the option pricing literature is the impact of truncation errors when employing a finite difference approach in the context of jump-diffusion models. These errors are introduced due to the fact that, typically, the integration domain cannot be fully encompassed by the computational domain and are of concern because options retain extrinsic value even after large jumps "out of the money". While in the context of our model, there is no upper truncation error due to the choice of jump size distribution, the lower truncation error is represented by the first integral in

$$\int_{-\infty}^{Z_j} S(Y_j+Z)f(Z)dZ + \int_{Z_j}^{0} S(Y_j+Z)f(Z)dZ = \int_{-\infty}^{0} S(Y_j+Z)f(Z)dZ.$$

However, as we aim to accurately estimate the default boundary, we set $Y_1 < \ln(X_D)$. Coincidentally, this eliminates any lower truncation error concerns as $S(X_i) = 0$ for all $X_i < X_D$ due to the equity owner's limited liability.

Stacking row vectors J_j for $j = 1, \cdots, n_Y$ we construct the following $n_Y \times n_Y$ matrix

$$\mathrm{J} = \begin{pmatrix}
1 & 0 & \cdots & 0 & 0\\
\frac{f(Z_2)}{2}h & \frac{f(Z_1)}{2}h & \cdots & 0 & 0\\
\vdots & & \ddots & & \vdots\\
\frac{f(Z_{n_Y-1})}{2}h & f(Z_{n_Y-2})h & \cdots & \frac{f(Z_1)}{2}h & 0\\
\frac{f(Z_{n_Y})}{2}h & f(Z_{n_Y-1})h & \cdots & f(Z_2)h & \frac{f(Z_1)}{2}h
\end{pmatrix}$$

where we define the first row vector to be a unit vector as starting out from Y_1 there is nowhere left to jump on the grid. Once again, because upward jumps are not possible, J is a lower triangular matrix. Furthermore, because of the change of variables from the original state variable X to Y, h is a constant and identically indexed Z take identical values across all rows. As a result, starting from the second column onward, J is also a Toeplitz matrix. Values on the main diagonal

[25] In particular, $Y_j + Z_j = Y_j + [Y_{n_Y-(j-1)} - Y_{n_Y}] = Y_j - (j-1)\Delta Y = Y_1$.

represent the probability of observing a jump of size zero, whereas values in the first column represent the probabilities of jumping from the starting value Y_j associated with row j to Y_1.

Returning to (C7), when integrating, one has to consider that jumps also impact equity prices through their impact on beliefs, in other words, the second argument of the integrand. While Z_k and J are both independent of p_t, i.e., the earnings jump sizes and probabilities of observing them do not vary with the agent's belief, the estimated risk-neutral jump intensity and equity prices do change in response to a change in p_t. Thus, first, as a further auxiliary step toward constructing A_J, we define

$$\hat{\mathrm{J}}(k) = \hat{\lambda}_k \mathrm{J},$$

where k, as defined earlier, identifies elements on the p grid, as opposed to the firm index k. Next, while A_J is of the same dimension as A_G and sorted according to the same lexicographical order, our double indexing will now refer to one of the $n_p \times n_p$ submatrices (blocks) of size $n_Y \times n_Y$ with k_1 identifying row and k_2 identifying column partitions. Note that p_{k_1} and p_{k_2} correspond to pre- and post-jump belief levels. While the integrand depends on the post-jump belief $p_{k_1}[1 + J_p(p_{k_1})]$, that value may not lie on the p grid, i.e., there might be no k_2 such that $p_{k_2} = p_{k_1}[1 + J_p(p_{k_1})]$. To account for this, we define $k_{2,l}(k_1)$, $k_{2,r}(k_1)$ to represent the indices of the two closest on-grid, post-jump belief values for a given pre-jump belief with index k_1 and $w_l(k_1)$, $w_r(k_1)$ to be the linear interpolation weights, i.e., $w_l(k_1)$ equals the relative distance from $p_{k_1}[1 + J_p(p_{k_1})]$ to $p_{k_{2,r}(k_1)}$ and vice versa. Then in each block row $k_1 \in \{1, ..., n_p\}$ of A_J we set $A_{J,[k_1,k_{2,i}(k_1)]} = w_i(k_1)\hat{\mathrm{J}}(k_1)$ for $i \in \{l, r\}$ while all other blocks are zero matrices. Placing $\hat{\mathrm{J}}(k)$ according to this scheme accounts for the second argument of the integrand.

We illustrate a hypothetical A_J in Figure C11.

Figure C11: : Schematic representation of jump operator matrix A_J.

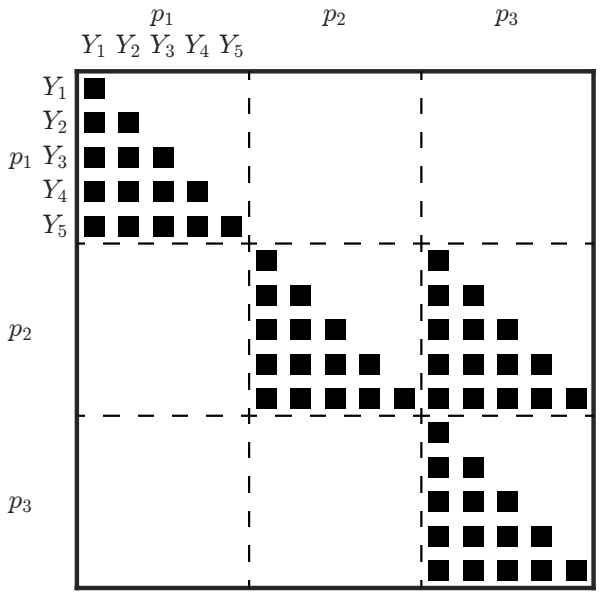

As before, we represent the case where $n_Y = 5$, $n_p = 3$ with $p_1 = 0$ and $p_3 = 1$. Given that p_{k_2} will always be 0 and 1 for $p_{k_1} = 0$ and $p_{k_1} = 1$ respectively, the top-left and bottom-right blocks of A_J will always be populated, while the remaining blocks in those rows are zero matrices. Looking at the middle block row, it is implicitly assumed that $p_2[1 + J_p(p_2)]$ is between p_3 and p_2 and thus we approximate the true $E_{t-}\left[S_t \mid p_t = p_{t-}[1 + J_p(p_{t-})]\right]$ by a weighted average of $E_{t-}\left[S_t \mid p_t = p_2\right]$ and $E_{t-}\left[S_t \mid p_t = p_3\right]$ resulting in sub-matrices $[p_2, p_2]$ and $[p_2, p_3]$ being populated. Multiplying A_J with S will yield 15 approximations of (C7) for 3 levels of pre-jump beliefs and 5 levels of pre-jump earnings each.

C.2.5 Setting up a Linear Complementarity Problem

To solve the problem numerically, we first rewrite (C1) as

$$\min\{\rho \circ S - u - AS, S\} = 0$$

with equivalent formulation

$$\begin{aligned} S'(\rho \circ S - u - AS) &= 0 \\ S &\geq 0 \\ \rho \circ S - u - AS &\geq 0. \end{aligned}$$

Substituting terms $z = S$, $B = \text{diag}(\rho) - A$ and $q = -u$ we obtain a standard Linear Complementarity Problems (LCP) form

$$\begin{aligned} z'(Bz + q) &= 0 \\ z &\geq 0 \\ Bz + q &\geq 0, \end{aligned}$$

which can be solved numerically for z using, e.g. a Newton-type method for positive-semidefinite linear complementarity problems.

C.2.6 Finding the prices to the remaining earnings flow claims

Having determined the price of levered equity, we next explain how to obtain the prices of the remaining claims to earnings. The table below lists individual claim holders and their respective payoffs.

Equity holders receive residual earnings after paying the coupon and taxes up until default. Limited liability allows them to declare default without incurring any further costs.

Debt holders receive coupon payments until default is declared. In default, they gain control over the remaining after-tax EBIT flow with present value $(1-\eta)p_X(p_{\tau_D})X_{\tau_D}$ of which a share of $(1-\alpha)$ is lost due to bankruptcy costs.

In bankruptcy, a share of $(1-\alpha)$ of the after-tax residual value of earnings is lost, and no additional costs of this kind are accrued while the firm is solvent.

The tax entity collects a flow $\eta(X_t - c)$ up until default and a one-off payment of $\eta\left[p_X(p_{\tau_D})X_{\tau_D}\right]$ in the event of default.

Stakeholder	$0 < t < \tau_D$	$t = \tau_D$
Equity	$(1-\eta)(X_t - c)$	0
Debt	c	$\alpha(1-\eta)\left[p_X(p_{\tau_D})X_{\tau_D}\right]$
Bankruptcy costs	0	$(1-\alpha)(1-\eta)\left[p_X(p_{\tau_D})X_{\tau_D}\right]$
Taxes	$\eta(X_t - c)$	$\eta\left[p_X(p_{\tau_D})X_{\tau_D}\right]$

Ultimately, the present values of all four claims have to sum to the present value of the claim to unlevered and untaxed earnings $p_X(p_t)X_t$. This means that once three out of four claims have been priced, we can use this identity to determine the present value of the remaining last claim as a difference.

The present value of bankruptcy costs

Solving the Equity owner's optimal stopping problem yields not only the prices of levered equity but simultaneously divides the earnings-belief space into a default and continuation region. This division applies in the same way to all other claims and allows one to treat them as regular partial integro-differential boundary value problems with known boundaries.

As a first step towards pricing the three remaining claims, we will determine the present value of bankruptcy costs given by

$$BC(X_t, p_t) = (1-\alpha)(1-\eta)\tilde{E}_t\left[\frac{\pi_{\tau_D}}{\pi_t}\ p_X(p_{\tau_D})X_{\tau_D}\right],$$

where $\tau_D = \inf\{\tau > t : X_\tau \leq X_D(p_\tau)\}$ and function $X_D(p_t)$ is now known from having solved the equity owners optimal default problem. Note that in contrast to levered equity, claim holders receive only a terminal instead of only intermediate payoffs. This means that the claim loses value the less likely default with non-zero residual earnings, i.e., $0 < X_{\tau_D} \leq X_D(p_{\tau_D})$, becomes. Thus, the present value of bankruptcy costs $BC(X_t, p_t)$ solves the HJB-VI embedded PDE after dropping the intermediate payoff term

$$\Big[r(p) + \lambda_x + \tilde{\lambda}(p)\omega(p)\Big]BC(Y,p) - \Big[(\mu_x - \gamma\sigma_c\sigma_x^{\text{sys}}\rho_{cx}) - \frac{1}{2}\sigma_x^2\Big]BC_Y(Y,p)$$
$$- \frac{1}{2}\sigma_x^2 BC_{YY}(Y,p) - \mu_p(p)BC_p(Y,p) - \tilde{\lambda}(p)\omega(p)\int_{-\infty}^{0} BC\Big(Y + Z_k,\ p + \sigma_p(p)\Big)f(Z_k)dZ_k = 0$$

and adjusting the boundary conditions to

$$BC(X_t, p_t) = (1-\alpha)(1-\eta)\left[p_X(p_t)X_t\right], \text{ for } X_t \leq X_D(p_t)$$

and

$$\lim_{X_t \to \infty} BC(X_t, p_t) = 0. \tag{C9}$$

We solve this PDE likewise with a finite difference approach. Once vector S has been obtained, the default region D corresponds to the set of points for which the value of levered equity is zero. We define $D = \{i | S_i = 0\}$ as the set of lexicographical indices in the default region. To determine the present values of bankruptcy cost, we adjust B and q for the default region boundary condition. We set $B_{i,j} = 0$ for all $(i \in D) \wedge (j \neq i)$ and $B_{i,j} = 1$ for all $(i \in D) \wedge (j = i)$. We set $q_i = -(1-\alpha)(1-\eta)\left[p_X(p_i)X_i\right]$ for all $(i \in D)$ and $q_i = 0$ for all $(i \notin D)$. Boundary condition (C9) holds trivially. The resulting system

$$Bz + q = 0$$

can be solved in a straightforward fashion.

Pricing corporate debt

Once we have determined the present value of the bankruptcy cost claim, we can combine it with the levered equity claim to form a portfolio that replicates the present value of tax payments. From the distribution of payoffs listed in the Payoff Table, it follows that

$$TAX(X_t, p_t) = \frac{\eta}{1-\eta}S(X_t, p_t) + \frac{\eta}{(1-\eta)(1-\alpha)}BC(X_t, p_t).$$

Finally, we can find the price of corporate debt by evaluating

$$D(X_t, p_t) = p_X(p_t)X_t - S(X_t, p_t) - BC(X_t, p_t) - TAX(X_t, p_t).$$

C.2.7 The issue of sparsity

When decomposing A and comparing the number of non-zero elements in A_G and A_J, it is immediately obvious that the presence of the compound Poisson process in the earnings process substantially increases the computational burden. By breaking the banded structure of the overall system matrix A, it prohibits the usage of specialized solvers and substantially increases calculation time and memory usage. This problem is compounded when dealing with free boundary value problems, which involve solving a linear complementarity problem instead of just a system of equations. This, e.g., renders the estimation of model parameters employing a reasonably fine grid computationally infeasible, as that requires the repeated solving of multiple LCPs.

For this reason, we employ the following strategy: To retain maximum sparsity in A we use the following approximation when constructing A_J

$$E_t\left[S\Big(Y_t + Z_{k,t}, p_t + \sigma_p(p_t)\Big)\right] \approx S\Big(E_t\left[Y_t + Z_{k,t}\right], p_t + \sigma_p(p_t)\Big).$$

This reduces the number of elements in every populated block in A_J from $\frac{n_Y(n_Y+1)}{2}$ down to only n_Y as J_j simplifies from a probability mass function to a unit vector indicating the location of $\int_{-\infty}^{0}[Y_j + Z_k]f(Z_k)dZ_k$ on the Y grid. We use this approximation to speed up the solving of LCPs. However, once approximative prices are determined, we only retain the numerically determined default region represented by the set $\tilde{D}$. Then we solve for exact levered equity prices using the original A_J defined earlier, now taking $X_D(p_t)$ via $\tilde{D}$ as given, thus transforming the problem from a free boundary value problem to one with a known boundary. The approach for a known boundary is the same as that described for the bankruptcy costs claim. All remaining steps of our solution strategy remain the same.

C.2.8 Optimal capital structure

Up to this point, we have discussed how to determine the prices of equity and debt for an exogenously specified coupon c. Next, we turn to determining the optimal level of debt to be issued at the point of firm inception. We use the standard approach of maximizing the portfolio value of initial firm owners, taking into account the optimal default strategy of future equity owners. For simplicity, we assume that firms start with normalized earnings $X_0 = 1$ and thus, the optimal coupon will only be a function of the current belief about the state of the economy, i.e., of the form $c^*(p_0)$. Formally, assuming debt is subject to issuance costs ι, at the time of firm inception, initial owners aim to maximize $F_0 = S_0 + (1-\iota)D_0$ and the problem of choosing an optimal capital structure can be written as

$$c^*(p_0) = \arg\max_c \; F_0\left(c, p_0, X_D(p_0, c)\right),$$

where c is a static control, p_0 is a state variable and $X_D(p_0, c)$ highlights the dependence of the future equity owners' optimal default strategy on the initial owners' capital structure choice. As a result, when endogenizing the optimal capital structure, all claims to firm earnings are functions of three variables, i.e., a firm's current earnings, the current beliefs as well as the coupon determining initial belief at the time of firm inception, e.g., we write $S(X_t, p_t, c^*(p_0)) = S(X_t, p_t, p_0)$. X_t and p_t are time-varying while p_0 remains static over the lifetime of a firm. X_t and p_0 are firm-specific, while p_t is the market-held belief about the current state of the economy.

We approximate $c^*(p_0)$ numerically in two steps. First, we compute $S(X, p, c_j)$ and $D(X, p, c_j)$ for $c_j \in \{\underline{c}, \cdots, \overline{c}\}$. Second, for each p_i on the belief grid, we estimate $c^*(p_i)$ by evaluating $S(1, p_i, c_j) + (1-\iota)D(1, p_i, c_j)$, approximating $F(c, p_i)$ by fitting a fourth-order polynomial through this set of points and searching for the firm value maximizing $c^*(p_i)$ in $[\underline{c}, \overline{c}]$.

Having obtained $c^* = \{c^*(0), \cdots, c^*(1)\}$, we approximate $S(X_t, p_t, p_0)$ and $D(X_t, p_t, p_0)$ by computing $S(X, p, c^*(p_j))$ and $D(X, p, c^*(p_j))$ for all $c^*(p_j) \in c^*$ and linearly interpolating.

C.2.9 Grid parameters

When simulating the model, we use the grid parameters below. We use the same grid in both the p_t and the p_0 dimension.

Parameter	Symbol	Value
Min Log Earnings	Y^{min}	log(0.01)
Max Log Earnings	Y^{max}	log(5)
Number of Grid Points	n_Y	1300
Lower bound for p	p^{min}	0
Upper bound for p	p^{max}	1
Number of Grid Points	n_p	11

C.3 CDX spreads

In our model, we aim to price a Markit CDX.NA.IG equivalent derivative, which is composed of 125 of the most liquid North American firms with investment-grade credit ratings that trade in the CDS market. Therefore, we set $N_F = 125$, $\mathcal{N}_F(t_{\text{roll}}) = \{1, 2, \cdots, 125\}$ and assume that the index provider's credit screening effectively eliminates the risk of including firms that could experience an extremely rare, idiosyncratic, exogenous exit shock over the lifetime of the contract, i.e., we set $dN_{k,\tau} = 0$ for all k while $\tau \in [t_{\text{roll}}, T]$. For simplicity, we set $t_{\text{roll}} = t$ and omit the explicit dependence of the relevant variables on the roll date in the following.

The key variables which impact the value of the CDX index are $\{R_{\tau_{D,k}}\}_{k \in \mathcal{N}_F}$ and the stochastic process n as they determine the contract's payoffs to both parties. The former variable is the set of stochastic recovery rates. Let time $t_{0,k}$ be the time firm k was incepted and issued debt and $\tau_{D,k}$ denote its default time defined as $\tau_{D,k} = \inf\{\tau > t_{0,k} : X_{k,\tau} \leq X_D(p_\tau, p_{t_{0,k}})\}$, we compute the firm's recovery rate as

$$R_{k,\tau_{D,k}} = \frac{D_{k,\tau_{D,k}}}{D_{k,t_{0,k}}}. \tag{C10}$$

which is the ratio of the corporate debt value for firm k at default relative to its value at issuance. In the case of a singular default, a CDX with \$1 notional entitles the protection buyer to a pay-off of $\$1 \cdot \frac{1}{N_F} \cdot (1 - R_{k,\tau_{D,k}})$. We denote by $n_{t,s}(t_{\text{roll}})$ the fraction of firms in the index that have defaulted between the times t and $s > t$:

$$n_{t,s}(t_{\text{roll}}) = \frac{1}{N_F} \sum_{k \in \mathcal{N}_F(t_{\text{roll}})} 1_{\{t < \tau_{D,k} \leq s\}}. \tag{C11}$$

A CDX with \$1 notional entitles the protection seller to quarterly insurance premia amounting to $\$1 \cdot (S_{\text{CDX}} \cdot \frac{1}{4}) \cdot (1 - n_{t,s})$ plus additional accrued premia in the case of default since payments are made in arrears. The latter are computed on a pro rata temporis basis.

In the context of our model, for a set of initial conditions, that is 125 initial beliefs, 125 current earnings levels and the market belief at the date of contract commencement, we can determine CDX spreads by means of Monte Carlo pricing. We will discuss our simulation approach next.

C.3.1 Pricing the CDX for given initial conditions

By convention, CDX spreads are set such that the value of the contract is zero at inception. Thus, we need to determine the present values of premium and protection payments first and solve for the spread subsequently. Given a set of initial conditions $\left\{\{X_{k,\tau}\}_{k \in \mathcal{N}_F(\tau)}, \{p_{0,k}\}_{k \in \mathcal{N}_F(\tau)}, p_\tau\right\}_{\tau = t}$ we can do this in straightforward fashion by simulating a panel of 125 firms under the SDF implied pricing measure $\mathbb{Q}$, calculating discounted realized payoffs of both contracts and aggregating them to their respective present values. In our simulations, we proceed as follows: For a given path of the economy (u) and time to maturity ($T - t$), we first simulate the following system

$$dp_t = \kappa(f_H - p_{t-})dt + \sigma_p(p_{t-})\ (dN_t - \tilde{\lambda}(p_{t-})dt) \tag{C12a}$$

$$E^{\mathbb{Q}}_{t-}[dN_t] = \lambda^{\mathbb{Q}}(p_{t-})dt \tag{C12b}$$

$$\lambda^{\mathbb{Q}}(p_{t-}) = \omega(p_{t-})\tilde{\lambda}(p_{t-}) \tag{C12c}$$

$$\tilde{\lambda}(p_{t-}) = p_{t-}\lambda_H + (1 - p_{t-})\lambda_L. \tag{C12d}$$

While, objectively, Poisson process N_t is assumed to be Markov Modulated, the agent cannot observe switches in its intensity λ_t as they occur. Instead, she updates her belief p_t that $\lambda_t = \lambda_H$ depending on whether she does or does not observe jumps over dt. For example, notice that whenever $dN_t = 1$, $dp_t \geq 0$ as

$$\sigma_p(p) = \frac{\lambda_H - \lambda_L}{\tilde{\lambda}(p)} p(1 - p) \geq 0,$$

i.e., the probability of observing future increments in N_t increases. Thus, from her perspective, as described by system (C12), N_t evolves as a self-exciting point process, i.e., a process for which the occurrence of past jumps increases the likelihood of future jumps. One can simulate this system directly using Ogata's modified thinning algorithm, see e.g. Ogata (1981). This method for simulating Hawkes processes is a modification of an algorithm for inhomogeneous Poisson processes with an intensity bounded from above. It is particularly suitable for our application as the risk-neutral intensity $\lambda^{\mathbb{Q}}(p_{t-}) = \omega(p_{t-})\tilde{\lambda}(p_{t-})$ decays between arrivals as p_t drifts toward p^*, provided $\lambda^{\mathbb{Q}}(p)$ is monotonically increasing in p. This condition holds at the estimated parameters because the linear growth of $\tilde{\lambda}(p)$ in p dominates the decline of the uncertainty premium $\omega_L(p)$ past its peak. The algorithm uses the current intensity as the local bounding rate for each inter-arrival interval.[26]

Our assumed time continuity implies default boundaries are monitored continuously. Therefore, to mitigate simulation bias, we simulate all state variables at a daily frequency setting $\Delta t = 1/252$. For a sequence of jump arrivals at $0 < \tau_1^{(u)} < \tau_2^{(u)} < \cdots \leq (T - t)$ from N_t we proceed with simulating 125 earnings growth series. Let the number of realized jumps between days t and $t + \Delta t$ be $n_J^{(u)}(t + \Delta t) = |\{\tau_i \in \tau^{(u)} : t < \tau_i \leq t + \Delta t\}|$, then risk-neutral earnings growth rates for firm k are approximated by

$$\Delta \log\left(X^{(u)}_{k,t+\Delta t}\right) = \left[(\mu_x - \gamma\sigma_c\sigma_x^{\text{sys}}\rho_{cx}) - \frac{1}{2}\sigma_x^2\right]\Delta t + \sigma_x^{\text{id}}\sqrt{\Delta t}B^{(u)}_{x,k,t+\Delta t} + \sigma_x^{\text{sys}}\sqrt{\Delta t}B^{(u)}_{x,c,t+\Delta t} - Z^{(u)}_{k,t+\Delta t},$$

[26] Monotonicity of $\lambda^{\mathbb{Q}}(p)$ can be verified numerically on the belief grid for any parameter configuration. The belief decay and jump after N_t arrivals are described by (C13) and (C14).

where $\sigma_x = \sqrt{(\sigma_x^{\text{id}})^2 + (\sigma_x^{\text{sys}})^2}$, $B^{(u)}_{x,k,t+\Delta t}$ and $B^{(u)}_{x,c,t+\Delta t}$ are independent draws from the standard normal distribution and $Z^{(u)}_{k,t+\Delta t}$ is the sum of $n_J^{(u)}(t+\Delta t)$ independent draws from an exponential distribution with mean $1/\epsilon_x$.

Having simulated a full set of state variables for one path of the economy, we proceed with processing all derivative quantities. Default times determine the payoffs to both parties. Thus, we first evaluate $\tau^{(u)}_{D,k} = \inf\{\tau > t : X^{(u)}_{k,\tau} \leq X_D(p_\tau, p_{0,k})\}$ for all k. From this, we construct a daily time series of the cumulative loss

$$L^{(u)}_{t,s} = \frac{1}{N_F} \sum_{k \in \mathcal{N}_F} 1_{\left\{t < \tau^{(u)}_{D,k} \leq s\right\}} \left(1 - R^{(u)}_k\right),$$

where $R^{(u)}_k$ are computed using definition (C10) and $s \in \{t, t+\Delta t, \cdots, T\}$. Subsequently, we aggregate discounted realized loss function increments over the simulation horizon

$$\text{Prot}^{(u)}(T-t) = \sum_{i=1}^{\frac{(T-t)}{\Delta t}} e^{-\sum_{j=0}^{(i-1)} r(p^{(u)}_{t+j\Delta t})\Delta t} [L^{(u)}_{t,t+i\Delta t} - L^{(u)}_{t,t+(i-1)\Delta t}].$$

Likewise, setting $S_{\text{CDX}} = 1$, we evaluate (C11) and aggregate discounted realized scheduled and accrued premia

$$\begin{aligned}\text{Prem}^{(u)}(T-t,1) =& 1 \cdot \frac{1}{4} \cdot \sum_{j=1}^{4(T-t)} \left[e^{-\sum_{m=0}^{\frac{j}{4\Delta t}-1} r(p^{(u)}_{t+m\Delta t})\Delta t} \left(1 - n^{(u)}_{t+\frac{1}{4}j}\right) \right. \\ &\left. + \sum_{i=\frac{j-1}{4\Delta t}+1}^{\frac{j}{4\Delta t}} e^{-\sum_{m=0}^{(i-1)} r(p^{(u)}_{t+m\Delta t})\Delta t} \; 4\left(i\Delta t - \frac{1}{4}(j-1)\right) \left[n^{(u)}_{t+i\Delta t} - n^{(u)}_{t+(i-1)\Delta t}\right] \right].\end{aligned}$$

The present values of both legs are then approximated by averaging

$$\text{Prot}(T-t) = \frac{1}{N_u} \sum_{u=1}^{N_u} \text{Prot}^{(u)}(T-t)$$

and

$$\text{Prem}(T-t,1) = \frac{1}{N_u} \sum_{u=1}^{N_u} \text{Prem}^{(u)}(T-t),$$

where N_u denotes the number of simulated paths. Finally, the spread is obtained by

$$S_{\text{CDX}} = \frac{\text{Prot}(T-t)}{\text{Prem}(T-t,1)}.$$

C.3.2 Generating initial conditions

The procedure we described requires a full set of initial conditions for initializing the CDX pricing simulations. We denote this set by $\mathcal{F}_t = \left\{\{X_{k,t}\}_{k \in \mathcal{N}_F(t)}, \{p_{0,k}\}_{k \in \mathcal{N}_F(t)}, p_t\right\}$. However, in practical terms, data on constituents' earnings are difficult to obtain, and beliefs are unobservable. Moreover, even when this data is available, as in the case when we are simulating economies for estimating model parameters via the Simulated Method of Moments (SMM), computing spreads across entire time series of initial conditions by means of repeated simulations is computationally unfeasible. Guided by the fact that, unlike for earnings, an empirical proxy for leverage can be constructed from available data and that, through the lens of our model, firm-level leverage subsumes information on a firm's current earnings, initial belief and the current market-wide held belief, we will use the current average CDX leverage $\bar{L}_t$ and belief p_t as the starting point to generate initial conditions for our simulation approach.[27] In particular, let $\tilde{\mathcal{F}}_t = \{\bar{L}_t, p_t\}$, where of course $\tilde{\mathcal{F}}_t \subset \mathcal{F}_t$, the goal is to perform the following approximation

$$E^{\mathbb{Q}}\left[\,\cdot \mid \mathcal{F}_t\right] \approx E^{\mathbb{Q}}\left[\,\cdot \mid \tilde{\mathcal{F}}_t\right].$$

Aside from required data being easier to obtain, allowing us ultimately to compare empirical CDX spreads to model-implied ones, introducing this approximation comes with the additional benefit of reducing the number of initial conditions we need to specify. Whereas originally, one had to specify $2 \times 125 + 1$ values, now the present values and thus

[27] Within our model, a firm's leverage ratio can be defined as $L(X_t, p_t, p_0) = \frac{D(X_t,p_t,p_0)}{D(X_t,p_t,p_0)+S(X_t,p_t,p_0)}$.

CDX spreads are fully determined by just two values. This, in turn, makes pre-pricing the CDX on a grid practical and allows one to substantially reduce computation time when having to determine CDX spreads repeatedly for varying initial conditions.

To facilitate this reduction in dimensionality, we make simplifying assumptions about the joint distribution of CDX' constituents leverages and initial beliefs at the time of contract commencement t. In particular, to generate initial conditions we proceed as follows: For a given pair $(\bar{L}_i, p_i)$, for a given path (u), we draw 125 firm-level leverage ratios $L_{k,t}^{(u)}$ from a shifted, right-truncated log-normal distribution and 125 initial beliefs $p_{0,k}^{(u)}$ from the stationary distribution of p_t. The leverage distribution is truncated at 0.90 and then shifted right by 0.05, thus $L_{k,t}^{(u)} \in [0.05, 0.95]$ for all k. We set the remaining parameters of the distribution such that $E[L_{k,t}^{(u)}] = \bar{L}_i$ and $V[L_{k,t}^{(u)}] = (0.1589)^2$, equivalent to the unconditional, cross-sectional variance of leverage. The distribution of initial beliefs is obtained by simulating p_t to stationarity, as described at the beginning of Appendix C.1. Then, we solve for earnings by numerically inverting

$$X_{k,t}^{(u)} = L^{-1}(L_{k,t}^{(u)}, p_i, p_{0,k}^{(u)})$$

for all k, where $L(X_{k,t}, p_t, p_{0,k})$ denotes the leverage function. Having determined a set of initial conditions, we proceed with the simulation as described in C.3.1.

C.3.3 CDX grid parameters

When simulating the model, we use the following grid parameters.

Parameter	Symbol	Value
Min CDX Leverage	L^{min}	0.15
Max CDX Leverage	L^{max}	0.45
Number of Grid Points	n_L	7
Lower bound for p	p^{min}	p^*
Upper bound for p	p^{max}	1
Number of Grid Points	n_p	7

C.4 Simulations

C.4.1 SMM

We simulate 1,000 economies each populated with 125 firms over 29 years to estimate our model with the SMM. We allow for consumption drops of at most -5.1%, measured peak-to-trough, as observed in the data. The first 10 years act as burn-in.

In our simulations we proceed as follows. We reset the time origin to the start of each simulated panel, so that t denotes elapsed time. For a given economy (u), we first simulate the Markov Modulated Poisson process N_t for 29 years to obtain a sequence of jump arrival times $0 < \tau_1^{(u)} < \tau_2^{(u)} < \cdots \leq 29$.[28] As before, the assumed time continuity implies default boundaries are monitored continuously. Therefore, to mitigate simulation bias, we simulate all state variables at a daily frequency setting $\Delta t = 1/252$. Let the number of realized jumps between days t and $t + \Delta t$ be $n_J = |\{\tau_i \in \tau : t < \tau_i \leq t + \Delta t\}|$, we simulate daily consumption growth rates according to

$$\Delta \log(C_{t+\Delta t}) = (\mu_c - \frac{1}{2}\sigma_c^2)\Delta t + \sigma_c \sqrt{\Delta t} B_c - Z_c,$$

where B_c is a draw from standard normal distribution and Z_c is the sum of n_J independent draws from an exponential distribution with mean $1/\epsilon_c$. Subsequently, we time-aggregate daily consumption and compute annual growth rates. We only proceed with simulating all other parts of the economy if the worst cumulative annual consumption decline does not exceed 5.1% in magnitude; otherwise, we redraw the consumption path.

Next, we simulate 125 earnings growth series, each according to

$$\Delta \log\big(X_{k,t+\Delta t}\big) = (\mu_x - \frac{1}{2}\sigma_x^2)\Delta t + \sigma_x^{\text{id}} \sqrt{\Delta t} B_{x,k} + \sigma_x^{\text{sys}} \sqrt{\Delta t} B_{x,c} - Z_k,$$

[28] For notational clarity we suppress the explicit dependence on simulation path index (u) in the following.

where $\sigma_x = \sqrt{(\sigma_x^{\text{id}})^2 + (\sigma_x^{\text{sys}})^2}$, $B_{x,c} = \rho_{cx} B_c + \sqrt{1-\rho_{cx}^2} B_a$, $B_{x,k}$ and B_a are independent draws from the standard normal distribution and Z_k is the sum of n_J independent draws from an exponential distribution with mean $1/\epsilon_x$. We treat default causing Poisson process $N_{k,t}$ separately. We refer to these types of defaults as *exogenous*, as they would occur under any default policy $X_D(p_t, p_0)$.

Then, setting the agent's prior at $t = 0$ to the long-run state of the Markov chain $p_0 = \frac{\phi_{LH}}{\phi_{LH}+\phi_{HL}}$, we compute the dynamics of the agent's belief for the given sequence of realized jump times τ. In the absence of jumps, between two points in time t_1 and t_2, the belief decays according to

$$p_{t_2} = p^* + \frac{1}{(p_{t_1} - p^*)^{-1} e^{(\lambda_H - \lambda_L)\Delta(t_2 - t_1)} + \Delta^{-1}[1 - e^{(\lambda_H - \lambda_L)\Delta(t_2 - t_1)}]}, \tag{C13}$$

where $t_2 > t_1$, and

$$\Delta = (1 + \overline{\kappa})\sqrt{1 - \frac{4 f_H \overline{\kappa}}{(1+\overline{\kappa})^2}}.$$

Note that t_1 and t_2 do not have to coincide with t and $t + \Delta t$ as jumps can occur at any time between two days. On the other hand, upon observing a jump the pre-jump belief p_{t-} sharply jumps upwards to

$$p_t = p_{t-}[1 + J_p(p_{t-})], \tag{C14}$$

where $J_p(p) = \sigma_p(p)/p$ is the proportional belief jump.

Because firms default and are replaced, the identity of the firm occupying each index slot k changes over time. We track each slot's inception belief as a piecewise-constant time series that resets whenever a replacement firm enters. Finally, we account for defaults in the 125 firm earnings- and generate 125 *initial belief* time series which we denote by $\{p_{0,k,i} : i \in \{0, \Delta t, \cdots, 29\}\}$. For this, for a given k, starting from $t_0 = 0$, we draw an exogenous default arrival time $\tau_X > t_0$ with intensity λ_x. Next, setting $X_{k,t_0} = 1$ and $p_{0,k,i} = p_{t_0}$ for all i, we evaluate $\tau_E = \inf\{t > t_0 : X_{k,t} \leq X_D(p_t, p_{0,k,t})\}$. Whenever $\tau_D = \min(\tau_E, \tau_X) < 29$, we update $t_0 = \tau_D + \Delta t$, rescale the remaining earnings level observations such that the new $X_{t_0} = 1$ and set $p_{0,k,i} = p_{t_0}$, for all $i \geq t_0$. We repeat this until $\tau_D > 29$ for each $k \in \{1, \cdots, 125\}$. Effectively, this means that the day after a default occurs, we reinject a new firm into the economy. The replacement firm starts with one unit of earnings, an initial belief equal to the market belief at the time of its inception and inherits index k of the firm it supersedes. While over the course of the simulated 29 years, more than 125 firms can exist, at any point in time exactly 125 firms simultaneously operate in the market. A particular firm is identified by the index pair $\{k, t\}$ and prices of claims to its earnings stream are fully characterized by its current earnings $X_{k,t}$, its initial belief $p_{0,k,t}$ and the current market-wide belief p_t.

Having simulated a full set of state variables for one economy, we proceed with processing all derivative quantities. To simplify notation, we drop index k and denote initial beliefs as p_0 given that they are constant over the lifetime of a firm. We compute daily before-tax returns of unlevered firms as

$$R^{UL}_{t+\Delta t} = \frac{p_X(p_{t+\Delta t}) X_{t+\Delta t} + X_{t+\Delta t}\Delta t}{p_X(p_t) X_t}.$$

We compute daily returns of levered firms as

$$R_{t+\Delta t} = \frac{S(X_{t+\Delta t}, p_{t+\Delta t}, p_0) + (1-\eta)(X_{t+\Delta t} - c)\Delta t}{S(X_t, p_t, p_0)}.$$

The daily risk-free rate is computed as

$$R^{rf}_t = e^{r(p_t)\Delta t}.$$

To obtain monthly excess returns, we compound daily gross returns until the end of the month and subtract the compounded risk-free return. We set the monthly return of a defaulting firm to $R^m_{\tau_D} = -1$. The replacement firm only enters the sample in the subsequent month. By then, at least 21 daily returns will have been observed for the new firm. We define the market excess return to be the cross-sectional average of levered firm-level excess returns. Firm-level daily leverage ratios are computed as

$$L_t = \frac{D(X_t, p_t, p_0)}{D(X_t, p_t, p_0) + S(X_t, p_t, p_0)}.$$

On the day of default, a firm's leverage ratio equals $L_{\tau_D} = 1$. We compute the average leverage ratio $\bar{L}_t$ as the cross-sectional average of firm-level leverage ratios. We compute monthly CDX spreads as the 21-trading-day average of daily spreads, matching the empirical time-aggregation convention described in Section 4.1:

$$S^T_{\text{CDX}\,t} = \frac{1}{21}\sum_{i=0}^{20} S_{\text{CDX}}(\bar{L}_{t-i\Delta t}, p_{t-i\Delta t}, T).$$

CDX moments are computed from end-of-the-month observation.

C.5 Large Heterogeneous Pool Approximation

Both our large heterogeneous pool approximation (LHetPA) and the large homogeneous pool approximation (LHomPA) of Doshi, Ericsson, Fournier, and Seo (2024) address the same computational challenge: pricing a CDX index whose exact valuation depends on the full cross-section of firm states. Both reduce the state space to two variables. The methods differ in how they treat the cross-section after reduction, and the formal error analysis below clarifies the economic consequences.

In Doshi, Ericsson, Fournier, and Seo (2024), the two state variables are the representative firm's asset value A^r_t and systematic variance V_t. At each pricing date, all firms are set identical ($A^j_t = A^r_t$ for all j), so the index collapses to a single representative firm: $I_t = f(A^r_t, V_t)$. For Monte Carlo pricing, 500 firms are simulated from these identical initial conditions; firms subsequently diverge through future idiosyncratic shocks, but all share the same default boundary A_D and the same recovery rate. This homogeneity assumption eliminates the cross-sectional distribution of distances-to-default at the pricing date: the distribution is a point mass at A^r_t/A_D.

Our two state variables are average leverage $\bar{L}_t$ and the current belief p_t. Rather than collapsing the cross-section, we regenerate it: for each grid point, we draw 125 firm-level leverage ratios from a truncated log-normal distribution with the empirical unconditional dispersion ($\sigma_L = 15.89\%$) and 125 initial beliefs from the stationary distribution. Each firm therefore carries a different optimal coupon $c^*_k(p_{0,k})$ and faces a different default boundary $X_D(p_t, c_k)$. We simulate the full finite pool via Monte Carlo and compute heterogeneous recovery rates R_{k,τ_D} for each defaulting firm.

As shown formally below, this distinction has three quantifiable consequences. First, Proposition C9 and Corollary 1 establish that the homogeneous pool understates the average expected loss by a convexity bias of approximately $\frac{1}{2}G''(\bar{d})\,\text{Var}_{\text{cross}}(d_k)$, where G is the expected loss function, $\bar{d}$ is the mean distance-to-default, and the cross-sectional variance of distances-to-default is driven by the leverage dispersion $\sigma_L = 15.89\%$. Because G is convex for investment-grade firms, evaluating it at the cross-sectional mean (as the LHomPA does) misses the contribution of firms in the left tail — precisely those closest to default. Our non-degenerate leverage draws capture this correction. Second, Proposition C10 shows that uniform recovery understates the protection leg when recovery and default probability are negatively correlated, as they are in structural models where firms closer to the boundary have lower asset values at default. Third, the convexity bias is state-dependent: it grows during stress episodes as firms migrate toward the default boundary and G'' increases. The LHomPA is therefore least accurate when the fear-driven financing channel is most active.

C.5.1 Error analysis of the state-space reduction

The preceding subsections describe how we reduce the 251-dimensional state $\mathcal{S}_t = \{(X_{k,t}, p_{0,k})\}_{k=1}^{N_F} \cup \{p_t\}$ (where $c_k = c^*(p_{0,k})$) to two variables $(\bar{L}_t, p_t)$ and regenerate cross-sectional heterogeneity via Monte Carlo draws. We now formalize the approximation error and compare it to the standard homogeneous-pool approach.

Proposition C8 (Error decomposition) *The approximation error in the protection leg decomposes as*

$$\text{Prot}^{exact}(\mathcal{S}_t) - \text{Prot}^{approx}(\bar{L}_t, p_t) = \underbrace{\text{Prot}^{exact}(\mathcal{S}_t) - \mathbb{E}[\text{Prot}^{exact} \mid \bar{L}_t, p_t]}_{\textit{(I) Information loss}} + \underbrace{\mathbb{E}[\text{Prot}^{exact} \mid \bar{L}_t, p_t] - \text{Prot}^{approx}(\bar{L}_t, p_t)}_{\textit{(II) Distribution approximation}}.$$

Term (I) is common to any method that reduces the state to $(\bar{L}_t, p_t)$. Term (II) depends on the assumed cross-sectional distribution: it is zero if the assumed distribution equals the true conditional distribution $\mathcal{L}(\{L_k, p_{0,k}\} \mid \bar{L}_t, p_t)$.

Proposition C9 (Convexity bias) *Let $G(d) = E^{\mathbb{Q}}_t[(1-R)\,\mathbf{1}_{\{\tau_D \le T\}} \mid d]$ denote the risk-neutral expected loss for a single firm with distance-to-default d. Suppose G is convex on the support of the cross-sectional distribution $\{d_1, \ldots, d_{N_F}\}$ with mean $\bar{d}$. Then*

$$\frac{1}{N_F}\sum_{k=1}^{N_F} G(d_k) \ge G(\bar{d}).$$

The homogeneous-pool approximation evaluates $G(\bar{d})$ (all firms at the mean distance-to-default), which understates the average expected loss. Our approach evaluates $\frac{1}{N_F}\sum_k G(d_k^{(u)})$ with draws from a non-degenerate distribution, capturing the convexity correction.

Proof. Direct application of Jensen's inequality to the convex function G and the discrete distribution $\{d_1, \ldots, d_{N_F}\}$. ■

Corollary 1 (Jensen gap magnitude) *A second-order Taylor expansion of G around $\bar{d}$ gives*

$$\frac{1}{N_F}\sum_{k=1}^{N_F} G(d_k) - G(\bar{d}) \approx \frac{1}{2}G''(\bar{d}) \cdot \mathrm{Var}_{cross}(d_k) + O\big(\mathbb{E}[|d_k - \bar{d}|^3]\big)\,,$$

where $\mathrm{Var}_{cross}(d_k) = \frac{1}{N_F}\sum_k (d_k - \bar{d})^2$. Under the homogeneous pool, $\mathrm{Var}_{cross} = 0$ and the gap vanishes. Under our approach, $\mathrm{Var}_{cross} > 0$ (driven by the cross-sectional leverage dispersion $\sigma_L = 15.89\%$), capturing the leading-order correction.

Proof. Taylor expand $G(d_k)$ around $\bar{d}$: $G(d_k) = G(\bar{d}) + G'(\bar{d})(d_k - \bar{d}) + \frac{1}{2}G''(\bar{d})(d_k - \bar{d})^2 + O(|d_k - \bar{d}|^3)$. Average over k: the linear term vanishes by definition of $\bar{d}$. ■

Proposition C10 (Recovery-default correlation bias) *Suppose recovery R_k and default probability $\mathbb{Q}(\tau_{D,k} \le T)$ are negatively correlated across firms. Then*

$$\frac{1}{N_F}\sum_k E^{\mathbb{Q}}\Big[(1 - R_k)\mathbf{1}_{\tau_{D,k}\le T}\Big] \ge (1 - \bar{R}) \cdot \frac{1}{N_F}\sum_k \mathbb{Q}(\tau_{D,k} \le T),$$

where $\bar{R}$ is the cross-sectional average recovery. The homogeneous pool with uniform recovery uses the right-hand side; heterogeneous recovery uses the left-hand side.

Proof. Recovery R_k is determined by firm k's characteristics at entry, so $E^{\mathbb{Q}}[(1 - R_k)\mathbf{1}_{\tau_{D,k}\le T}] = (1 - R_k)\, q_k$, where $q_k \equiv \mathbb{Q}(\tau_{D,k} \le T)$. Decomposing $(1 - R_k) = (1 - \bar{R}) + (\bar{R} - R_k)$ and averaging across the N_F firms:

$$\frac{1}{N_F}\sum_k (1 - R_k)\, q_k = (1 - \bar{R})\, \bar{q} - \frac{1}{N_F}\sum_k (R_k - \bar{R})(q_k - \bar{q}),$$

where $\bar{q} = \frac{1}{N_F}\sum_k q_k$, using $\sum_k (R_k - \bar{R}) = 0$. The last term is the negative of the cross-sectional sample covariance of R_k and q_k. When R_k and q_k are negatively correlated across firms—firms closer to the default boundary have both higher default probability and lower recovery—this term is positive, yielding the inequality. ■

C.5.2 Finite-pool effects

Under the homogeneous pool with $N \to \infty$, the realized default fraction converges to its expectation and the protection leg becomes deterministic conditional on the systematic path. With our finite pool of $N_F = 125$ firms:

$$\mathrm{Var}\left(\frac{1}{N_F}\sum_{k=1}^{N_F} \mathbf{1}_{\tau_{D,k}\le T}\right) = \frac{1}{N_F}\,\mathrm{Var}(\mathbf{1}_{\tau_{D,k}\le T}) + \frac{N_F - 1}{N_F}\,\mathrm{Cov}(\mathbf{1}_{\tau_{D,j}\le T}, \mathbf{1}_{\tau_{D,k}\le T}).$$

The first term ($O(1/N_F)$, idiosyncratic) is small. The second term (systematic default correlation) is non-diversifiable and captures the CDX's exposure to joint default risk, which matters for the nonlinear spread formula $S_{\mathrm{CDX}} = \mathrm{Prot} \,/\, \mathrm{Prem}$.

C.5.3 State-dependence of the approximation error

The convexity bias from Corollary 1 is state-dependent: $G''(\bar{d})$ is largest when the mean distance-to-default is intermediate (firms neither far from nor at the boundary). During crisis episodes, when fear raises default boundaries and leverage increases, firms migrate toward the boundary and G'' grows. The homogeneous-pool approximation is therefore least reliable precisely when the fear-driven financing channel is most active. Our approach, by preserving cross-sectional dispersion, captures the convexity correction in all states.